Guarding the vacuole: how *Legionella* T4SS substrate SdhA maintains vacuole integrity

A thesis submitted by

Ila S. Anand

In partial fulfillment of the requirements

for the degree of

Doctor of Philosophy

in

Molecular Microbiology

Tufts University

Sackler School of Graduate Biomedical Sciences

August 2019

Advisor: Ralph R. Isberg, PhD

Abstract

Legionella pneumophila is a Gram-negative, intracellular pathogen that targets amoebal species in aquatic environments and alveolar macrophages in humans. To sustain intracellular replication, *L. pneumophila* uses a type IV secretion system (T4SS) that translocates bacterial protein substrates into the host cytoplasm. These T4SS substrates are involved in the biogenesis of a membrane-bound compartment known as the *Legionella* containing vacuole (LCV). Our knowledge of LCV membrane integrity has been greatly enhanced by studying the T4SS substrate SdhA. The SdhA substrate plays an important role in maintaining LCV integrity, as a *sdhA* mutant exhibits a defect in vacuole integrity and intracellular growth. However, the specific mechanism by which SdhA maintains vacuole integrity is not well understood. To understand how SdhA maintains vacuole integrity during infection, we performed high-throughput RNAi screens against host membrane trafficking genes to identify factors that antagonize vacuole integrity in the absence of SdhA. Host proteins that emerged from the screen were involved in endocytic and recycling pathways. We focused our study on three Rab GTPases and found that depletion of Rab5 isoforms, Rab11b isoform, or Rab8b isoform partially rescued vacuole integrity and intracellular growth of *Legionella* in the absence of SdhA. Additionally, depletion of downstream effectors, EEA1, Rab11FIP1, or VAMP3 rescued vacuole integrity and intracellular growth of the *sdhA* mutant. Localization analyses revealed EEA1 and Rab11FIP1 colocalize with the *sdhA* mutant at a higher frequency than the WT vacuole. These findings provide insights into the host pathways that SdhA is regulating to maintain vacuole integrity during infection.

Dedication

This thesis is dedicated to my Dadi and Nani, who consistently exemplify the character of a strong, academic woman.

Acknowledgements

During my six years of graduate school, there have been numerous individuals who have played invaluable roles in my development as a scientist. Without their support, I would not have been able to achieve the goals that I had set out to accomplish as a graduate student. I am particularly grateful for those individuals who had consistent faith in my abilities to perform as a scientist, especially from the very beginning of graduate school.

First, I would like to thank my advisor, Ralph Isberg, for the opportunity to be a part of his lab. The example he sets as an accomplished principle investigator as well as a prolific scientific writer has been inspiring. I am grateful for his guidance and optimism over the years, which has helped me overcome major obstacles during my thesis research.

Furthermore, I am greatly appreciative of my Thesis Advisory Committee: Bree Aldridge, John Leong, Shumin Tan, and Joan Mecsas. The direction and advice they provided during the progression of my thesis project vastly improved the quality of my research and helped me to hone my analytical skills. I would also like to thank Jonathan Kagan for coming to Tufts to serve as my outside examiner on my defense day.

I would like to express my sincerest gratitude to my family for their love, unwavering support, and encouragement during my time in graduate school. My family has been especially influential in my path to pursuing a PhD and I would not have been able to achieve the goals without them. My mother, a fellow scientist, has served as both a mentor and 'Boston buddy' over the years and I am incredibly grateful for her kindness and support. My father, a physician-researcher, has offered many words of wisdom and astute advice during my time in graduate school and I am ever so thankful for his support

and encouragement to keep persisting through this entire journey. To my sister and best friend, Neha—thank you for your love and steadfast support over the years. Your drive and work ethic is consistently a source of inspiration for me.

I would like to thank members of the Tufts Sackler School of Biomedical Sciences for lending a helping hand and making the graduate school experience enjoyable. Stacie—thank you for being a great friend and making working in the Isberg lab so much more fun. I'm grateful for all the times you lent a listening ear and for both the serious and entertaining conversations we've had together. It's amazing to see how much we've both grown from the beginning. Erion, Efrat, Kristen—thank you for all the laughs, being supportive friends, and providing an uplifting spirit in the Isberg Lab. Our lunchroom conversations will always be memorable. Giang and Matt—thanks for being my first friends in graduate school, reaching out to see how I was doing between experiments, and exploring the Boston food and music scene with me. I would additionally like to thank Kathleen Riendeau for assistance and post-docs Asaf, Won Young, and Wenwen for their scientific advice during my time in the Isberg Lab.

Lastly, I would like to express my gratitude to my significant other, Paresh, for his love, compassion, and support in my final year of graduate school. I am incredibly grateful for all your advice, patience, and encouragement. I feel very blessed to have you in my life and I look forward to starting many new beginnings with you.

Table of Contents

List of Tables

List of Figures

List of Copyrighted Materials

Das, S. and D.G. Lambright, Membrane Trafficking: An Endosome Tether Meets a Rab and Collapses. Curr Biol, 2016. 26(20): p. R927-R929.

Isberg, R.R., T.J. O'Connor, and M. Heidtman, The Legionella pneumophila replication vacuole: making a cosy niche inside host cells. Nat Rev Microbiol, 2009. 7(1): p.13-24.

Marie, N., A.J. Lindsay, and M.W. McCaffrey, Rab coupling protein is selectively degrade by calpain in a Ca2+-dependent manner. Biochem J, 2005. 389(Pt 1): p. 223-31.

Mellouk, N. and J. Enninga, Cytosolic Access of Intracellular Bacterial Pathogens: The Shigella Paradigm. Front Cell Infect Microbiol, 2016. 6: p. 35.

Prekeris, R., Rabs, Rips, FIPs, and Endocytic Membrane Traffic. TheScientificWorldJOURNAL, 2003. 3.

Stenmark, H., Rab GTPases as coordinators of vesicle traffic. Nat Rev Mol Cell Biol, 2009. 10(8): p. 513-25.

List of Abbreviations

BMDM	Bone marrow-derived macrophage
CBM	Clathrin binding motif
CDC	Center for Disease Control & Prevention
Dot/Icm	Defective in organelle trafficking/intracellular multiplication
EE	Early endosome
eEF1A	Eukaryotic translation elongation factor 1A
ER	Endoplasmic reticulum
ERC	Endocytic recycling compartment
F-actin	Actin filaments
FIB/SEM	Focused ion beam scanning electron microscopy
G-actin	Globular actin
GAP	GTPase-activating proteins
GDP	Guanosine diphosphate
GEF	Guanine exchange factor
GTP	Guanosine-5'-triphosphate
HOPS	HOmotypic fusion and Protein Sorting
Hpi	Hours post-infection
IDTS	Icm/Dot translocated substrates
IF	Intermediate filaments
KIFs	Kinesin superfamily proteins
LCV	*Legionella*-containing vacuole
LE	Late endosome
MAPs	Microtubule associated proteins
MT	Microtubule
Mtb	*Mycobacterium tubercuolosis*
MTOCs	MT-organizing centers
PA	Phosphatidic acid
PI	Phosphatidylinositol
Rab	"Ras genes from rat brain"
RE	Recycling endosome
SCV	*Salmonella*-containing vacuole
SIF	*Salmonella*-induced filament
SKIP	SifA-and-Kinesin-Interacting-Protein
SNAP	Synaptosomal nerve-associated protein
SNARE	"SNAP Receptor"
T2SS	Type II Secretion System
T4SS	Type IV Secretion System
TB	Tuberculosis
TGN	Trans-Golgi network
VAMP	Vesicle-associated membrane protein

Chapter 1: Introduction

1.1 Pathogenesis of Legionella pneumophila

Legionella pneumophila is a Gram-negative bacterial pathogen that is naturally found in aquatic habitats. The bacterium can infect a diverse range of fresh water amoebae, which provide a niche for the microorganism to intracellularly replicate [1]. These amoebal species include *Hartmannella*, *Acanthamoeba*, and *Naegleria* [1-3]. In addition to residing in fresh water ponds, the bacterium has been isolated in numerous human-made structures associated with water, including cooling towers, air conditioning units, fountains, and spas [4, 5]. These environments are a source of exposure for humans and individuals may be infected if they inhale aerosolized water particles contaminated with *L. pneumophila* [6-10]. It is believed that humans are dead-end hosts for the pathogen, since person-to-person spread has never been reported [11]. After inhalation, the bacteria are able to replicate within alveolar macrophages [12]. The infection can result in two distinct diseases: a mild flu-like illness known, as Pontiac fever, and a severe form of pneumonia, known as Legionnaires' disease [4, 9, 13].

1.1.1 History & Epidemiology of Legionnaires' Disease

The term Legionnaires' disease was first coined after a mysterious illness had swept through the American Legion Convention in July of 1976. War veterans who had attended the conference presented high fever and pneumonia symptoms, and within one month there were reports of deaths in the news. Overall, 34 of 221 infected individuals past away from this unknown disease [14]. Due to the scale of the epidemic, two congressional investigations were set in motion to determine the source of the outbreak

[15]. For months, laboratory tests ruled out common causative agents of pneumonia, which caused public criticism of the Center of Disease Control and Prevention (CDC). After six months of investigation, a clue as to the causative agent of the disease came from Joseph McDade, a CDC scientist who specialized in researching the intracellular pathogen *Rickettsia*. Guinea pigs that he had inoculated with tissue from infected individuals harbored a novel bacterial species in their livers. CDC researchers named this novel type of bacterium *Legionella pneumophila*, in recognition of the outbreak that resulted in its discovery [16]. Investigators determined that *L. pneumophila* was indeed the source of the pneumonia symptoms at the American Legion Convention [14]. Additionally, researchers investigated into previous outbreaks where people presented similar symptoms and found that the bacterium was responsible for 4 outbreaks between 1957 and 1974 [15] [14] [17]. Moreover, *L. pneumophila* was identified as the agent responsible for an outbreak in 1968 that presented high fevers, but without pneumonia in Pontiac, Michigan [18]. This disease was later coined Pontiac fever.

Currently, the CDC estimates that 8,000-18,000 individuals in the United States are hospitalized each year as a result of Legionnaires' disease. Cases tend to be seasonal, with a higher frequency of cases reported during the summer and early fall [18] [15]. Most healthy individuals are able to effectively eliminate bacterial infection by their innate immune response [4]. However, immunocompromised individuals, the elderly, and smokers are particularly susceptible to disease by the pathogen, as their innate immune response is not as robust [19]. Symptoms usually present 2-14 days after exposure [15] (CDC, 2018). It is estimated that one in ten people who has Legionnaires' disease will die (CDC, 2018). Because the bacterium replicates intracellularly within alveolar

macrophages, cell permeable antibiotics, such as erythromycin, are used to treat *Legionella* infection [20].

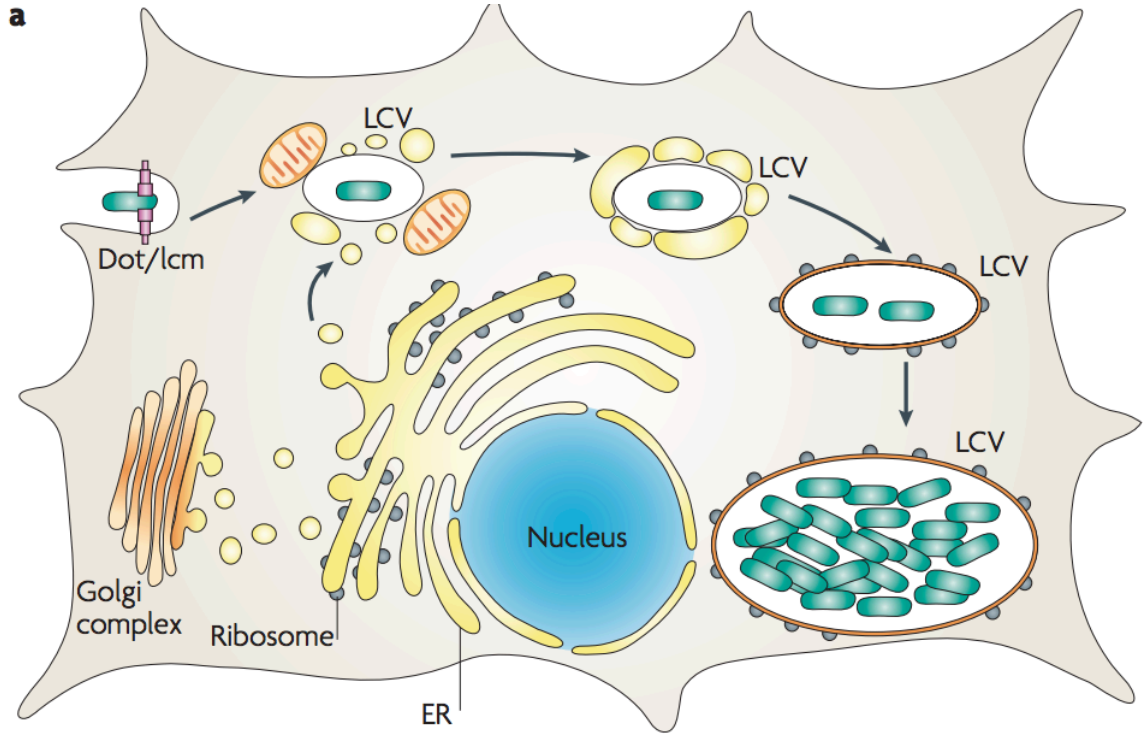

Figure 1. 1 Intracellular Life Cycle of *Legionella pneumophila* in Macrophages Immediately after uptake by macrophages, *L. pneumophila* establishes a membrane-bound replication compartment known as the Legionella-containing vacuole (LCV). The pathogen evades transport to the lysosomal network and hijacks host cell processes via secreted bacterial substrates of the type IV secretion system (Dot/Icm). Within minutes after uptake, vesicles derived from the endoplasmic reticulum (ER, yellow compartments) and mitochondria appear in close proximity to the LCV. The LCV membrane eventually resembles the rough ER in appearance and becomes studded with ribosomes. Within this ER-like compartment, the pathogen undergoes 3-4 cell divisions before eventually lysing the host cell after 14 hours of infection. Reprinted with permission from Isberg, R.R., T.J. O'Connor, and M. Heidtman, *The Legionella pneumophila replication vacuole: making a cosy niche inside host cells.* Nat Rev Microbiol, 2009. **7**(1): p. 13-24.

1.1.2 *Legionella pneumophila* Intracellular Life Cycle

When non-pathogenic bacteria are phagocytosed by a host cell, the phagosome is trafficking down the endocytic-lysosomal degradation pathway and the bacteria are

quickly destroyed by the fusion of the phagosome with low pH lysosomes [21]. *L. pneumophila* is a pathogen that also avoids fusion with acidic lysosomes containing hydrolytic proteases [22, 23] [24]. The detailed intracellular life cycle *L. pneumophila* within the macrophage is described next.

At a glance, *L. pneumophila* intracellular life cycle within macrophages is approximately 14 hours. *L. pneumophila* is phacytosed by macrophages through a unique uptake process called "coiling phagocytosis" [25]. Immediately after uptake*, L. pneumophila* establishes the LCV in which the bacterium replicates (Figure 1.1). This compartment is distinct by the absence of endocytic and lysosomal markers, and as a result is less acidic [12] [25]. Within minutes after uptake, the LCV is decorated with smooth vesicles and enriched with mitochondria [26] [27] [28] [29]. These smooth vesicles are postulated to be ER-Golgi "vesicles" and are repeatedly observed during early time points of infection, but are less prevalent during later time points. This interpretation has been challenged, with recent data showing the "vesicles" are derived from rearranged tubular ER [30]. At 4 hours after uptake, ribosomes that are derived from the rough ER begin to associate with the vacuole, and at 8 hours after uptake, ~95% of LCVs are studded with ribosomes or rough ER, indicating the pathogen is recruiting host translation machinery [23]. After host resources are spent and the bacteria has undergone 3-4 cell divisions, the bacterial progeny egress from the infected cell by host cell lysis and infect neighboring macrophages. Although several mutants showing defective egress from mammalian cells have been identified, how *L. pneumophila* exits the host is still ongoing research [31].

1.1.3 Dot/Icm T4SS and translocated substrates

Successful formation of the *Legionella*-containing vacuole and replication of the bacterium is dependent on its type IVb secretion system (Icm/Dot T4SS). This T4SS is encoded by ~27 genes termed *intracellular multiplication/defect in organelle trafficking* (*icm/dot*) [32] [33] [34]. Of the 27 genes, 7 of the genes are responsible for translocation of ~300 bacterial proteins into the host cytoplasm. These bacterial proteins are also known as Icm/Dot translocated substrates (IDTS).

The core complex of the Icm/Dot T4SS spans the bacterial membrane and forms a pore to allow the transfer of IDTS. The core complex is composed of five proteins DotC, DotD, DotF, DotG, and DotH [35]. The DotG protein forms the central channel that spans both the inner and outer bacterial membrane [36] [37] [38]. All Dot proteins, except DotF, are required for intracellular replication, as a strain lacking *dotF* demonstrates only a slight defect in Icm/Dot-dependent translocation and intracellular replication [35]. The Icm/Dot system additionally contains a second complex, which contains the type IV coupling protein DotL [39]. The coupling protein provides energy for the T4SS through the hydrolysis of ATP. Moreover, DotL binds to two other Icm/Dot proteins, IcmS and IcmW [40]. Icm proteins are soluble and directly interact with translocated substrates [41]. IcmS and IcmW are hypothesized to recruit translocated substrates to the core Icm/Dot system and maintain the substrates in their secretion competent form prior to translocation [42] [41].

Studies of Icm/Dot T4SS translocated substrates have revealed a vast amount of information about *L. pneumophila* and the host that it infects. Although ~300 IDTS have been identified, deletion of a single gene encoding for a substrate rarely results in an

intracellular growth defect for the pathogen [43] [44]. This is most apparent from a study demonstrating that a *Legionella* strain lacking 71 IDTS (31.4% of all identified translocated substrates) is still able to replicate in tissue cultured bone marrow-derived macrophages [5]. It is believed that many IDTS play functionally redundant roles in targeting multiple pathways to accomplish similar outcomes during infection. Interestingly, strains lacking single substrates have been shown to have defects in certain amoebal species but not in human or mouse macrophages [40] [45] [46]. These results indicate that many IDTS may only be required for intracellular replication in certain hosts, but not others. Furthermore, the large number of predicted translocated substrates is revealing of the broad host range *L. pneumophila* can infect.

Legionella translocated substrates serve various purposes inside the host cell, including avoidance of lysosomal degradation, recruitment and regulation of ER-derived membrane to the LCV, manipulation of host ubiquitin pathway, and regulation of innate immune responses and host protein translation, and maintenance of vacuole integrity (Figure 1.2) [47] [48] [8] [29] [49] [50]. *L. pneumophila* translocated substrates implicated in avoidance of lysosomal degradation are VipD and SidK. VipD is a phospholipase that localizes to early endosomes where it binds Rab5b and depletes PI3P from the endosome membrane, preventing the LCV from interaction with downstream effectors of the endocytic pathway [51] [52] [53]. SidK directly binds to host v-ATPase subunit VatA and prevents v-ATPase proton translocation and, as a result, the acidification of the vacuole [54]. Overexpression or injection of VipD or SidK in cells can also prevent acidification of the LCV as well as an *E. coli*-containing phagosome [53] [54]. Interestingly, deletion strains of VipD or SidK do not affect *Legionella*

intracellular growth and this indicates that the pathogen uses other strategies to prevent traffic through the endocytic-lysosomal pathway [55] [10].

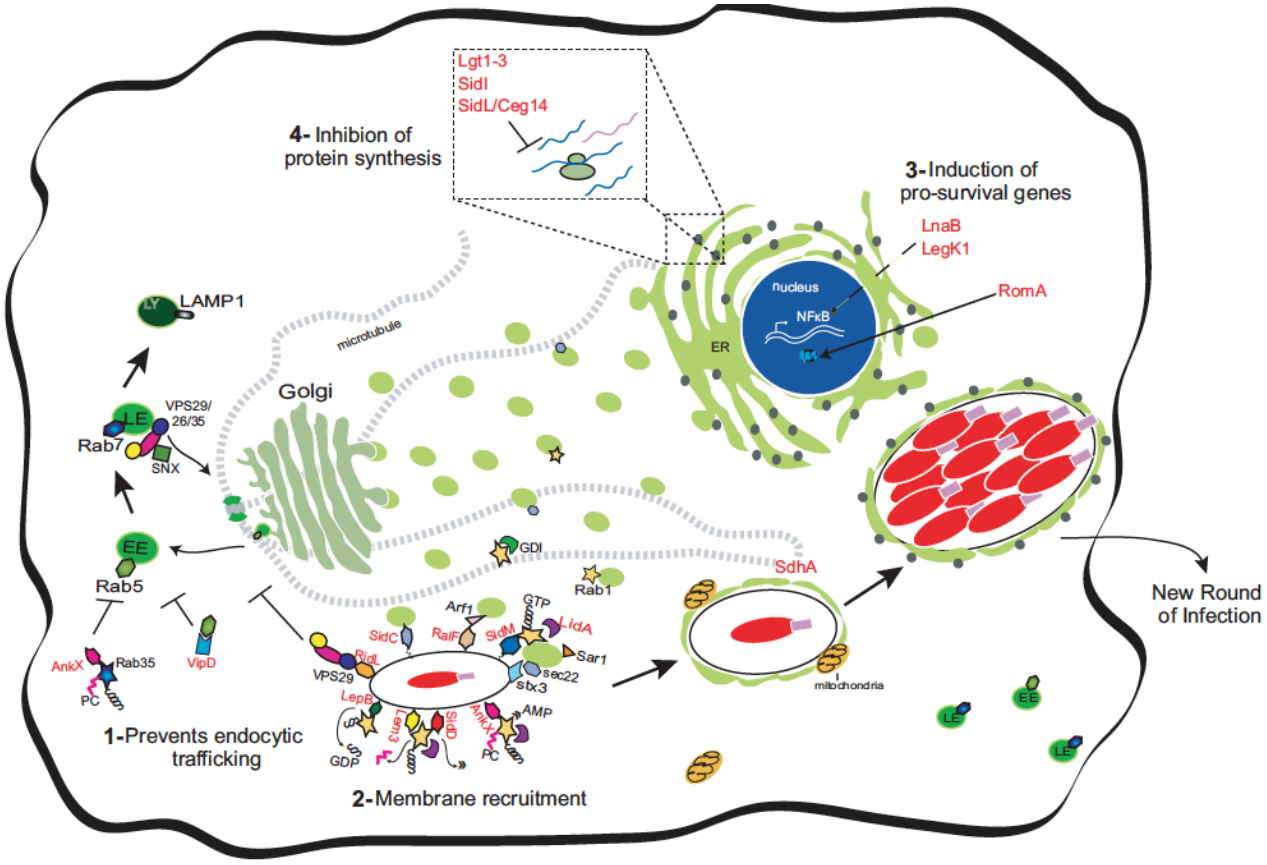

Figure 1. 2 Legionella pneumophila manipulates host cell pathways via T4SS substrates.
Within the macrophage host, *L. pneumophila* controls host factors (black font) through the action of type 4 secretion system (T4SS) substrates (red font). 1) *L. pneumophila* prevents trafficking through the endocytic-lysosomal pathway by the T4SS substrates VipD, a phospholipase that binds Rab5, and by AnkX phosphocholination of Rab35. The pathogen also inhibits retrograde trafficking to the Golgi by RidL. 2) Formation of the *Legionella*-containing vacuole (LCV) requires hijacking components of the secretory pathway in order for ER-derived vesicles to fuse with the LCV. Examples of T4SS substrates that control host secretory Rab1 activity are SidM, LidA, AnkX, SidD, Lem3, and LepB. 3) T4SS substrates LnaB and LegK3 induce expression of NF-kB and its translocation to the nucleus to activate pro-survival host genes. 4) *L. pneumophila* inhibits host protein synthesis by substrates Lgt1, Lgt2, Lgt3, SidI, and SidL/Ceg14. Used with permission from Ralph Isberg.

Many *Legionella* translocated substrates are involved in recruiting ER-derived membrane to the LCV during infection inside macrophages. The IDTS SidM (also known as DrrA) binds to PI4P on the vacuole membrane and recruits host Rab1 to the LCV [56]. Rab1 is a GTPase involved in vesicle trafficking between the ER and the Golgi. When SidM binds and activates Rab1, membrane fusion between the LCV and ER-derived vesicles occurs [26]. Specifically, SidM acts a guanine exchange factor (GEF) for Rab1 and efficiently displaces the protein from its host guanine nucleotide dissociation inhibitor partner [57] [58]. Once Rab1 is activated, host t-SNARE proteins Stx3 and Stx4 and ER-derived v-SNARE Sec22b complex together and facilitate ER-derived membrane fusion with the LCV [49] [59] [60].

Translocated substrate LidA is also involved in Rab-mediated ER recruitment and membrane fusion with the LCV. LidA is known to bind various GTPases *in vitro*, including Rab1, Rab6, and Rab8 [56] [61] [62]. Similar to SidM, LidA has been shown to enhance vesicle tethering and membrane fusion by recruiting SNAREs Stx2, Stx3, Stx4 and ER-derived Sec22b [56].

Other *Legionella* substrates, such as RalF and SidC, promote docking and fusion of ER-derived vesicles at the LCV. RalF acts as a GEF for the host GTPase Arf1, which controls ER-Golgi and Golgi-plasma membrane trafficking [63] [64] [65]. SidC is an IDTS that binds to PI4P on the LCV membrane and is involved in vesicle fusion and ER-recruitment [66] [67] [68]. SidC was also shown to have ubiquitin ligase activity at the LCV, which will be discussed later [69].

In addition to recruiting ER-derived membranes, *Legionella* also tightly regulates trafficking dynamics. Translocated substrates LepB, SidD, and AnkX specifically control

Rab1-mediated trafficking dynamics. LepB stimulates GTP hydrolysis of active Rab1, thereby converting Rab1 to the inactive form. It was shown that as LepB concentration increases at the LCV, there is a corresponding decrease in Rab1 localization around the LCV [70] [71]. LepB phosphosinosidyl-4- kinase activity has been suggested to function in antagonism with another translocated substrate SidF, which is a bacterial phosphoinositide phosphatase. Together, LepB and SidF control the amount of PI3P relative to PI(3,4)P2, and ultimately PI(4)P on the LCV membrane [72]. Another IDTS, SidD, modifies Rab1 by de-AMPylation, thereby reversing the effects of SidM ampylation [73] [74]. IDTS AnkX enhances the activity of both Rab1 and Rab35 (a GTPase involved in endocytic recycling) by adding a phosphocholine moiety to these GTPases and also blocking GDI and GAP binding to the GTPases [75] [74] [76]. Altogether, these translocated substrates play an important role in regulating Rab1 secretory trafficking to the LCV. Another noteworthy IDTS is RidL, which inhibits retrograde trafficking towards the LCV. Once RidL is secreted by the T4SS, the substrate localizes to the LCV and binds VPS29, a member of the retromer complex. This binding inhibits the accumulation of cargo receptors from coming in contact with the LCV and prevents the stability of the vacuole from being compromised [77].

An important class of *L. pneumophila* translocated substrates are those that interfere with host cell ubiquitination. Four IDTS, LubX, LegU1, SidC, and AnkB functionally mimic eukaryotic E3 ubiquitin ligases [78]. E3 ubiquitin ligases mark bacterial and host proteins for either modification of activity or proteasomal degradation. LubX acts in cooperation with E2 enzymes to polyubiquitinate and modify host protein Clk1, which is involved in pre-mRNA processing. LubX also acts as a “meta-effector” by

targeting another IDTS, SidH, for proteosomal degradation during later stages of infection [79]. LegU1 uses the E3 ligase activity to ubiquitinate BAT3, which is a host chaperone protein that regulates the ER stress response [80]. As mentioned earlier, translocated substrate SidC has ubiquitin ligase activity in addition to recruiting ER vesicles to the LCV. However, the substrate of the SidC is unknown [69]. Lastly, AnkB recruits host protein Skp1 to promote polyubiquitination of proteins at the LCV [81]. It has been proposed that AnkB-mediated polyubiquitination of LCV-associated proteins promotes protein turnover, thereby generating necessary metabolites for bacterial replication. Recently, investigators have shown that translocated substrates SidE, SdeA, SdeB, and SdeC (the SidE family) catalyze the ubiquitination of host proteins reticulon 4 and Rab33b. Two studies demonstrated that this process is independent of the host ubiquitin conjugation system [30] [82].

The inhibition of protein synthesis also benefits *L. pneumophila* during intracellular replication. Five translocated substrates, Lgt1, Lgt2, Lgt3, SidI, and SidL have specifically shown to inhibit protein synthesis in mammalian cells by radiolabeled methionine incorporation studies [83] [84] [45] [85]. Lgt1 was the first putative *L. pneumophila* translocated substrate shown to modify the elongation factor 1a (eEF-1A). During translation elongation, eEF-1A is responsible for loading charged amino acids to the A site of the ribosome [86]. Lgt1, Lgt2, and Lgt3 have glucosyltransferase activity that promotes mono-O-glucosylation of eEF-1A, thereby inhibiting ribosomal loading [85] [83].

Other translocated substrates that target members of the eukaryotic translation elongation machinery are SidI and SidL. In contrast to Lgt1-3, SidI does not have

glucosyltransferase activity. However, SidI has been shown to bind to not only eEF-1A but also eEF-1Bgamma. The mechanism of translation inhibition by SidI remains to be determined [84]. Little is known about SidL and the mechanism of inhibition also remains to be determined. It is postulated that SidL might possess actin depolymerization activity, as a connection for efficient translation and stable actin cytoskeleton has been established [87] [88] [86].

In addition to translocated substrates that control host translation, secretory, and ubiquitin pathways, *L. pneumophila* also possesses a subset of proteins that are involved in preventing host cell death responses. Previous studies have shown that *L. pneumophila* infection in macrophage-like U937 cell line results in the activation of transcription factor NF-kB as well as genes involved in inhibition of apoptosis [50]. The IDTS LegK1 is a Ser/Thr kinase that is able to activate NF-kB *in vitro*, although its role *in vivo* remains unclear [89]. LnaB is another translocated substrate that activates NF-kB, but by an unknown mechanism [90]. The activation NF-kB leads to enhanced transcription of pro-survival factors, as well as inflammatory cytokines [50] [91].

1.1.4 Dot/Icm T4SS substrate SdhA

Avoiding exposure to the host cytoplasm is essential for *L. pneumophila* intracellular replication. Unlike other pathogens such as *Shigella* and *Listeria*, *L. pneumophila* has not evolved strategies to cope with the hostile cytoplasmic environment [92]. Establishment and maintenance of vacuole integrity is critical for bacterial survival. Permeability of LCV membrane leads to recognition of the bacterium by cytosolic innate immune sensors and ultimately clearance of the pathogen [93] [94]. Our understanding of

LCV membrane integrity has been greatly enhanced by studying the Dot/Icm T4SS substrate SdhA.

The SdhA IDTS was first identified by an insertional mutant screen, which was designed to determine if any *Legionella* translocated substrates exist that are required for maximal intracellular growth. One of the two mutants identified had an insertion in the gene *sdhA*. The SdhA protein is a 1429 amino acid protein and it is a paralog of two other predicted IDTS, sidH and sdhB [95] [96] [55]. Single deletions of *sidH* or *sdhB* had no detectable effects on *L. pneumophila* growth, although a triple mutant (Δ*sdhA*Δ*sidH*Δ*sdhB*) did increase the severity of the *sdhA* defect. Interestingly, the intracellular growth of the triple mutant could be fully rescued by complementation of only *sdhA* on a multicopy plasmid [55]. This result indicated that it is only the *sdhA* gene that is required for *Legionella* intracellular replication. In the absence of *sdhA* during *Legionella* infection, a profound intracellular defect in macrophages is observed. This defect is visualized as early as 14 hours post-infection (hpi) by microscopy and is additionally observed by CFU count at 24 hpi [55] [97]. There is also a defect in intracellular growth in amoebal species, although the defect is less severe [55].

By immunofluorescnce microscopy, extensive staining of SdhA is observed around the LCV when *sdhA* is overproduced on a multi-copy plasmid during *Legionella* infection. This staining is absent when the plasmid-encoded *Legionella* strain lacked the Dot/Icm translocator, indicating that SdhA is an Icm/Dot translocated substrate. Additionally, cell fractionation studies demonstrated that SdhA is present in the digitonin or saponin-soluble (translocated) fraction of infected U937 macrophage-like cells. It was

also determined by hybrid construction that SdhA possesses a carboxyl-terminal translocation signal that is required for translocation by the T4SS [55].

As early as 4hpi, strains harboring a deletion of *sdhA* are found, by microscopy, to be within vacuoles that are permeable and exposed to the cytosol (Figure 1.3A) [97]. The base level of cytosol-detected bacteria during WT infection is approximately 5-10% throughout the entire course of infection. During Δ*sdhA* infection, the percent of cytosol-detected bacteria is approximately 10% at 1hpi. However, this observed phenotype rises to 40% and 60% at 5hpi and 8hpi, respectively. On average, the percent cytosol-detected *Legionella* is approximately 5-fold more when comparing ΔsdhA infection to WT infection at 5hpi (Figure 1.3B). The percent of cytosol-detected Δ*sdhA* bacteria can be rescued to WT levels if SdhA is complemented on a plasmid (Figure 1.3C).

Legionella exposed to the cytoplasm are susceptible to host innate immune recognition and activation of caspase-11-dependent cell death known as pyroptosis. Vacuole disruption of the Δ*sdhA* vacuole is a precursor for caspase-11 activation and degradation of bacteria (Figure 1.4C). After vacuole disruption, bacteria are degraded by an unknown mechanism, resulting in downstream caspase-11 activation. Degraded bacteria are evident by swollen, blebbed, and puntae phenotypes that are observed by microscopy (Figure 1.4A). The percent of degraded Δ*sdhA* bacteria steadily increases over time and is directly correlated with an increase in activated caspases with time (Figure 1.4C). The activation of caspase-11-dependent pyroptosis is promoted by the recruitment of guanylate binding proteins (GBPs) to the disrupted vacuole [98] [99]. Basal IFN signaling is sufficient to maintain GBP expression at steady-state levels [93].

GBP recruitment to the disrupted vacuole mediates the release of LPS and bacterial DNA [93] [94].

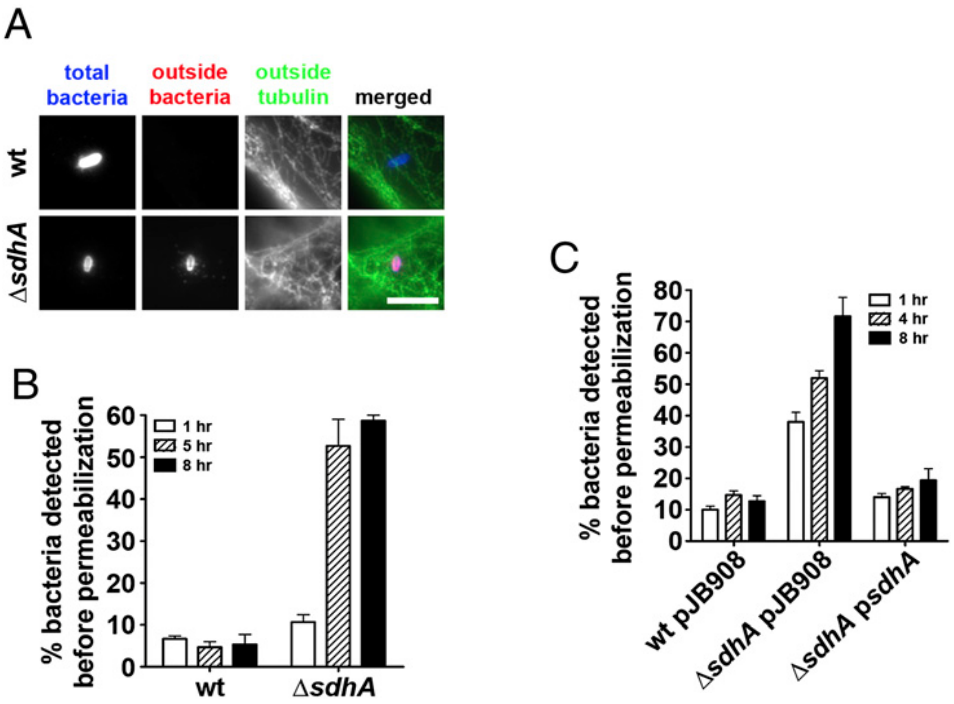

Figure 1. 3 Absence of SdhA results in loss of *Legionella*-containing vacuole integrity A) Fixation of mouse bone marrow-derived macrophages (BMDMs) is sufficient to detect cytosolic markers, such as tubulin and cytosol-exposed bacteria. Infected macrophages were stain before bacteria permeabilization (red) and after BMDM permeabilization (blue). B) Percent bacteria detected before permeabilization was quantified. Percent cytosol-detected *Legionella* is approximately 5-fold more when comparing ΔsdhA infection to WT infection at 5hpi. C) Loss of Δ*sdhA* vacuole integrity can be rescued by over-expression of SdhA on a multi-copy plasmid. Used with permission from Ralph Isberg.

The release of bacterial DNA into the cytoplasm triggers two parallel pathways: cGAS/STING pathway for IFN induction and the AIM2 inflammasome pathway for IL-1 maturation. Secreted IFN and IL-1 play non-redundant roles in alerting other innate immune cells to clear the infection. The GBP-mediated LPS leakage into the cytoplasm results in LPS binding directly to the CARD domain of caspase-11, which triggers its

oligomerization and activation. Activated caspase-11 cleaves gasdermin D and this protein oligomerizes to form plasma membrane pores and ultimately causing host cell death [94].

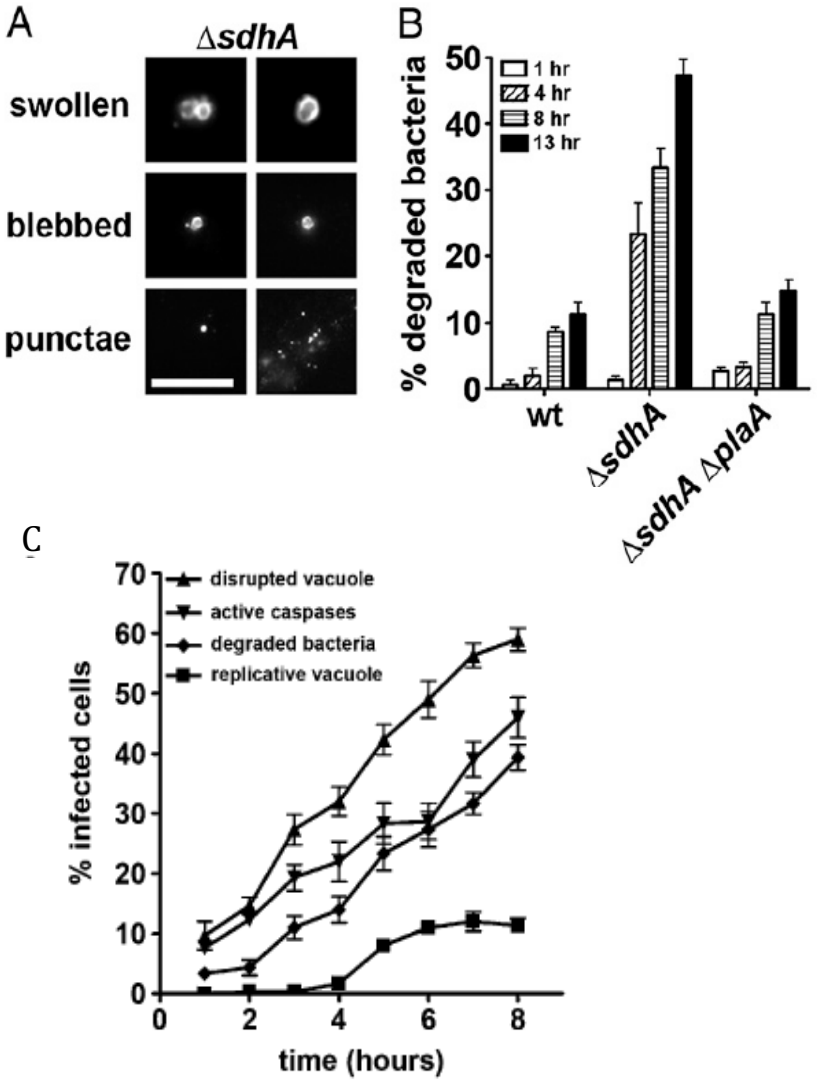

Figure 1. 4 Cytosolic *L. pneumophila* is degraded after vacuole disruption
A & B) Mouse bone marrow-derived macrophages (BMDMs) were challenged with *L. pneumophila* for 8 h, then fixed and stained for *Legionella*. Degraded bacteria were quantified based on aberrant bacterial morphology. C) BMDMs were challenged with Δ*sdhA* at indicated times and FITC-VAD was added before fixation to stain and quantify activated caspases. Disrupted vacuoles, replicative vacuoles, and degraded bacteria were also quantified. Used with permission from Ralph Isberg.

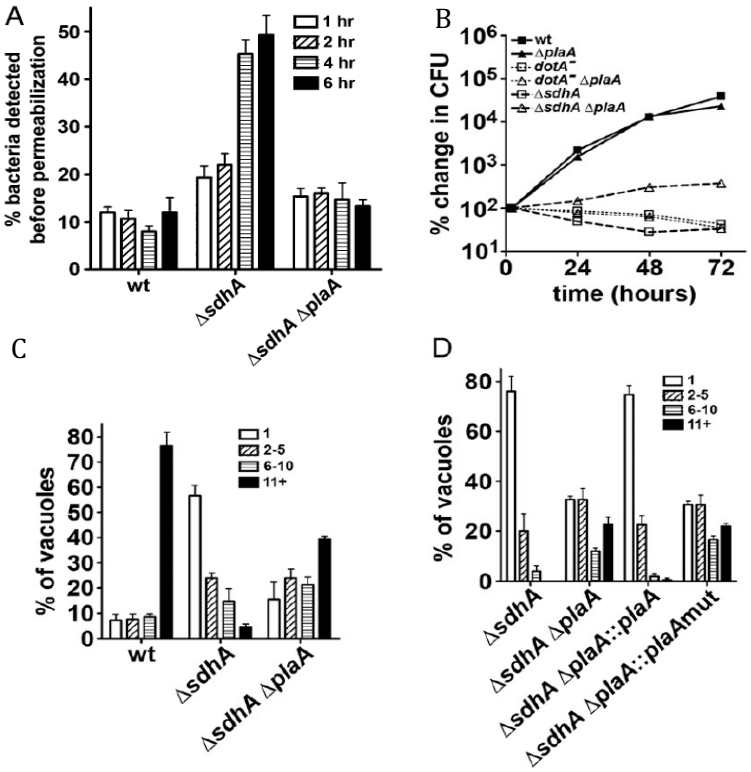

Figure 1. 5 Growth defect of ΔsdhA strain is suppressed by absence of PlaA phospholipase activity.
A) Mouse bone marrow-derived macrophages (BMDMs) were challenged with *L. pneumophila* for 6 h, then fixed and stained for *Legionella*. Percent cytosol-detected bacteria was quantified. B) Growth of L. pneumophila in BMDMs was determined by plating for CFU. Δ*sdhA*Δ*plaA* (open triangle) partially restores intracellular growth compared to Δ*sdhA* (open square) and WT (black square). C&D) BMDMs were challenged with *L. pneumophila* for 14 h, then fixed, stained for *Legionella,* and visualized by immunofluorescence microscopy. Used with permission from Ralph Isberg.

The Δ*sdhA* vacuole integrity defect can be restored by disruption of the gene encoding the *L. pneumophila* type 2 secretion system (T2SS) substrate PlaA. The percent detected degraded bacteria is reduced to WT levels during infection with Δ*sdhA*Δ*plaA* double mutant (Figure 1.4B). PlaA is a phospholipase that bears homology to *Salmonella* SseJ and cleaves phospholipids and lysophospholipids [100, 101]. Similar to the function of SseJ, PlaA destabilizes the vacuole in the absence of SdhA. A double mutant Δ*sdhA*Δ*plaA* strain restores vacuole integrity and partially restores intracellular growth

[97] (Figure 1.5A-C). If the double mutant Δ*sdhA*Δ*plaA* strain is complemented with PlaA on a plasmid, then the vacuole permeability defect returns to ΔsdhA levels. However, when the double mutant is complemented with PlaA containing a mutation in the phospholipase active site, growth remains at similar levels as the non-complemented Δ*sdhA*Δ*plaA* strain (Figure 1.5D).

The specific mechanism by which SdhA maintains vacuole integrity is not well understood. It is hypothesized that SdhA is a structural protein that prevents a host compartment carrying a toxic lipid substrate from contacting the *Legionella*-containing vacuole. The toxic lipid coming in contact with the Δ*sdhA* vacuole may be a substrate for PlaA phospholipase activity, resulting in the vacuole disruption phenotype observed during Δ*sdhA* infection. Because the Δ*sdhA*Δ*plaA* strain fully restores vacuole integrity at 4hpi but only partially restores Δ*sdhA*Δ*plaA* intracellular growth over time, we believe a toxic lipid substrate may accumulate on the vacuole. The toxic lipid may be a substrate for host factors to bind, causing vacuole instability and disruption. This would explain why there is only partial restoration of intracellular growth for the Δ*sdhA*Δ*plaA* strain.

Evidence that corroborates a toxic lipid is accumulating at the vacuole and host proteins are involved in vacuole disruption is the recent finding that SdhA directly interacts with host protein OCRL. The OCRL protein contains a 5-phosphatase domain that hydrolyzes PI(4,5)P_2 to PI(4)P (Figure 1.6) [102] [103]. The N-terminal region of OCRL contains a PH domain that binds host clathrin and AP2 and the C-terminal region contains an ASH and Rho-GAP domain that binds clathrin and small GTPases. Strikingly, SdhA shows some sequence motifs that are both found in OCRL and predicted to bind OCRL, where the N-terminal region of SdhA contains a clathrin and

AP2 binding site (CBM1) and the C-terminal region also contains a clathrin binding site (CBM2). Recently, it was determined that the SdhA CBM2 region directly binds to OCRL based on pull-down and immunoprecipitation assays (Figure 1.6). This result led us to believe that SdhA is sequestering OCRL from performing its 5-phosphatase activity on vesicle membranes and/or interacting with small GTPases involved in vesicle trafficking. However, OCRL is involved in numerous membrane trafficking events in the cell. Therefore, it is challenging to decipher which membrane trafficking pathway SdhA is preventing from coming in contact with the LCV through the sequestration of OCRL.

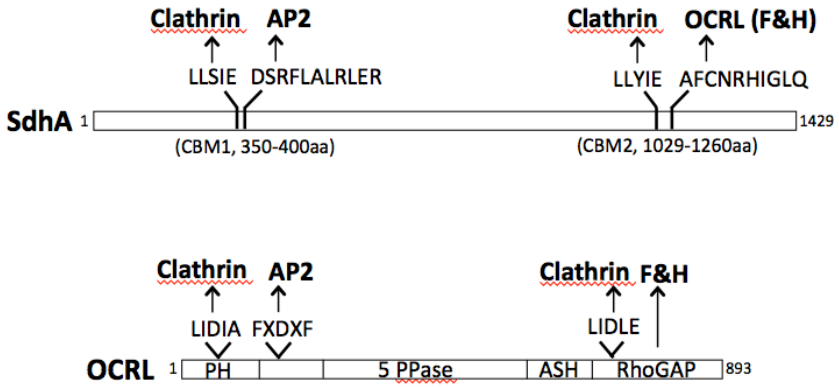

Figure 1. 6 Domain Map of SdhA and OCRL
(Top) SdhA N-terminal region contains a clathrin and AP2 binding site (CBM1) and the C-terminal region contains a clathrin binding site (CBM2) and OCRL binding site. (Bottom) OCRL N-terminal region contains a PH domain that binds host clathrin and AP2 and the C-terminal region contains an ASH and Rho-GAP domain that binds clathrin and small GTPases. Used with permission from Won Young Choi.

In Chapter 2, I investigate which specific host membrane trafficking compartments are involved in interfering with growth of the Δ*sdhA* strain by performing an RNAi screening against membrane trafficking genes. Before discussing the details of the screen and research, I will first review how other intracellular pathogens maintain vacuole integrity and the types of host membrane trafficking events that occur in the cell.

Many pathogens evade particular membrane trafficking events and this can provide insights into understanding how SdhA maintains vacuole integrity during *L. pneumophila* intracellular replication.

1.2 Maintenance of vacuole integrity by intracellular pathogens

Intracellular bacterial strategies have evolved various strategies to maintain membrane integrity after establishment of the vacuole. Vacuolar maintenance is critical during the initial stages of infection, even for pathogens that eventually rupture the vacuole and replicate in the cytoplasm. Pathogens have encoded "guard" proteins to protect against membrane damage during intracellular replication. In this section I explore the various guard strategies employed by pathogens to maintain their vacuole membrane. These strategies include hijacking host cytoskeleton and ER-Golgi trafficking, regulating lysosomal fusion and endocytic-recycling compartments, and regulating autophagy and retromer-mediated trafficking. The different strategies pathogens use to maintain the vacuole can provide insights into understanding how SdhA maintains vacuole integrity during *L. pneumophila* intracellular replication.

1.2.1 Hijacking Host Cytoskeleton

One strategy used by bacterial pathogens to maintain vacuole integrity is by manipulating host cytoskeleton dynamics. This strategy also allows the pathogen to maneuver where the vacuole is localized to in the host cell. *Salmonella typhimurium* is a facultative intracellular bacterium that can cause gastroenteritis and enteric fever. In both epithelial cells and macrophages, *S. typhimurium* manipulates the host cytoskeleton to

form abundant tubule aggregates known as *Salmonella*-induced filaments (SIFs). These SIFs emanate outward from the *Salmonella*-containing vacuole (SCV) in the cytoplasm. SIFs link *Salmonella* to both the endocytic and exocytic trafficking pathways [104]. SIFs biogenesis is dependent on the SPI2 type III secretion system and six secreted bacterial substrates: SifA, SseJ, PipB2, SopD2, SseF, and SseG. Deletion mutants of any of the six bacterial proteins produce an aberrant SIF morphology and altered SIF frequency [105].

SifA was first identified as the main driver of SIF formation after infection of HeLa cells with the Δ*sifA* mutant failed to induce SIFs and attenuation with this strain was observed in mice [106]. Galectin-3, a marker for vacuole lysis, was found recruited to the *sifA* mutant vacuole at a higher frequency compared to wild-type bacteria [107]. Later, the N-terminal region of SifA was found in a complex with the host factor SifA-and-Kinesin-Interacting-Protein (SKIP) [108, 109]. This interaction promotes kinesin-1-dependent movement along microtubules, enabling vesicle budding from the SCV and the formation of SIFs that maintain vacuole integrity.

Interestingly, transfection of HeLa cells with a SifA-encoded plasmid produces extensive vacuolation of LAMP-1-positive lysosomal compartments [110]. Overexpression of SKIP also induces kinesin-1-dependent anterograde movement of lysosomal compartments [111]. It was also shown recently that SifA-SKIP recruit HOPS (HOmotypic fusion and Protein Sorting) complex to the SCV in order to access host late endosomal and lysosomal membrane [112]. These results presented the conundrum that fusion of lysosomal membrane maintains the vacuole but also delivers toxic lysosomal enzymes to the SCV. It was later demonstrated that SifA-SKIP interaction sequesters lysosomal Rab9, thereby inhibiting Rab9-dependent M6PR recruitment of the SCV [113].

Therefore, through the actions of SifA, *Salmonella* is able to hijack cargo movement for membrane acquisition while simultaneously evading fusion of toxic cargo the SCV.

The activities of SifA are tightly coordinated with another substrate, SseJ. SseJ has phospholipase activity and glycerophosphlipid:cholesterol acyltransferase activity that alters the lipid composition of the SCV membrane. Recently, it was demonstrated that SseJ clusters around the SCV by a pearling transition, which is a force-driven mechanism for endosomal tubulation [114]. A Δ*sifA*Δ*sseJ* double mutant can suppress the loss of integrity phenotype by a Δ*sifA* mutant [115]. Thus, loss of vacuolar membrane of the *sifA* mutant requires the action of SseJ. This suggests that SseJ is recognizing a lipid accumulating on the SCV of the Δ*sifA* mutant and degrading the membrane. Interestingly, the vacuole permeability of a *sifA* mutant can be harnessed for cancer therapy. Recently, an engineered *sifA* mutant was shown to release a cytotoxic peptide into the cytoplasm of proliferating tumor cells, thereby inducing host cell death [116].

SPI2 substrates PipB2, SopD2, SseF, and SseG also stabilize the SCV membrane. PipB2 promotes SIF extension by linking SIFs to kinesin-1[117]. From live cell analyses, infection with *a* Δ*pipb2* mutant produces bulky SIFs that have reduced peripheral extension [105]. In contrast, SopD2 antagonizes the activity of SifA to regulate membrane dynamics and SIF biogenesis [118]. SseF and SseG are required for converting single-membraned SIFs to double-membraned SIFs [119]. SseG also influences SCV motility by restricting vacuole speed [120]. Strains lacking *sseF* or *sseG* present a decreased recruitment of LAMP1 to SCVs as well as a decrease in *Salmonella* intracellular replication [121].

Chlamydia trachomatis is a common sexually transmitted pathogen that replicates within epithelial cells in a compartment known as the inclusion. *C. trachomatis* creates microtubule cages to support the development of the inclusion [122]. The chlamydial protein CT813 stabilizes microtubules and consequently the inclusion itself by interacting with GTPases Arf1 and Arf4 [123, 124]. The inclusion scaffold is also made up of F-actin and intermediate filaments (IF). Disruption of the actin scaffold results in rupture of the inclusion membrane and exposure of *C. trachomatis* to the cytoplasm [125]. IFs have shown to be processed by chlamydial protease CPAF in order to stabilize the vacuole [125, 126].

1.2.2 Hijacking ER-Golgi Trafficking

Chlamydia trachomatis hijacks the ER and Golgi to acquire lipids and maintain inclusion membrane integrity. The inclusion membrane requires host sphingomyelin biosynthesis [127]. In the mammalian host, ceramide, the precursor of sphingomyelin, is synthesized on the cytosolic surface of the endoplasmic reticulum [128-130]. The host protein CERT binds to ER membrane proteins VAP-A and VAP-B and extracts newly synthesized ceramide [129]. Ceramide is subsequently transported to the trans-Golgi by CERT and converted to sphingomyelin by sphingomyelin synthases [130]. The *Chlamydia* protein IncD acquires spingomyelin by directly recruiting host CERT-VAP complex to the inclusion [131, 132]. Sphingomyelin synthases have shown to localize at the inclusion membrane by a GBF1-dependent vesicular pathway, thereby allowing the conversion of ceramide to sphingomyelin to occur directly on the membrane [133]. Sphingomyelin biosynthesis is required for inclusion growth and stability; without

sphingomyelin, inclusion membrane disruption occurs. The *Chlamydia* inclusion also establishes direct contacts with the ER by *Chlamydia* protein IncV, which inserts into the inclusion membrane and directly interacts with VAP by IncV FFAT motif [134]. This interaction is thought to tether the ER in close proximity to the inclusion and allow for efficient access to lipid biosynthesis machinery.

1.2.3 Regulation of Lysosomal Fusion

Mycobacterium tubercuolosis (*Mtb*) is the causative agent of human tuberculosis (TB) and its pathogenesis largely depends on the type VII secretion system ESX-1 [135]. ESX-1-induced rupture of the phagosomal membrane and access to the cytosol is important for *Mtb* survival. Using a fluorescence-based method, investigators demonstrated that *M. tuberculosis* is able to rupture the vacuole in an ESX-1 secretion system-dependent manner [136]. A strain lacking ESX-1 secreted substrate ESAT-6 showed reduced levels of phagolysosome rupture. However, it was recently found that restriction of phagosome acidification during initial steps of infection is a prerequisite for mycobacterial phagosome rupture. It was shown that *M. tuberculosis* induces partial blockage of phagosomal acidification prior to vacuolar break through the bivalent cation transporter Nramp-1 [137]. Therefore, regulation of lysosome-mediated *Mycobacterium*-vacuole rupture is regulated in a temporal fashion.

1.2.4 Regulating Endocytic-Recycling Compartments

Current studies have provided evidence that the endocytic-recycling compartment is involved in destabilizing the pathogen-containing vacuole. *Shigella* is an intracellular pathogen that causes bacillary dysentery in humans. A crucial step of *Shigella* infection

after internalization is to escape the vacuole and replicate within the cytosol. However, deciphering the mechanism of *Shigella*-containing vacuole rupture has been challenging to study because vacuole escape occurs rapidly after entry. Recently, from a high-throughput siRNA screen, endosomal and recycling factors were identified as being involved in rupturing the *Shigella*-containing vacuole [138]. Notable host factors included early endosomal markers Rab5 and EEA1, sorting nexins SNX1 and SNX2, and recycling endosomal markers Rab4 and Rab11 [138].

Rab11 was further investigated to understand its role during *Shigella* vacuole rupture. By immunofluorescence staining, Rab11 recruitment to the vacuole was dependent on the *Shigella* T3SS substrate IpgD, which is a PI(4,5)P_2 phosphatase that generates PI(5)P [138]. In the absence of IpgD or in Rab11-depleted cells, rupture of the vacuole was delayed. Additionally, using ion beam scanning electron microscopy (FIB/SEM), Rab5 and Rab11-positive macropinosomes were observed to accumulate at the *Shigella*-containing vacuole before rupture [139]. It is thought that possible fusion and fission events occur between the macropinosomes and the vacuole, promoting vacuolar rupture. Furthermore, it is believed that the recruitment of the endocytic-recycling compartments to the vacuole is dependent on the phosphoinositide composition of the vacuole that is remodeled by IpgD. Altogether, these recent findings reveal a critical role of endocytic and recycling compartments for *Shigella* vacuolar escape as well as the composition of phosphoinositides (Figure 1.7).

1.2.5 Regulation of Autophagy

Autophagy is a conserved cellular pathway in eukaryotic cells that delivers cytoplasmic proteins and organelles to the lysosome for degradation. During bacterial

uptake, carbohydrates that are exposed on the outside of cells face inward on vacuole membranes. These carbohydrates are signals for recruitment of autophagic machinery. Bacterial intracellular division within a vacuole ultimately causes damage to vacuole membrane and carbohydrates on the inner membrane of the vacuole are now exposed to the cytoplasm. Galectin-8 recognizes these carbohydrates and recruits autophagy adaptors such as NDP52 to the damaged membrane. Autophagy protein LC3 binds these adaptors and recruits the damaged vacuole to the autophagosome, where it ultimately fuses with the lysosome. Many pathogens inhibit recognition of disrupted vacuoles by the autophagy system. *Legionella pneumophila* interferes with the autophagy process of the host by the Icm/Dot translocated substrate RavZ, which is a cysteine protease that irreversibly cleaves ubiquitin-like protein Atg8 on membranes of nascent autophagosomes [141]. *L. pneumophila* spingosine-1 phosphate lyase (LpSpl) also inhibits autophagy by targeting host sphingolipid metabolism, which regulates the progression of autophagy [142]. *S. flexneri* secreted substrate IcsB also helps evade autophagy by recruiting host Toca-1, which prevents recruitment of LC3 to the ruptured vacuole [143-145].

In some cases, autophagy has shown to enhance the membrane integrity of the *Salmonella*-containing vacuole and the *Mycobacterium*-containing vacuole. It was demonstrated that autophagy proteins might repair SCV membrane that is damaged by the SPI-1 secretion system early on in infection. Investigators found that SCV dye retention was reduced in autophagic-deficient cells compared to WT cells [146]. Similarly, autophagy machinery was shown to repair the *Mycobacterium*-containing vacuole damage caused by the ESX-1 secretion system. Specifically, Atg8 was found localized around the damaged *Mycobacterium*-containing vacuole [147].

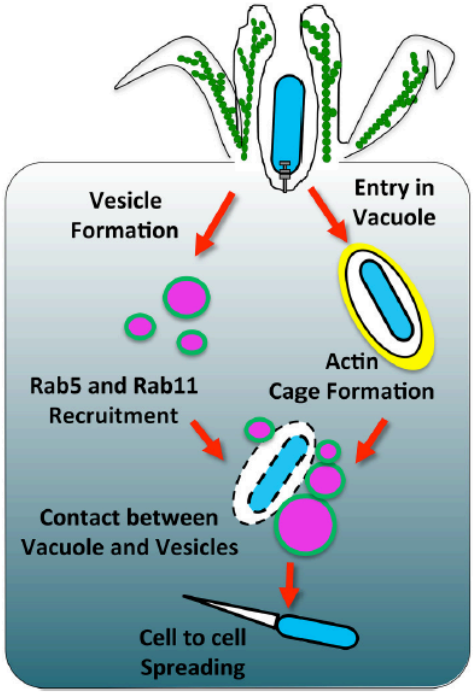

Figure 1. 7 The involvement of Rab5 and Rab11 during *Shigella* vacuolar rupture

Shigella induces its own uptake into a vacuole compartment, which is surround by an actin cage. At the same time, macropinosomes around the invasion site are modulated by IpgD to deplete $PI(4,5)P_2$ and form PI(5)P. This change in lipid content recruits Rab5-positive and Rab11-positive macropinosomes to the *Shigella*-containing vacuole. Macropinosomes around the *Shigella*-containing vacuole make contact with the bacterial compartment, resulting in vacuolar rupture. Reprinted with permission from Mellouk, N. and J. Enninga, *Cytosolic Access of Intracellular Bacterial Pathogens: The Shigella Paradigm.* Front Cell Infect Microbiol, 2016. 6: p. 35.

1.2.6 Regulation of Retromer & Sorting Nexins

The retromer is a multi-subunit protein complex that mediates retrograde trafficking of cargo from endosomes to the trans Golgi network [148]. Cargo typically trafficked by the retromer are lysosome-related, such as MPRs and sortilin [149]. Regulation of retromer-dependent trafficking has emerged as a common strategy amongst intracellular pathogens to prevent vacuolar membrane damage and bacterial degradation by lysosomal components. *Chlamydia* substrate IncE disrupts retromer trafficking by

directly binding to PX domains of retromer component SNX5/6 [150]. By binding SNX5, IncE inhibits the interaction between CI-MPR and SNX5, thus counteracting CI-MPR-mediated host restriction of *Chlamydia* [151]. *Legionella* translocated substrate RidL also inhibits retromer trafficking by binding to retromer subunit Vps29 [77]. RidL binds to a specific site of Vps29 that is also the competitive binding site TBC1d5, which regulates the interaction of the VPS complex with the targeted membrane [152-154]. In *D. discoideum*, deletion of host phosphoinositide 5-phosphatase OCRL reduced the amount of another retromer subunit, Vps5, recruited to the LCV [155]. Therefore, OCRL-mediated retromer trafficking has also been implicated in restricting *L. pneumophila* intracellular growth.

In contrast to other pathogens, the *Salmonella*-containing vacuole and the *Coxiella*-containing vacuole, interaction with the retromer was shown to maintain vacuole integrity. From yeast genetic interaction profiling, investigators found that *Salmonella* substrate SseC physically interacts with components of retromer [156]. Depletion of the retromer complex was found to disrupt the integrity of the SCV. Additionally, the *Salmonella* phosphoinositide phosphatase substrate, SopB, recruits SNX3, a retromer-associated protein, to the SCV. This recruitment induces formation of SNX3-containing tubules and promotes SCV maturation [157]. Similarly, retromer components have been implicated in regulating the formation of *Coxiella*-containing vacuole (CCV). *Coxiella burnetti* is the causative agent of zoonosis Q fever. RNAi treatment against retromer cargo-adapter genes VPS26, VPS29, and VPS35 or treatment against retromer-associated STX17 was shown to abrogate *C. burnetti* intracellular

replication [158]. Recently, it was also shown that actin patches form around the CCV membrane require the retromer, WASH, and Arp2/3 for biogenesis [159].

Over the years, various studies have elucidated the mechanisms by which bacterial pathogens maintain vacuole integrity during intracellular replication. From these studies, investigators have been able to identify membrane trafficking pathways that pathogens manipulate to survive within the host cell. Mammalian membrane trafficking is a broad field and is continuously growing. The mammalian cell cytoskeleton will be summarized next, as it is the basis for all membrane trafficking events. Additionally, membrane trafficking pertinent to this dissertation will be reviewed.

1.3 Host Membrane Trafficking

The cytoskeleton plays crucial roles in the cell; it provides the frame that determines cell shape, organizes cellular contents, and harnesses energy to generate mechanical force for cargo transport [160]. The cytoskeleton is not a static structure. In fact, a number of cellular processes require dynamic rearrangements of cytoskeletal networks [161]. For example, cell division, chromosome segregation and cell cleavage require force-generating activities of the microtubule and actin cytoskeletons [160]. Cytoskeletal filaments can be divided into three main categories: actin, microtubules, and intermediate filaments. For the purpose of this dissertation, actin and microtubules will be reviewed below.

1.3.1 Actin Cytoskeleton

Actin filaments (F-actin) are polymeric structures assembled through the head-to-tail assembly of actin monomers (globular or G-actin) [162]. Actin is an inherently polar

filament with a barbed “plus” end and a pointed “minus” end [160]. The plus end is the preferred site of monomer addition and the minus end is the site of monomer disassembly. A single actin filament is made of two protofilaments wound around each other [162]. These filaments can assemble into more complex arrays [163]. Actin organization is regulated by nucleation factors that promote the assembly of branched or linear actin arrays [164]. Actin can polymerize itself by the monomeric G-actin hydrolyzing ATP, and at steady state, the plus end growth is matched to minus end disassembly (phenomenon termed “treadmilling”) [165]. Although actin filaments can generate force on their own, actin can also work together with molecular motors to produce forces that alter cell shape [166]. Motor protein superfamily myosin carries out a number of diverse, actin-based processes in mammalian cells, including endocytosis, muscle contraction, cell migration, and cytokinesis [160]. Myosin generates force on F-actin networks by hydrolyzing ATP [167]. Formins can also be involved in the polymerization of actin by removing a capping protein from the plus end of the filament and preventing re-capping, thus allowing continued growth of filaments and cross-linked bundles. Many formins are the effectors of Rho GTPases, a subfamily of small GTPases discussed in a later section [168].

1.3.2 Microtubule Cytoskeleton

Microtubules (MTs) are cylindrical tubes that are assembled from alpha- and beta-tubulins [160]. Like actin, MTs are polar polymers with a fast growing plus end and a slow growing minus end [162]. MTs switch between states of growth and shrinkage, a phenomenon known as “dynamic instability” [169] [170]. Compared to actin, MTs are sturdier and can withstand greater force due in part that a MT is built from thirteen

protofilments held together through lateral non-covalent bonds [162] [171]. Cellular organization of MTs is controlled by MT-organizing centers (MTOCs), such as the centrosome, which anchors MT minus ends [172].

Proteins that associate with MTs can alter either the growth or disassembly at the plus end of the MT [160]. MT-associated proteins can be divided into two major classes: non-enzymatic proteins (MAPs) and ATP-hydrolyzing molecular motor proteins [173]. MAPs organize the MT cytoskeleton by cross-linking MT bundles and mediating interactions with other cellular proteins [174]. MT-associated motor proteins include kinesin and dynein. Despite sharing the same microtubule track, dynein and kinesin are very different motor proteins.

The kinesin superfamily is larger than the dynein superfamily and consists of forty-five genes identified in humans [175] [176]. Most kinesins transport cargo towards the plus end of the microtubule. There are six kinesin motor protein subfamilies (KIFs) that traffic cargo in the anterograde direction away from the nucleus: kinesin-1, kinesin-2, kinesin-3, kinesin-4, kinesin-11, and kinesin-13 [175]. Kinesins consists of two heavy chains and light chains. Each heavy chain contains a head region and a stalk region, and each light chain consist of a tail region [177]. The two heavy chains and light chains together form a homodimer [178]. The head region binds to the plus end of the microtubule and the tail region interacts either directly with the cargo or with adaptor proteins that link the motor to the cargo. Cargo movement in the anterograde direction is propelled by ATP hydrolysis of kinesin motor heads. Kinesin takes 16 nm forwards steps in a “hand-over-hand” manner, where intramolecular strain prevents simultaneous detachment of the two heads [179] [180] [181].

Dynein is involved in minus-end directed cargo transport along microtubules (retrograde transport). The dynein superfamily consists of fifteen dynein motor genes in the human genome [182]. In contrast to kinesin, dynein often takes larger, irregular steps (32 nm) and can even take backwards steps [183]. Dynein is a larger, more complex motor than kinesin. While kinesin contains two heavy and light chains, dynein consists of two heavy chains, two intermediate chains, two intermediate light chains, and a few pairs of light chains [184]. The heavy chains bear ATPase force-generating and microtubule binding domains [185] [186]. Dynein associates with the cargo through the interactions of its intermediate and light chains as well as by the adaptor dynactin. Dynactin is a large complex of 11 protein subunits [187]. The largest and primary functional subunit of dynactin is the *DCTN1* gene product $p150^{Glued}$, which binds dynein intermediate chain, microtubules, and another dynactin subunit Arp1 [188] [189]. Arp1 is a rod that mediates dynactins's interaction with many membranous cargoes by binding directly to spectrin-family proteins that is found on the surface of certain vesicles and organelles [190]. Given its interactions with cargo, dynein, and microtubules, the dynactin complex is generally understood to improve processivity of the dynein motor by enhancing its attachment to microtubule tracks, thereby increasing the average run length of transport [191] [192].

1.3.3 Phosphoinositide signaling & OCRL

Phospholipid vesicles contain the cargo trafficked along the cytoskeleton network. Phosphoinositides are important for directing vesicle trafficking. Phosphoinositides are signaling molecules that are polyphosphorylated derivatives of phosphatidylinositol (PI),

a phospholipid that resides almost entirely on the cytosolic surface of cell membranes. Differential phosphorylation at the hydroxyl groups 3,4, and 5 of the inositol ring in PI generates seven distinct phosphoinositides contributing to their signaling diversity [193]. These seven are PI(3)P, PI(4)P, PI(5)P, PI (3,4)P_2, PI(3,5)P_2, PI(4,5)P_2, and PI(3,4,5,)P_3. Phosphoinositides constitute about 10% of the total phospholipids in the cell but they regulate major cellular processes such as protein trafficking, cytoskeletal rearrangements, cell growth, proliferation, and motility [194] [195] [196] [197] [198]. Aberrant phosphoinositide signaling has been implicated in numerous human disease including cancer, neurological disorders, and diabetes [199] [200] [201].

The major functional roles of phosphoinositides are to define organelle identity and recruit regulatory proteins to cellular compartments [202]. Each type of phosphoinositide has a distinct localization in the cell through which a specific function is carried out. PI(3)P is found on early endosomes and PI(3,5)P_2 regulates late endosomes-lysosome trafficking. PI(4)P is enriched at the Golgi, and PI(3,4)P_2 and PI(3,4,5)P_3 are enriched at the plasma membrane where they are involved in Akt signaling [203]. PI(4,5)P_2 is especially enriched at the plasma membrane and is involved in actin dynamics and in endocytosis. One protein that associates with PI(4,5)P_2 and is of interest to this body of work is the 5-phosphatase OCRL.

OCRL is a multi-domain protein with an N-terminal PH domain, a central 5' phosphatase domain, and C-terminal RhoGAP-like and ASH domains. The PH domain has a loop with a clathrin-binding motif that helps OCRL tether to endocytic clathrin coated pits [204]. The PH domain is connected to the 5'-phosphatase domain through an unstructured linker containing an FEDNF consensus motif, which binds directly to AP-2

[204]. OCRL preferentially hydrolyzes PI(4,5)P2 to PI(4)P *in vitro* and *in vivo* [205]. The RhoGAP-like domain mediates interactions with both Rac1 and Cdc42 small GTPases [206] [207]. This domain is not catalytically active and does not behave like a GAP. However, it tethers OCRL to sites of Cdc42 activity, which is associated with actin assembly. The ASH domain of OCRL is known to mediate interactions with the Rab family of small GTPases [208]. OCRL is known to interact with Rab5, Rab6, Rab8, Rab14, Rab31, Rab35 through the ASH domain [208] [209] [210]. This domain is important for the proper sub-cellular localization of OCRL. The interactions with Rab GTPases recruits OCRL to compartment where it hydrolyzes $PI(4,5)P_2$.

In mammalian cells, OCRL is broadly distributed but primarily localizes to endosomal and TGN compartments [211] [212] [213] [214]. OCRL has been implicated in modulating clathrin-dependent endocytosis. OCRL is recruited to clathrin-coated pits at late stages of endocytosis, immediately before the vesicle is pinched off from the plasma membrane [215]. Loss of OCRL results in the loss of un-coating clathrin coated pits, and this is responsible for phenotypic defects associated with the disease Lowe syndrome [213]. OCRL also interacts with Pacsin2, which is an F-BAR protein that sculpts membranes by tubulating lipids [216]. In addition to OCRL, $PI(4,5)P_2$ and other phosphoinositides associate with numerous types of proteins, such as adaptors, protein kinases, and small GTPases. The small GTPases typically contain specialized phosphoinositide-binding domains (i.e. PH, FYVE, PX, ENTH, FERM PHD, Tubby domains) [217] [218]. For the purpose of this dissertation, I will focus on describing small GTPases and their interactions with phosphoinositides and downstream effector proteins.

1.3.4 Rab GTPases

Small GTP-binding proteins are monomeric proteins with molecular masses 20-40 kDa [219]. The small GTPase superfamily Ras has been divided into five subfamilies: Ras, Rho/Rac/Cdc42, Ran, Arf/Sar, and Rab. Each of these small GTPases share structural homology but have different functions in the cell. The Ras subfamily was found to regulate cell proliferation, differentiation, morphology, and apoptosis [219]. The Rho/Rac/Cdc42 proteins regulate cytoskeletal reorganization in response to extracellular signals in mammalian cells [220]. The Ran subfamily regulates nuclear import and export through the nuclear pore complex [221]. The Arf/Sar subfamily was shown to regulate vesicle budding and formation [222]. Finally, the Rab subfamily regulates vesicle trafficking [219].

The Rab subfamily ('Ras genes from rat brain') regulates many diverse aspects of vesicle trafficking within both polarized and non-polarized cells [223]. Researchers have identified over sixty mammalian Rabs to date, each with a unique role in vesicle trafficking. Rabs are critical for regulation of vesicle budding and fusion during trafficking. Studies have revealed that Rabs have a high conservation from yeast through mammals and they can often be substituted for each other in *in vitro* experiments [224]. Rab family members have a carboxyl-terminal CC or CXC sequence that allows isoprenylation with its geranylgeranyl motif [225]. Isoprenylation of the Rab allows for membrane association and activation of Rabs [226]. Rab proteins cycle between an active (GTP-bound) and inactive (GDP-bound) state. The transition between these states utilizes guanine-nucleotide exchange factors (GEFs) to exchange GDP for GTP and activate the Rab, and GTPase-activating proteins (GAPs) to aid in hydrolysis of GTP to GDP and de-

activate the Rab [227]. The carboxy-terminal domain of the Rab confers specificity to that particular membrane compartment [228]. Therefore, Rab localization depends on C-terminal protein interactions [229].

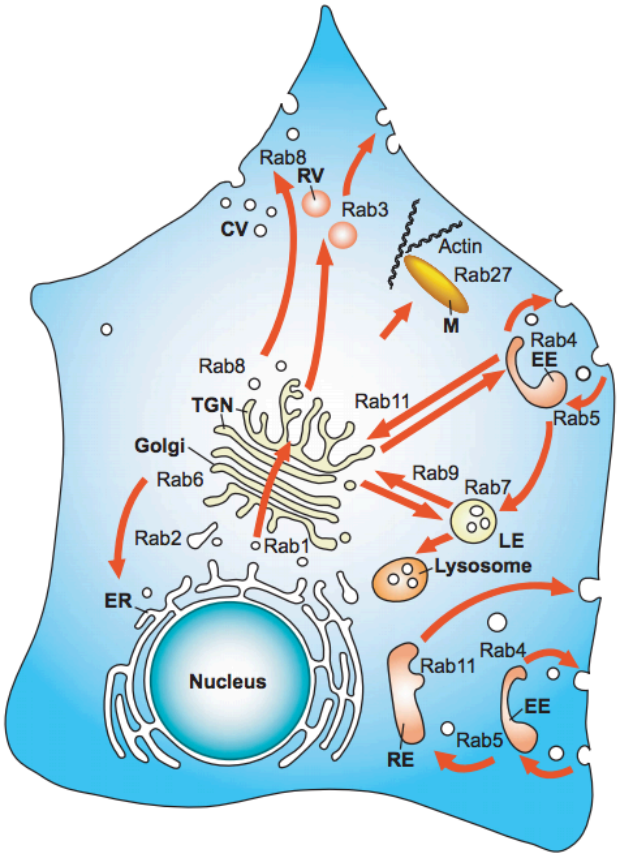

Figure 1. 8 Subcellular localization of selected Rab proteins
The endocytic and exocytic circuits are shown (arrows). Abbreviations: endoplasmic reticulum (ER), trans-Golgi network (TGN), constitutive secretory vesicles (CV), early endosomes (EE), late endosomes (LE), recycling endosomes (RE). Reprinted with permission from Stenmark, H., *Rab GTPases as coordinators of vesicle traffic.* Nat Rev Mol Cell Biol, 2009. 10(8): p. 513-25.

Each Rab protein defines a distinct vesicular membrane compartment (Figure 1.8) [230]. It has become standard practice in the trafficking field to use Rabs to define subcellular compartments [229]. For example, Rab1 specifically localizes to the ER and

the pre-Golgi intermediate compartment, as it is involved in the tethering of ER-derived vesicles to the Golgi complex [224]. Rab6 is localized to the Golgi and mediates intra-Golgi trafficking [231] [232]. Rab3 regulates exocytic vesicle trafficking [233]. Rab5 is localized to plasma membrane and sorting endosome, mediating endocytosis and homotypic early endosome fusion of clathrin-coated vesicles [234] [235]. Rab4 regulates the fast endocytic recycling and Rab11 is involved in slow endocytic recycling [224]. Rab7 plays a role in the maturation of late endosomes that fuse with lysosomes. Rab9 also reside on late endosomes and mediates trafficking from late endosomes to the TGN [233]. Rab8 mediates traffic of vesicles from TGN to plasma membrane [224]. Because Rab5, Rab11, and Rab8 are important to this body of work, I will focus on reviewing these Rab GTPases and their downstream effectors.

Rab5 is important for regulating early endosomal motility and fusion [236]. Over-expression of the active form of Rab5 induces formation of enlarged endosomes in cells [237]. Furthermore, knockdown of Rab5 results in loss of early and late endosomal compartments [238]. Rab5 has three subgroup isoforms (Rab5a, Rab5b, and Rab5c) [239]. The abundance of each Rab5 isoform is cell-type dependent [240] [241]. All Rab5 isoforms have been shown to co-localize with internalized transferrin and are involved in endocytic trafficking. Furthermore, all Rab5 isoforms cooperate together to transport endosomes [242].

The role of active Rab5 is to recruit effector proteins that bind specifically to Rab5-GTP. Active Rab5 is found at the plasma membrane as well as on early endosomes [243]. Rab5 regulates the production of PI(3)P on early endosomal membranes by its downstream effectors. PI(3)P is an important regulator of early endosome function and is

generated by two Rab5 effectors: hVps34 kinase and PI3Kbeta [244]. Rab5-activated hVps34 can directly generate PI(3)P on early endosomes while PI3Kbeta function is restricted to the plasma membrane [245] [244]. Upon stimulation by Rab5, PI3Kbeta converts PI(4,5)P_2 to PI(3)P [246]. Local increase of PI3P on membrane facilitates the recruitment of other Rab5 effectors containing a conserved FYVE finger domain that binds specifically to PI(3)P [247]. These PI(3)P-binding Rab5 effectors include EEA1 and Rabenosin-5. The most well characterized effector is EEA1 and this protein will be described in more detail, as it is relevant to this dissertation.

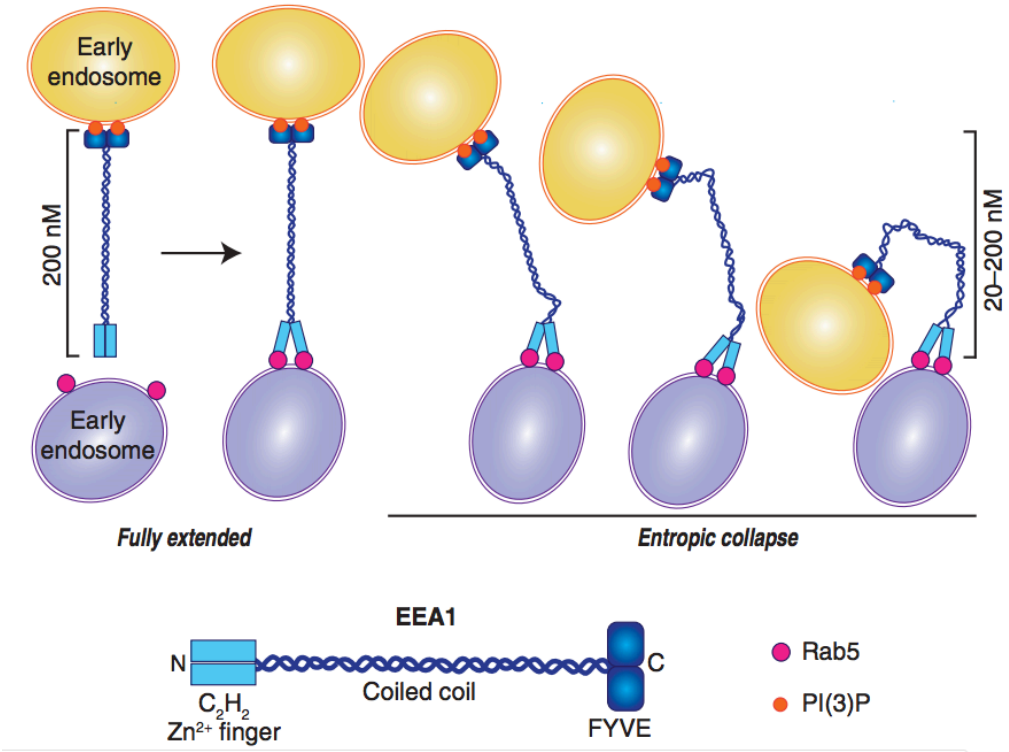

Figure 1. 9 Schematic illustrating entropic collapse cause by Rab5 binding to the N-terminus of EEA1 tethering factor
The N-terminus of EEA1 binds Rab5-positive early endosome, and the C-terminus of EEA1 binds PI(3)P on a different early endosome. Tethering of the two early endosomes allows the vesicles to come in proximal distance of each other. Reprinted with permission from Das, S. and D.G. Lambright, *Membrane Trafficking: An Endosome Tether Meets a Rab and Collapses.* Curr Biol, 2016. 26(20): p. R927-R929.

Early endosome antigen 1 (EEA1) is a tethering protein that predominately localizes to early endosomes. The C-terminus contains two zinc finger that contain eight cysteines called a FYVE domain [249]. The FYVE domain of EEA1 specifically binds to PI(3)P [250]. EEA1 also contains two binding sites for Rab5, one at the N-terminus and one at the C-terminus close to the FYVE domain [251] [252] [245]. The protein is a dimer and has a rod-like shape that allows interactions with Rab5 and PI(3)P from one end of the dimer and Rab5 interactions only at the other end (Figure 1.9) [251]. EEA1 is important for facilitating the tethering between early endosomes and allowing homotypic fusion to occur. The bipolar organization of EEA1 with one end binding both Rab5 and PI(3)P and the other end binding only Rab5 is crucial for fusion between early endosomes and endocytosed vesicles derived from the plasma membrane [251] [250] [252] [245]. EEA1 has been shown to bind SNARE protein syntaxin-6, which enables vesicle fusion [253].

Another Rab GTPase that is important to this body of work is Rab11. Because Rab11 is involved in the slow recycling of vesicles back to the plasma membrane, it is found on endosomes and at the TGN and post-Golgi vesicles [254]. The majority of studies characterizing Rab11 have been performed in tissue culture cell lines. In MDCK cells, Rab11 has been shown to be involved in apical recycling and targeting of vesicles to apical membrane [255]. In parietal epithelial cells, Rab11 is enriched in tubulovesicular structures contain H+/K+ ATPase, where it regulates the delivery of H+/K+ ATPase to the apical membrane [256]. In CHO cells, Rab11 regulates the recycling of TfR from the ERC to the plasma membrane [254] [257]. It has also been shown that Rab11 plays a role in exocytic membrane trafficking [258]. In particular,

Rab11 has been shown to be involved in post-Golgi trafficking of rhodopsin to the photosensitive apical membrane of Drosophila photoreceptors, as well as trafficking and basolateral targeting of E-cadherin in polarized cells [259] [260].

There are three isoforms of Rab11: Rab11a, Rab11b, and Rab25. Rab11a and Rab11b share 91% sequence identity to each other, while Rab25 only shares 62% sequence identity to Rab11a and Rab11b [261]. To date, Rab11a is the best-characterized member of the Rab11 family. However, there are a few studies investigating the difference between Rab11a and Rab11b isoforms. In rabbit parietal cells and other epithelial cells Rab11b localizes to a compartment distinct from Rab11a, suggesting a division of function between the two isoforms [262]. Rab11b, but not Rab11a, is also believed to function in the apical recycling of protein CFTR (cystic fibrosis transmembrane conductance regulator) in polarized epithelial cells [263]. Additionally, Rab11b has been shown to be specifically involved in the exocytosis of insulin granules in pancreatic beta-cells, in the recycling of epithelial sodium channel, in the regulation of degradation of Ca^{2+} channels, and the regulation of acidosis-induced trafficking of V-ATPases in salivary glands [264] [265] [266].

Downstream effectors of the Rab11 isoforms have been identified as Rab11 family interacting proteins (Rab11FIPs) [267]. Five Rab11FIPs have been identified, and although the degree of sequence homology between Rab11FIPs is low, they all share a highly-conserved C-terminus motif referred to as the Rab11 binding domain (RBD). Class I Rab11FIPs (Rab11FIP1, Rab11FIP2, Rab11FIP5) contain the C2 domain that binds to membrane phosphoinositide required for docking to membrane [268]. Class II Rab11Fips (Rab11FIP3 and Rab11FIP4) do not contain a C2 domain and instead contain

calcium binding EF hand motif that is important for intracellular trafficking [269] [270]. The C2 domain of class I Rab11FIPs plays a crucial role in subcellular localization for the Rab11FIPs. It is believed that the C2 domain of class I Rab11FIPs target the protein to docking sites at plasma membranes and endomembranes.

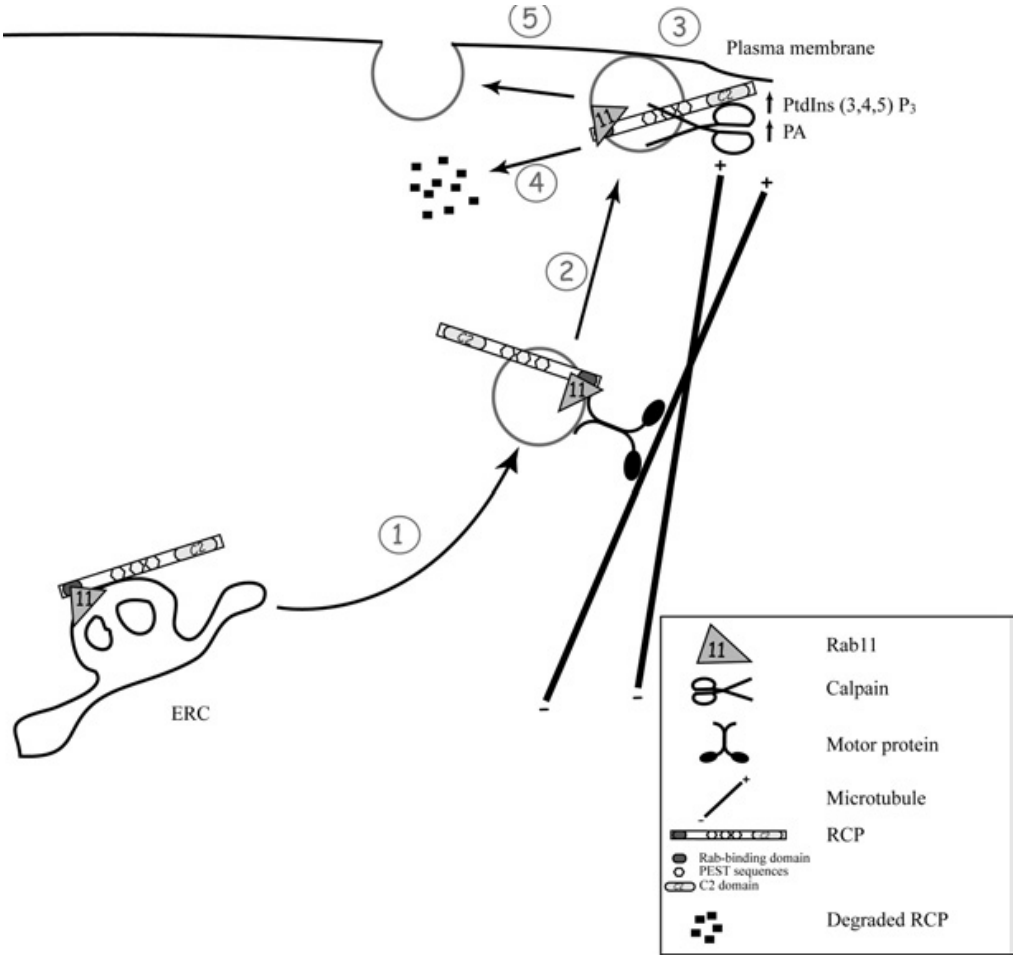

Figure 1. 10 Proposed model of Rab11FIP1 function
1) Recycling cargo is transported to the plasma membrane by Rab11 and Rab11FIP1 (RCP) in conjuction with motor protein after vesicle budding from the endocytic recycling compartment (ERC). 2 & 3) Phosphatidic acid (PA) and PtdIns(3,4,5)P3 (PI(3,4,5)P) at the plasma membrane provide signals for vesicle docking mediated by the C2 domain of Rab11FIP1 (RCP). 4) Rab11FIP1 (RCP) is then cleaved by calpains. 5) Fusion of the vesicle with the plasma membrane occurs. Reprinted with permission from Marie, N., A.J. Lindsay, and M.W. McCaffrey, *Rab coupling protein is selectively degraded by calpain in a Ca2+-dependent manner.* Biochem J, 2005. 389(Pt 1): p. 223-31.

One Rab11FIP that is of particular interest to this dissertation is Rab11FIP1. Rab11FIP1 has been shown to dock to the plasma membrane enriched in phosphatidic acid (PA) and PI(3,4,5)P_3 (Figure 1.10) [268]. Functionally, Rab11FIP1 has been involved in the sorting of TfR into the recycling pathway but not into the degradative pathway [272]. Recent work has also implicated Rab1FIP1 as crucial protein for cancer cell migration [273]. Rab11FIP1 was shown to be involved in the recycling of alpha5beta1 integrin and EGFR1 [274]. Interestingly, Rab11FIP1 can bind to Rab11 and Rab4 GTPases, implicating Rab11FIP1 in diverse recycling roles [275].

Lastly, Rab8 GTPase is of interest to this body of work. Very little is actually known about Rab8 function and its interacting proteins. Based on a couple of studies, Rab8 was shown to regulate transport of vesicles from the trans-Golgi network to the basolateral surface of polarized epithelial cells as well as to dendrites in nerve cells [276] [277] [278]. Only a few proteins have shown to interact with Rab8. These proteins include Rab8ip, Trip8b, Mss4, and AS160. Rab8ip is a kinase that has been implicated in mammalian stress responses [278]. Trip8b is a membrane receptor protein that interacts with Rab8b [279]. Mss4 is a small zinc binding protein that facilitates the dissociation of GDP from Rab8. However, Mss4 is not a true GEF for Rab8, since it does not stimulate binding of GTP [280]. AS160 has shown to have GAP activity for Rab8a [281].

There are two isoforms of Rab8 in mammals, Rab8a and Rab8b. These two Rab8 proteins are highly homologous and differ only in the C-terminal region. Rab8a has the highest level of expression in muscle lung and kidneys, whereas Rab8b is most abundant in brain, spleen, and testis [282]. Very little is known about the difference between the two Rab8 isoforms, although it is postulated that they function in both distinct and as well

as overlapping compartments in cilia and AtT20 cells. Interestingly Rab8 and Rab11 have shown to interact with the SNARE protein Vamp3, which facilitates membrane fusion [283] [284]. As Vamp3 is relevant to this dissertation, I will next discuss SNAREs in more detail.

1.3.5 SNAREs and membrane fusion

Membrane fusion is a fundamental process for vesicle trafficking in the cell. A key mediator of membrane vesicle fusion is the soluble NSF-attachment protein receptor (SNARE) [285] [286]. The C-terminal domain of SNAREs is attached to the membrane while the N-terminus points toward the cytosol. SNAREs are grouped according to their domain structure and sequence homology and three groups exist: members of the vesicle associated membrane protein (VAMP), syntaxins, or synaptosomal associated proteins (SNAPs) [287]. Furthermore, SNAREs are classified according to their localization: v-SNAREs for vesicle-associated proteins and t-SNAREs for target membrane-associated proteins. SNAREs have also been classified based on their structural features: R-SNAREs for those that have a conserved arginine residue and Q-SNAREs for those that have a conserved glutamine residue [288].

Membrane fusion begins with the docking of the donor membrane to the target membrane. When vesicles are trafficked to the vicinity of the target organelles, v-SNAREs on the vesicles and t-SNAREs on the target membrane come together to form a complex known as the trans-SNARE complex (Figure 1.11). This complex is an extremely stable four-helix bundle that builds lipid bilayers close together and pushes water molecules away from the fusion site, resulting in membrane fusion [290] [291]. After membrane fusion, the trans-SNARE complex becomes a cis-SNARE complex,

since the SNARE complex now resides in the same membrane [292]. The SNARE complex then dissociates and recycles back to its resident compartment. The recycling of SNAREs is mediated by N-ethylmaleimide-sensitive factor (NSF) and cofactor alpha-SNAP. Alpha-SNAP binds to the cis-SNARE complex and recruits NSF, which leads to ATP hydrolysis and the dissociation of the complex [293].

Like Rab proteins, individual SNAREs localize to distinct subcellular cellular compartments, suggesting that each has a selective role in intracellular trafficking [287]. The VAMP subfamily of SNAREs are v-SNAREs contain 7 members: Vamp1, Vamp2, Vamp3, Vamp4, Vamp5, Vamp7, and Vamp8 [294]. VAMPs are anchored to membranes by their C-terminal transmembrane tail and they are distributed in various cellular compartments [287]. Vamp1 and Vamp2 are primarily found in synaptic vesicles of neurons and secretory granules of endocrine and exocrine cells. Vamp4 is associated with the TGN and Vamp5 is primarily distributed on the cell surface of muscle myotubes [295] [296]. Vamp7 has been reported to act on the lysosome as well as the apical surface of epithelial cells. Vamp8 is detected primarily in early and late endosomes [297] [298]. Finally, Vamp3 is found primarily in sorting and recycling endosomes [294].

Vamp3 bears homology to Vamp2, however, unlike Vamp2, Vamp3 has a broad tissue distribution [299]. Because Vamp3 is present on sorting and recycling endosomes, it localizes with endocytosed transferrin receptors, glucose transporter GLUT4 in adipocytes, and alpha-granules in platelets [299] [300] [301]. VAMP3 has been implicated in recycling of transferrin receptors back to the plasma membrane, secretion of alpha-granules in platelets, recycling of T-cell receptors to the immunological synapses, and membrane trafficking during cell migration [302] [303]. Biochemical

studies reveal that VAMP3 binds t-SNAREs syntaxin1, syntaxin4, SNAP-23, and SNAP-25 to form the trans-SNARE complex during membrane fusion [304].

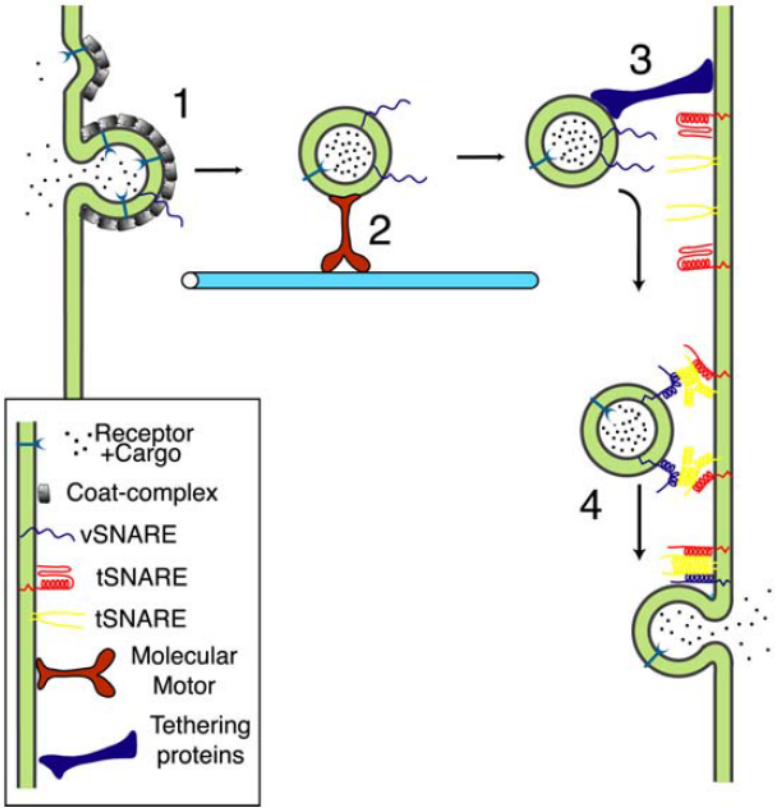

Figure 1. 11 Transport vesicle fusion model
1) Coat proteins mediate vesicle budding from donor compartment. 2) Actin and microtubule-based molecular motors are responsible for delivering vesicle to its final destination. 3 & 4) SNARE proteins, syntaxins and VAMPs, mediate membrane fusion and delivery of cargo to the acceptor compartment. VAMPs are present on transport vesicles (vSNAREs) and syntaxins are present on target membranes (tSNAREs). Reprinted with permission from Prekeris, R., *Rabs, Rips, FIPs, and Endocytic Membrane Traffic*. TheScientificWorldJOURNAL, 2003. 3.

1.4 Research aims

The aim of this dissertation work was to identify membrane trafficking proteins that are involved in the disruption of the *L. pneumophila* Δ*sdhA* vacuole. To this end, siRNA and shRNA screen strategies were used in RAW 264.7 cells and bone marrow-

derived macrophages (BMDMs), respectively, to identify mouse membrane trafficking proteins that cause defects in Δ*sdhA* intracellular growth and vacuole integrity. Rab GTPases and downstream effectors of endocytic and recycling vesicle trafficking pathways were identified, and the phenotypes of infected cells depleted of these factors were further validated (reviewed in Chapter 2). Ultimately, we focused our study on the localization of identified factors at the WT and Δ*sdhA* vacuole. The models developed through this work have significant implications regarding how *L. pneumophila* maintains vacuole integrity. Additionally, the tools to study membrane trafficking events in BMDMs can also be used to analyze a wide variety of interactions between *L. pneumophila* and its host.

Chapter 2: Components of the endocytic and recycling trafficking pathways exacerbate the integrity of the *Legionella*-containing vacuole[1]

This chapter contains written and experimental work of the first author, which has been reviewed by the second author and last author.

---

[1] Anand, IS., Choi, W., Isberg, RI. To be submitted to *Cellular Microbiology*.

2.1 Introduction

Legionella pneumophila is a fastidious Gram-negative bacterium that grows intracellularly in both fresh water amoebae and human alveolar macrophages [11]. The pathogen is able to infect humans after inhalation of aerosolized water particles contaminated with the bacterium [305]. Upon entry into the lungs, *L. pneumophila* is internalized by alveolar macrophages with its most severe manifestation being Legionnaires' disease pneumonia [306, 307]. In both amoebae and macrophages, the ability of *L. pneumophila* to replicate intracellularly is dependent on the Icm/Dot type IV secretion system (T4SS) [308]. This complex introduces more than 300 translocated substrates into the host cell cytosol, which promote establishment of the *Legionella*-containing vacuole (LCV) and exert a variety of regulatory controls on the host cell [43, 309].

Establishment and maintenance of LCV membrane integrity is essential for protection of *L. pneumophila* from innate immune cytosolic sensing [93, 310]. The inability of a bacterial mutant to properly form the LCV or maintain its integrity results in pathogen clearance and consequently a severe intracellular growth defect [97, 311]. The identification of the Icm/Dot-translocated substrate SdhA has greatly contributed to our understanding of the consequences of failure to properly maintain pathogen replication vacuoles [55]. In the absence of SdhA, the LCV becomes disrupted and *L. pneumophila* is detected in the cytoplasm of the infected macrophage [55, 97]. Bacteria exposed to the cytoplasm are susceptible to recruitment of the interferon-regulated GBP family of anti-microbial proteins, resulting in leakage of LPS and activation of caspase-11 [93, 97] [99].

As a consequence, gasdermin D is activated and pyroptotic cell death ensues [98] [312] [313].

We previously demonstrated that that removal of phospholipase activity of bacterial substrate PlaA rescues Δ*sdhA* vacuole integrity, thus demonstrating that PlaA promotes vacuole disruption [97]. PlaA bears homology to the translocated phospholipase SseJ from *Salmonella* Typhimuirium, which is also involved in vacuole disruption in the absence of another *Salmonella* translocated substrate, SifA [115] [100, 101, 115]. During infection, SifA binds host factor SKIP and sequesters Rab9 to prevent delivery of M6PR cargo to the vacuole [113]. The resemblance between SdhA/PlaA and SifA/SseJ suggests SdhA may also regulate host membrane trafficking events in order to maintain LCV integrity.

In addition to *Salmonella*, other pathogens have been reported to interface with host membrane trafficking pathway as a strategy for maintaining vacuolar integrity. The *Chlamydia* protein IncD was shown to recruit the host CERT-VAP complex to the inclusion and enable acquisition of host lipids that are essential for inclusion membrane stability [131]. Recently, the *Shigella* vacuole has been reported to interact with endocytic Rab5-positive vesicles and recycling Rab11-positive vesicles to facilitate vacuole membrane rupture, indicating that vacuole integrity can be disrupted by interfacing with appropriate cellular compartments [138, 139]. In this study, we determine if the disruption of LCV integrity that results from loss of *L. pneumophila* SdhA function can be attributed to a subset of host membrane trafficking pathways. Using high throughput screening strategies, we identified specific endocytic and recycling Rab GTPase isoforms and their downstream effectors and investigate their roles

in vacuole disruption after challenge with the Δ*sdhA* strain. The similarity between *Legionella* and *Shigella* interactions with a common endocytic-recycling pathway provides an example of how a host process can either promote or interfere with pathogen replication, depending on the strategy used for intracellular growth.

2.2 Materials & Methods

2.2.1 Bacterial culture and media

All *Legionella pneumophila* strains used in this study are derived from the Philadelphia 1 isolate and are described in Table 2.1 [32]. Luminescent *L. pneumophila* was constructed using P_{ahpC}::*luxCDABE* as previously described [314, 315]. *L. pneumophila* strains were grown on plates containing charcoal and yeast extract buffered with ACES [N-(2-acetamido)-2-aminoethanesulfonic; Sigma] adjusted to pH 6.9 and supplemented with 0.4 mg/mL of $_L$-cysteine and 0.135 mg/mL of ferric nitrate (CYE), as well as 0.1 mg/mL thymidine and/or kanamycin (Sigma) when necessary. Liquid cultures of *L. pneumophila* were prepared in the same medium, but without charcoal and agar (AYE) [316]. Overnight *L. pneumophila* cultures were prepared by inoculating AYE broth with a bacterial patch and serially diluting cultures 1 to 2. Liquid cultures were incubated overnight at 37°C with shaking. For infections, overnight cultures were used, and all strains were grown to post-exponential phase (A_{600} of 3.5 to 4.0) [317]. The approximate multiplicities of infection were determined by assuming that an A_{600} = 1.0 is equivalent to 10^9 bacteria/mL.

2.2.2 Mammalian cell culture

RAW 264.7 cells (ATCC TIB-71) were grown in Dulbecco modified Eagle medium (DMEM, Gibco) supplemented with heat-inactivated fetal bovine serum (FBS).

Bone marrow-derived macrophages (BMDMs) were isolated from femurs and tibias of female A/J mice as previously described and frozen in heat-inactivated FBS with 10% dimethyl sulfoxide (DMSO) [318]. BMDMs were plated in RPMI 1640 (Gibco) supplemented with 10% heat-inactivated FBS (Invitrogen) and 1mM $_{L}$-glutamine (Gibco) one day prior to challenge with *L. pneumophila*. Animal protocols were approved by the Institutional Animal Care and Use Committee of Tufts University.

2.2.3 Primary siRNA library screen

The Mouse siGENOME siRNA Library of 112 siRNA directed against membrane trafficking genes (Dharmacon, Lafayette, CO; GU-015500) was tested in a high-throughput screen. The library consists of a pool of four different oligos for each target gene. RAW 264.7 cells were seeded overnight in RPMI medium (Thermo Fisher Scientific) containing 10% (vol/vol) FBS at a density of 1.25 x 10^4 cells per well in a 96 well white-bottom plate (Thermo Fisher Scientific). The next day, the cells were transfected with 50nM siRNA using Lipofectamine RNAiMAX Reagent (Thermo Fisher Scientific). The screen was designed with three negative control wells, transfected with non-targeting siRNA, and one well for each experimental siRNA target. After 24 hours of transfection, the medium was replaced to reduce cell cytotoxicity. After 48 hours of transfection, cells were challenged at an MOI = 0.5 with *L. pneumophila* Δ*sdhA* Lux $^{+}$ grown to post-exponential phase. At 1 hr post-challenge, extracellular bacteria were removed by washing in PBS and cells were incubated at 37°C, 5% CO_2 in Phenol Red-free RPMI media containing 10% FBS. Relative light units (RLU) of each well were measured every 12 hours in a Tecan M200 Pro plate reader. A total of 8 plates were

screened to collect at least three replicate measurements for each gene target. RLU from each experimental well was normalized to the average RLU of the negative control wells on the same plate. Using normalized data, Z_{MAD} scores (equivalent the number of median absolute deviations (MAD) from the median) were calculated for each experimental siRNA target and were used for selection of hits [319]. The classification of the scale of the siRNA effects based on the ZMAD score was defined as follow: | ZMAD | ≥ 2 for extremely strong RLU, 2 > | ZMAD | ≥ 1.5 for very strong RLU, 1.5 > | ZMAD | ≥ 1 for strong RLU, 1 > | ZMAD | ≥ 0.5 for moderately strong RLU, 0.5 > | ZMAD | ≥ 0 for no effect, 0 > | ZMAD | ≥ -0.5 for moderately weak RLU, -0.5 > | ZMAD | ≥ -1 for weak RLU, -1 > | ZMAD | ≥ -1.5 for very weak RLU, -1.5 > | ZMAD | for extremely weak RLU. Only siRNAs that had a ZMAD of ≥ 1.5 were considered of interest for further analysis in the secondary shRNA library screen, as described next.

2.2.4 Secondary shRNA library screen

Selected hits from the primary siRNA library screen and additional related targets were tested in a screen using shRNA constructions introduced into BMDMs. The shRNA were obtained from the Broad Institute Genetic Pertubation Platform (https://www.broadinstitute.org/genetic-perturbation-platform). To this end, lentiviral vector library plates were constructed with three negative control shRNAs against LacZ and 92 experimental lentiviral shRNAs against 23 target genes (four shRNAs per target). All shRNAs were contained on third-generation transfer plasmid pLKO.1, which confers puromycin resistance. On day 0, progenitor cells derived from the bone marrow of A/J mice (Materials and Methods) were seeded at a density of 5×10^4 cells per well in a 96

well clear-bottom black plate (Corning) in RPMI medium containing 30% (vol/vol) L-cell supernatant, 20% FBS, and 1% penicillin-streptomycin (BMM media, Gibco). On day 4, polybrene (Sigma) and $2x10^5$ infectious units of lentivirus were added to the wells, and transduction was initiated by centrifugation at 2200 rpm at 37°C for 20 minutes. On day 5, conditioned medium was replaced to reduce cell cytotoxicity. On day 6, transductants were selected in conditioned medium containing 3μg/mL puromycin. On day 8, the supernatants were removed and replaced with puromycin-free conditioned medium to recover transduced clones. On day 10, the cultured medium was changed to RPMI containing 10% FBS. Terminally differentiated macrophage transductants were challenged with *L. pneumophila* Δ*sdhA* at MOI = 1 for 1 hr, followed by removal of extracellular bacteria by washing in PBS. After 6 hours, infected macrophages were fixed with 4% (vol/vol) paraformaldehyde in PBS and disrupted vacuoles were stained as described in "Vacuole Integrity & Intracellular Replication Assay." The screen was performed on triplicate shRNA library and plates were stored in PBS at 4°C until analysis.

After fixation and staining, images of each well were captured using ImageXpress (Molecular Devices) [320]. All images were captured using 20X Plan Apo lens. Images were captured with the FITC (ex. 490, em. 525) and Texas Red (ex. 590, em. 617) filter sets. Sixteen images were captured at the center of each well. A total of three plates were screened to acquire three replicates for each knockdown condition. The "Cell Scoring" function from the MetaXpress software was used to calculate the number of *Legionella*-containing vacuoles (LCV) in each channel per image. LCVs were defined as having a pixel intensity of at least 50 gray levels above background, with a minimum width of 6

pixels and a maximum width of 12 pixels. LCVs were scored as disrupted if the pixel intensity in the FITC channel overlapped with the pixel intensity in the Texas Red channel. The number of disrupted LCVs in each well were recorded and analyzed in Microsoft Excel. Raw data from each experimental well was normalized to the average of the negative control wells. Statistical analyses were performed on normalized data by unpaired t test (*$P < 0.05$).

2.2.5 Nucleofection

Frozen differentiated BMDMs were recovered and plated at a density of $5x10^6$ cells in a 10cm dish (Falcon) in RPMI medium containing 10% (vol/vol) FBS and 10% (vol/vol) L-cell conditioned supernatant. The next day, cells were lifted in cold PBS (Gibco) and resuspended in RPMI medium containing FBS [26]. Resuspended cells were aliquoted into 1.5 ml microfuge tubes at $1x10^6$ cells per tube and pelleted by centrifugations for 10 minutes at 200xg. Cell pellets were resuspended in nucleofector buffer (Amaxa Mouse Macrophage Nucleofector Kit (Lonza)) and 2ug of siRNA was added to each tube (Dharmacon). Cells were transferred to a cuvette and nucleofected in the Nucleofector 2b Device (Lonza) under Y-001 program settings. Nucleofected macrophages were immediately recovered in RPMI medium containing 10% FBS and 10% L-cell supernatant. Cells were plated in 8-well chamber slides (Millipore Sigma) for microscopy assays or in 12-well plates (Corning) to prepare extracts for immunoblotting.

2.2.6 Immunoblotting

Efficiency of siRNA silencing in nucleofected cells was determined by immunoblot. Nucleofected macrophages were plated in 12-well plates in RPMI medium

containing 10% (vol/vol) FBS and 10% (vol/vol) L-cell supernatant. After 48 hours, cells were lysed using 4X SDS Laemmli sample buffer (Bio-Rad) and boiled for 5 minutes. After fractionation on SDS-polyacrylamide gels (Bio-Rad), proteins were transferred to nitrocellulose membranes, blocked in 4% (vol/vol) milk in TBST [0.05 M Tris buffered saline (NaCl = 0.138 M, KCl = 0.0027 M); (Tween-20 = 0.05%, pH 8.0) (Sigma-Aldrich) and probed with antibodies to Rab5A (Cell Signaling, 1:500), Rab5B (Santa Cruz Biotechnology, 1:500), Rab5C (Novus Biologicals, 1:500), Rab11A (Cell Signaling, 1:500), Rab11B (Cell Signaling, 1:500), Rab8A (Cell Signaling Technologies, 1:500), Rab8B (Proteintech, 1:500), EEA1 (BD Biosciences, 1:500), Rab11FIP1 (Cell Signaling, 1:500), VAMP3 (Synaptic Systems, 1:500) or GAPDH (Santa Cruz Biotechnology, 1:1000) in 4% milk/TBST. Immunoblotting with primary antibodies was carried overnight at 4°C. After washing in TBST, secondary antibodies Dylight anti-rabbit IgG 680, Dylight anti-mouse IgG 680, Dylight anti-rabbit IgG 800, and Dylight anti-mouse IgG 800 (Cell Signaling 1:20,000) were incubated in 4% milk/TBST for 45 minutes at room temperature. Capture and analysis was performed using the Odyssey Scanner and the Image Studio software (LI-COR Biosciences).

2.2.7 Vacuole Integrity & Intracellular Replication Assays

For fluorescence microscopy experiments, nucleofected BMDMs were seeded in 8-well chamber slides (Millipore Sigma) at a density of 5 x10^4 cells per well in RPMI medium containing 10% (vol/vol) FBS and 10% (vol/vol) L-cell supernatant. After 48 hours, the medium was changed to RPMI containing 10% FBS only. Nucleofected macrophages were challenged with post-exponential phase *L. pneumophila* strains at a

MOI = 1. At 1h after challenge, extracellular bacteria were removed by washing in PBS, and at the indicated times, macrophages were fixed with 4% (vol/vol) paraformaldehyde in PBS and blocked in PBS containing 4% BSA overnight at 4°C.

For detection of *L. pneumophila* disrupted vacuoles, nucleofected BMDMs were incubated with rabbit anti-*L. pneumophila* antisera (1:20,000) for 1h at 37°C in PBS containing 4% BSA followed by anti-rabbit IgG Alex Fluor 488 (Invitrogen, 1:500) for 1h at 37°C in PBS containing 4% BSA. After washing three times in room temperature PBS, cells were permeabilized with ice-cold methanol for 20 seconds, blocked in PBS containing 4% BSA for 25 minutes at room temperature, and incubated again with *L. pneumophila* antisera (1:20,000) in PBS containing 4% BSA for 1h at 37°C, followed by anti-rabbit IgG Alex Fluor 594 (Invitrogen, 1:500) for 1h at 37°C in PBS containing 4% BSA. Disrupted vacuoles were identified by the simultaneous staining of bacteria with both Alexa Fluor 488 (bacteria detected prior to permeabilization) and Alexa Fluor 594 (bacteria detected after permeabilization) antibodies by fluorescence microscopy. BMDMs were permeabilized with ice-cold methanol for 20 seconds, blocked in 4% BSA for 25 minutes at room temperature, and then incubated with anti-*L. pneumophila* sera (1:20,000) for 1h at 37°C, followed by anti-rabbit IgG Alex Fluor 488 (1:500) for 1h at 37°C. The number of bacteria contained in each vacuole was quantified by fluorescence microscopy [97].

2.2.8 Localization of EEA1 or Rab11FIP1 at the *Legionella* vacuole

For EEA1 or Rab11FIP1 localization studies, BMDMs were challenged with *L. pneumophila* strains in 8-well chamber slides. After 4 hours of incubation, cells were

fixed with 4% paraformaldehyde in PBS and blocked in PBS containing 4% BSA for 1 hour at room temperature. For EEA1 staining, cells were incubated overnight at 4°C with anti-mouse EEA1 antibody (BD Biosciences, 1:50) in PBS containing 4% BSA. The next day, cells were incubated with anti-mouse IgG Alexa Fluor 488 (Invitrogen, 1:500) for 1h at 37°C in PBS containing 4% BSA. Cells were incubated with rabbit anti-*L. pneumophila* (1:20,000) for 1h at 37°C in PBS containing 4% BSA, followed by anti-rabbit IgG Dylight 405 (Invitrogen, 1:200) for 1h at 37°C in PBS containing 4% BSA. Cells were permeabilized with ice-cold methanol for 20 seconds, blocked in PBS containing 4% BSA for 25 minutes at room temperature, and incubated with rat anti-SidC antibody (1:200) for 1h at 37°C in PBS containing 4% BSA, followed by anti-rat IgG Alex Fluor 594 antibody (Invitrogen, 1:200) in PBS containing 4% BSA. Cells were incubated with *L. pneumophila* antisera (1:20,000) for 1h at 37°C in PBS containing 4% BSA, followed by anti-rabbit IgG Alex Fluor 647 (Invitrogen, 1:500) for 1h at 37°C in PBS containing 4% BSA. For Rab11FIP1 staining, cells were incubated overnight at 4°C with anti-rabbit Rab11FIP1 antibody (Cell Signaling Technologies) and staining procedures followed as described above. Chamber slides were mounted with ProLong Gold (Life Technologies) and imaged with a 63X objective lens, using a Zeiss Axio Observer.Z1 (Zeiss) fluorescent microscope, an Apotome.2 (Zeiss), and an ORCA-R^2 digital CCD camera (Hamamatsu). Images were acquired under Cy5 (ex. 650, em. 665), FITC (ex. 490 , em. 525), Texas Red (ex. 590 , em. 617), and DAPI (ex. 346, em. 442) filter sets, and 2.5μm z stacks were acquired per image (10 steps were imaged at 0.25μm step size). Three replicates for each strain were imaged.

Volocity image analysis software (Quorum Technologies) was used to measure colocalization between EEA1 or Rab11FIP1 and the *Legionella*-containing vacuole (LCV). Objects were gated based on signal intensity as the following: bacteria were thresholded on Cy5 intensity, SidC was thresholded on Texas Red intensity, EEA1 or Rab11FIP1 was thresholded on FITC intensity. The bacteria and SidC gates were combined to define the LCV gate. The numbers of disrupted vacuoles were manually quantified in the DAPI channel. The number of EEA1 or Rab11FIP1 objects overlapping in the LCV gate were quantified and correlated with the number of disrupted vacuoles for each image. Each experiment contained three replicates for each *Legionella* strain, and quantification of ~30 vacuoles for each *Legionella* strain. Statistical analyses were performed on each replicate by unpaired t test (*P < 0.05, **P < 0.01, ***P<0.001).

Strain/Plasmid	**Genotype**	**Description**	**Reference**
WT	Lp02, Philadelphia-1, rpsL hsdR thyA-	wild-type strain	[32]
ΔsdhA	Lp02 ΔsdhA	SdhA deletion	[55]
ΔsdhA lux+	Lp02 ΔsdhA kan^R P_{ahpC}::lux	SdhA deletion, Lux+	This study
pSdhA	pJB908*sdhA*	Expression vector for SdhA	[55]

Table 2. 1 Table Strains used in this study

2.3 Results

2.3.1 Identification of host proteins that contribute to disruption of *L. pneumophila* Δ*sdhA* intracellular growth

To identify host membrane trafficking pathways that interfere with growth of the *L. pneumophila* Δ*sdhA* mutant, we carried out a screen using an siRNA library targeting genes known to participate in membrane trafficking and remodeling. RAW 264.7 macrophages are known to be partially defective in the activation of pyroptosis and clearance of bacteria, allowing growth of the mutant to be followed without the confounding effects of premature host cell death downstream of cytoplasmic exposure of the bacteria [321]. This allowed subtle differences in intracellular growth to be detected. RAW 264.7 macrophages were seeded in 96-well plates and transfected with an arrayed siRNA library against 112 mouse genes involved in membrane trafficking (Supplemental Tables, Table 2.3). Each well contained 4-pooled siRNAs per gene target and each plate contained 6 non-targeting siRNA control wells. After 48 hours of transfection, cells were challenged with a Δ*sdhA* Lux^+ strain and luminescence was measured as a proxy for intracellular growth, performing the assay in at least triplicate samples for each gene target (Figure 2.1A). Candidates were identified by comparing the luminescence from each siRNA-treated well to the average luminescence of the non-targeting siRNA controls. The median absolute deviation score (ZMAD) was then determined for each gene target. We focused our analysis on early time points 12hpi and 24hpi, since siRNA knockdown effects diminish after 72 hours of transfection to identify candidates that stimulate Δ*sdhA* intracellular growth after depletion.

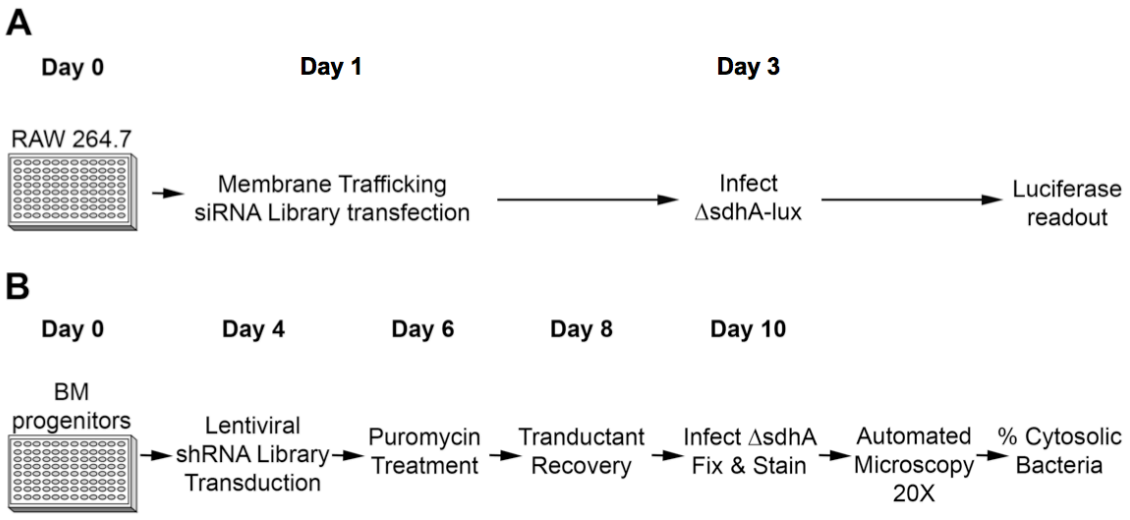

Figure 2. 1 Loss of function treatments that compensate for depressed vacuole integrity of intracellular *L. pneumophila* Δ*sdhA*.
(A) Identification of siRNA that enhance intracellular growth. RAW 264.7 macrophages were seeded in 96-well plates and transfected the following day with an siRNA library directed against transcripts encoding membrane trafficking proteins. After 2 days of treatment, transfected cells were challenged with *L. pneumophila* Δ*sdhA* Lux^{+} and luminescence was measured at 12 and 24 hours post infection (hpi). (B) Identification of shRNA that decrease vacuole permeability in primary macrophages. A/J bone-marrow derived progenitors were seeded in 96-well plates and incubated in differentiation medium for 4 days. Cells were transduced with shRNAs targeting genes identified in the siRNA screen (A). Transductants were selected by puromycin treatment for 2 days and recovered by further incubation in puromycin-free medium. Terminally differentiated BMDM transductants were challenged with Δ*sdhA* for 6h. Plates were fixed and stained for cytosol-detected *L.p.* and total *L.p.*. Automated Microscopy was performed with 20X objective and percent of cytosol-detected bacteria for each well was measured by image analysis.

A total of 20 genes were identified as hits in the siRNA screen based on increased intracellular growth relative to the nontargeting siRNA controls with a cutoff of ZMAD ≥ 1.5. Candidate genes spanned functional roles in endocytosis, endocytic recycling, and exocytosis (Figure 2.2A). Hits included arrestin subtypes (ARRB1 & ARRB2), clathrin heavy chain (CLTC), regulators of actin cytoskeleton (ROCK1, CDC42, DNM2, ARFIP2, WASF1, VAV2), E3 ubiquitin ligase (NEDD4L), phosphoinositide kinase (PI3K), components of vesicle fusion (VAMP1 & SYT1), specific Rab GTPase isoforms

(RAB3D, RAB4B, RAB5B, RAB5C, RAB8A, RAB11B), and a downstream Rab11 effector (RAB11FIP5). Interestingly, only five genes were identified as strong hits at both 12hpi and 24hpi (ARRB1, RAB3D, RAB4B, RAB5C, SYT1). The majority of the genes were identified as strong hits at only one time point, emphasizing the importance of membrane trafficking kinetics in controlling LCV dynamics. Hits identified at 12hpi may alter pathways that are toxic for growth of bacteria during early steps of vacuole biogenesis, while hits identified at later times could block pathways the cause decay to an already established vacuole.

2.3.2 Identification of shRNAs that partially rescue Δ*sdhA* vacuole integrity

The assay for increase bacterial yields allows identification of knockdown candidates that could improve intracellular growth of the Δ*sdhA* mutant in a number of ways. To directly test if improved growth were due to increased vacuole integrity, we selected hits from the siRNA screen and additional related targets for analysis in a secondary screen using a direct assay for vacuole integrity in bone marrow-derived macrophages (BMDM) from the mouse. The secondary screen took advantage of a fluorescence readout we previously described to detect disrupted Δ*sdhA* vacuoles in knockdown macrophages combined with shRNA knockdown in these primary cells [97]. Terminally differentiated BMDMs were used to facility microscopic readout, and to avoid the complication of having a portion of the cells in S phase, which results in a high proportion of unstable vacuoles [316]. This strategy allows subtle differences in vacuole integrity to be detected. BMDMS were transduced with a lentiviral shRNA library (Figure 2.1B) targeting 23 membrane trafficking genes arrayed as 4 individual shRNAs assayed separately (Supplemental Tables, Table 2.4).

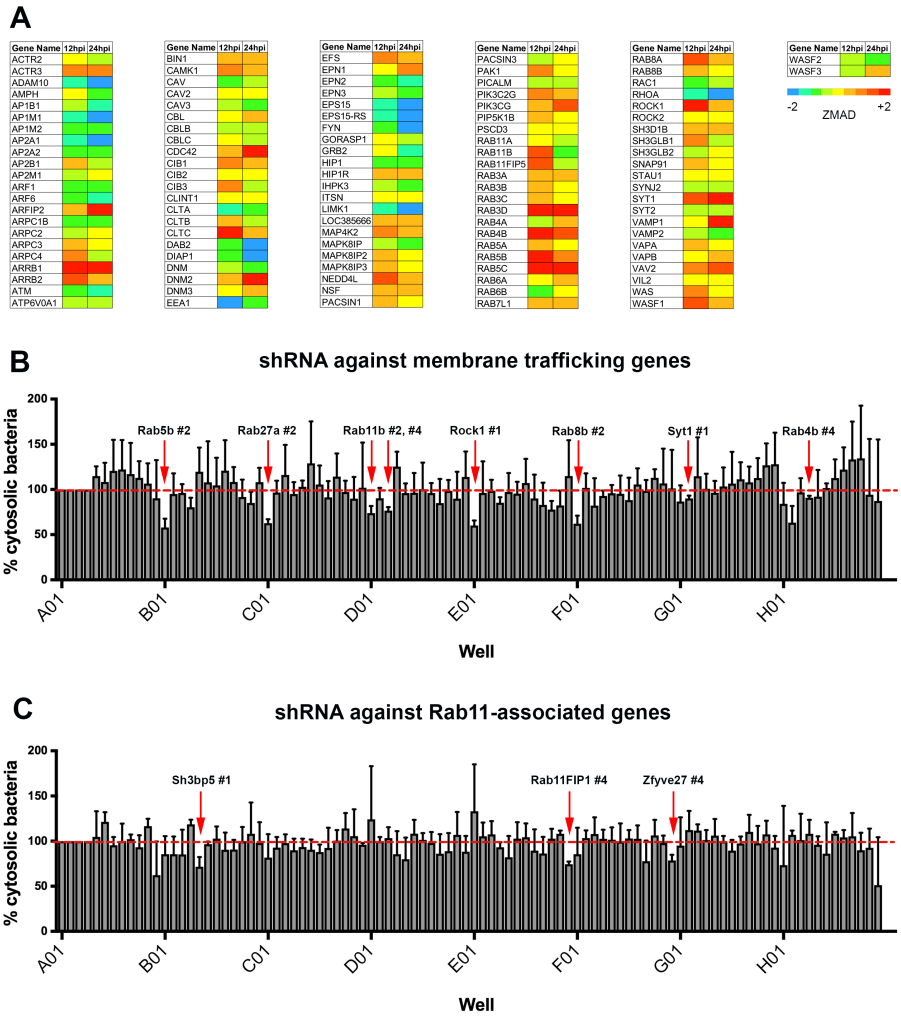

Figure 2. 2 RNAi screens identifies membrane trafficking proteins that antagonize Δ*sdhA* intracellular growth and vacuole integrity

(A) Results of high-throughput siRNA screen for enhanced intracellular growth of *L. pneumophila* Δ*sdhA* Lux^{+}. Experimental design, Fig 1(A), performing luminescence readings at 12 or 24 hpi, with least three replicate measurements for each gene target being performed Luminescence from each experimental well was normalized to the average luminescence of the non-targeting siRNA treated control wells of the same plate. Normalized ZMAD values are shown color-coded for each siRNA of the library. A cutoff of ZMAD $\geq$ 1.5 was used to select potential candidates. (B) Candidates identified in 2(A) and additional targets not covered in the original screen were tested in a high-throughput shRNA screen, performing assay detailed in Fig. 1B, detecting cytosolic exposure of bacteria. Three replicates for each knockdown condition were performed, capturing 16 images/well with automated microscopy. Image capture, analysis and normalization of data were performed as described (Materials and Methods). (C). Depletion of transcripts for a subset of Rab11 effectors results in increased vacuole integrity during *L. pneumophila* Δ*sdhA* intracellular growth. Assay conditions as in panel 2B. Statistical analyses were performed on normalized data by unpaired t test (*P < 0.05) (Materials and Methods).

After allowing differentiation and 6 days of knockdown, BMDMs were challenged in triplicate with the Δ*sdhA* strain for 6 hours, fixed and probed for permeable vacuoles using a previously described antibody accessibility assay [97]. After capturing multiple images per well and subjecting them to image analysis to quantitate permeable vacuoles, shRNAs that increased the integrity of the Δ*sdhA* vacuole relative to the shRNA-LacZ negative control were identified (Figure 2.2B).

In this fashion, eight shRNAs were identified that significantly reduced the number of permeable Δ*sdhA* vacuoles detected in macrophages (Table 2.2, t test, P = 0.0048-0.0346). The candidate genes included five members of the Rab family of GTPases that are associated with endocytic recycling, as well as ROCK1, and SYT1. Of this set, Rab5b, Rab11b, and Rab8b were of particular interest due to their robust phenotype and their tight association with recycling, based on STRING analysis [322]. Strikingly, two hits from the screen were shRNAs directed against Rab11b (Table 2.2), so this result was pursued further. Using the same screening procedures as described above, we performed a lentiviral shRNA library screen against gene targets related to Rab11 (Figure 2.2C). These gene targets included Rab11 guanine exchange factors (SH3BP5 & TRAPPC2L), motor proteins (MYO5B, KIF5A, KIF5B, KIF13A), adaptor protein (ZFYVE27), components of the exocyst complex (EXOC1-8), and downstream Rab11-family interacting proteins (RAB11FIP1-5) (Supplemental Tables, Table 2.5). ShRNAs against SH3BP5, ZFYVE27, and RAB11FIP1 significantly reduced the number of disrupted Δ*sdhA* vacuoles detected in macrophages (Table 2.2; P<0.0041 for RAB11FIP1). The gene target Rab11FIP1 was of particular interest since this downstream Rab11 effector is known to regulate membrane trafficking events and vesicle

docking events [261, 269]. We selected Rab5b, Rab11b, Rab8b, and Rab11FIP1 for further characterization in response to a Δ*sdhA* infection.

Figure	Well	shRNA	Description/Function	P value
2.2B	B01	Rab5b #2	Rab-GTPase. Endocytosis	0.0172
2.2B	C01	Rab27a #2	Rab-GTPase. Exocytosis	0.0048
2.2B	D01	Rab11b #2	Rab-GTPase. Endocytic Vesicle Recycling	0.0293
2.2B	D03	Rab11b #4	Rab-GTPase. Endocytic Vesicle Recycling	0.0091
2.2B	E01	Rock1 #1	Rho-associated Protein Kinase	0.006
2.2B	F01	Rab8b #2	Rab-GTPase. Endocytic Vesicle Recycling	0.0181
2.2B	G02	Syt1 #1	Synaptotagmin 1	0.0346
2.2B	H04	Rab4b #4	Rab-GTPase. Endocytic Vesicle Recycling	0.0172
2.2C	B05	Sh3bp5 #1	Rab11 GEF. Endocytic Vesicle Recycling	0.044
2.2C	E12	Rab11FIP1 #4	Rab11 Effector. Endocytic Vesicle Recycling	0.0041
2.2C	F12	Zfyve27 #4	Protrudin. Endocytic Vesicle Recycling	0.281

Table 2. 2 Hits from shRNA lentiviral screens

2.3.3 Depletion of specific Rab GTPase isoforms partially rescues Δ*sdhA* defect

Host membrane trafficking events are coordinated by small Rab GTPases in the cell [323]. Rab5 is involved in regulating endocytic trafficking events and Rab11 and Rab8 regulate recycling events [233]. Little is known about how the *Legionella* vacuole subverts interaction with these Rabs and, specifically, their individual isoforms. To understand how depletion of a subset of Rabs increases vacuole integrity, BMDMs were

nucleofected with siRNAs against individual Rab isoforms and knockdown efficiency was determined by immunoblot (Figure 2.3). Individual or group depletion of Rab5a, Rab5b, or Rab5c resulted in enhanced vacuole integrity in BMDMS challenged with *L. pneumophila* Δ*sdhA* (Figure 2.3A). Furthermore, each individual knockdown resulted in enhanced intracellular growth of the Δ*sdhA* strain (Figure 2.4A). Surprisingly, for Rab11 and Rab8, only depletion of Rab11b or Rab8b partially restored Δ*sdhA* vacuole integrity and intracellular growth (Figure 2.3B,C; 2.4B, 2.4C). Depletion of Rab11a or Rab8a did not rescue Δ*sdhA* phenotypic defects, while double knockdowns of Rab11a and Rab11b or Rab8a and Rab8b mimicked the defects exhibited by the single depletions that showed rescue. Of particular note regarding isoform specificity is the fact that siRNA in an immortalized cell line (Fig. 2.2A), shRNA (Fig. 2.2B) and siRNA in primary macrophages (Figs 2.3, 2.4), and using both vacuole integrity and intracellular growth as readouts gave identical results (Figs 2.3, 2.4).

2.3.4 Analysis of Rab GTPase downstream effectors: evidence for aberrant trafficking events in the absence of SdhA function

From the secondary shRNA screen in BMDMs, we found that silencing Rab11 downstream effector Rab11FIP1 restored Δ*sdhA* vacuole integrity (Fig. 2.2B). Nucleofection of BMDMs with siRNA targeting a different region of Rab11FIP1 provided the identical result and demonstrated that depletion of this protein rescued Δ*sdhA* vacuole integrity and growth (Figure 2.5B). We next tested the effects on BMDMs that were treated with siRNA against EEA1, a Rab5 effector involved in promoting early endosome vesicle tethering and VAMP3, a SNARE protein that promotes vesicle fusion

events and is a downstream effector of both Rab11 and Rab8 [283, 324, 325] [268, 326]. We found that individual depletion of EEA1 or VAMP3 was sufficient to partially restore Δ*sdhA* vacuole integrity and intracellular growth (Figure 2.5A & 2.5C). These findings point to a model in which early endosomes and recycling endosomes are trafficked in close proximity to the Δ*sdhA* vacuole, resulting in vacuole disruption in the absence of SdhA function.

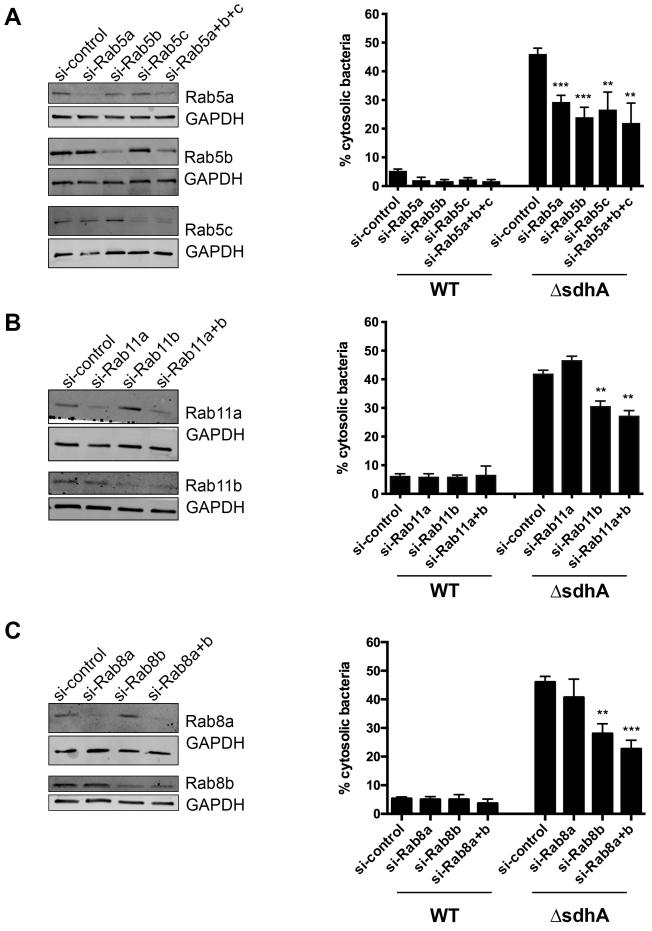

Figure 2. 3 Depletion of specific Rab GTPase isoforms results in increased vacuole integrity after BMDM challenge with *L. pneumophila* Δ*sdhA*.
(A-C) Depletion of Rab5 isoforms, Rab11b, or Rab8b partially rescues Δ*sdhA* vacuole integrity. A/J bone marrow-derived macrophages were nucleofected with noted siRNAs. Knockdown efficiency was assessed by immunoblots with noted antibodies (left panels). Nucleofected macrophages were challenged with either WT or Δ*sdhA Legionella*, fixed at 6hpi, and immunostained to determine cytosol exposure. Percent of cytosol-detected bacteria was quantified, as described (Materials and Methods).

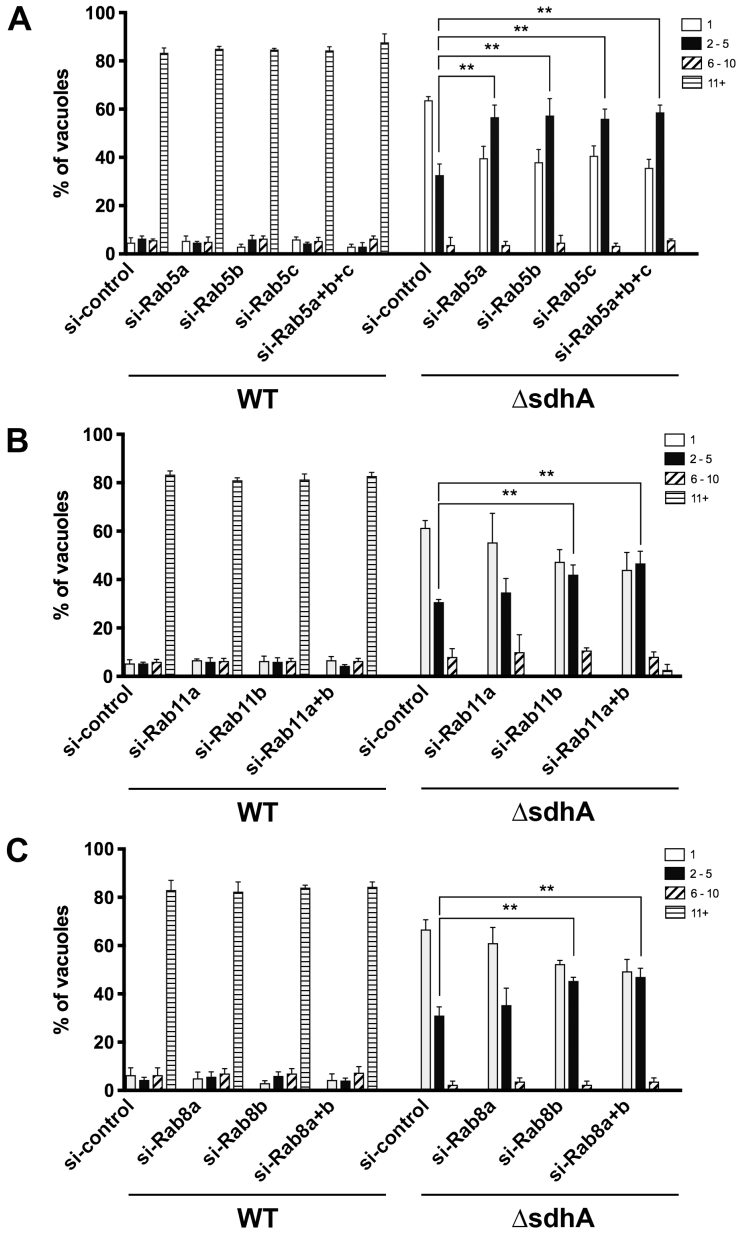

Figure 2. 4 Depletion of specific Rab GTPase isoforms partially rescue Δ*sdhA* vacuole intracellular growth

(A-C) Growth of noted *L pneumophila* strains in nucleofected BMDM. After BMDM were challenged for 14 h., the cells were fixed and probed to determine yield of bacteria in each macrophage. Number of bacteria per vacuole were quantified microscopically, and binned into 4 groups, displaying the binned vacuole size based on the graph legend (Materials and Methods; [95]). Knockdown efficiency for the shRNAs is displayed in Figure 2.3.

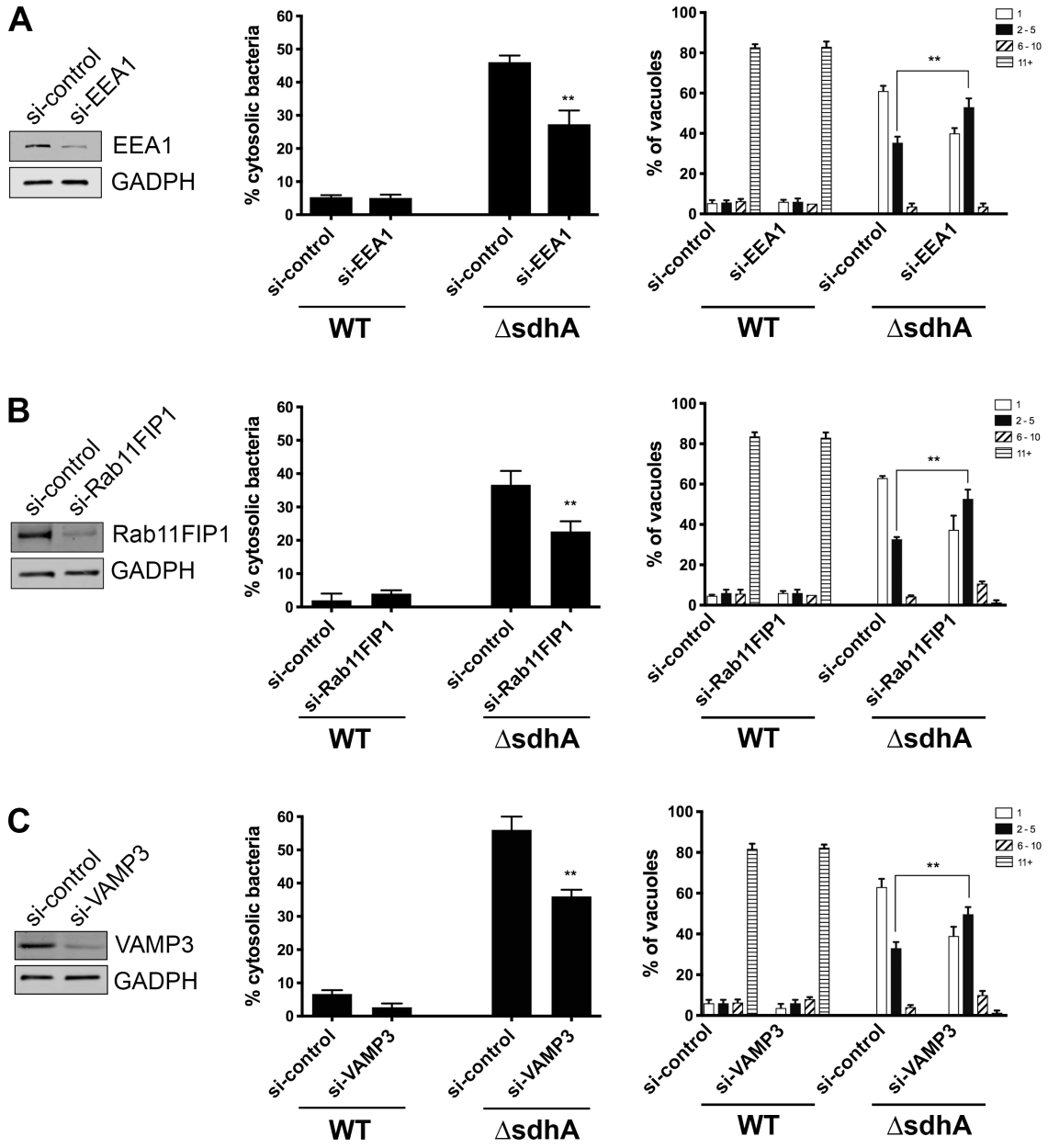

Figure 2. 5 Depletion of downstream effectors partially rescue Δ*sdhA* vacuole intracellular growth

(A-C) Depletion of downstream Rab effectors EEA1, Rab11FIP1, or VAMP3 rescues Δ*sdhA* vacuole integrity and growth defects. A/J bone marrow-derived macrophages were nucleofected with respective siRNAs. Knockdown efficiencies were determined by immunoblot. Left panels: nucleofected macrophages were challenged with noted *L. pneumophila* strains, fixed at 6hpi, and immunostained to detect cytosolic bacteria (Materials and Methods), calculating percent of cytosol-detected bacteria relative to total intracellular bacteria. Right panels: growth of *L. pneumophila* in nucleofected macrophages was measured after 14h of infection and number of bacteria in individual vacuoles was quantified (Materials and Methods).

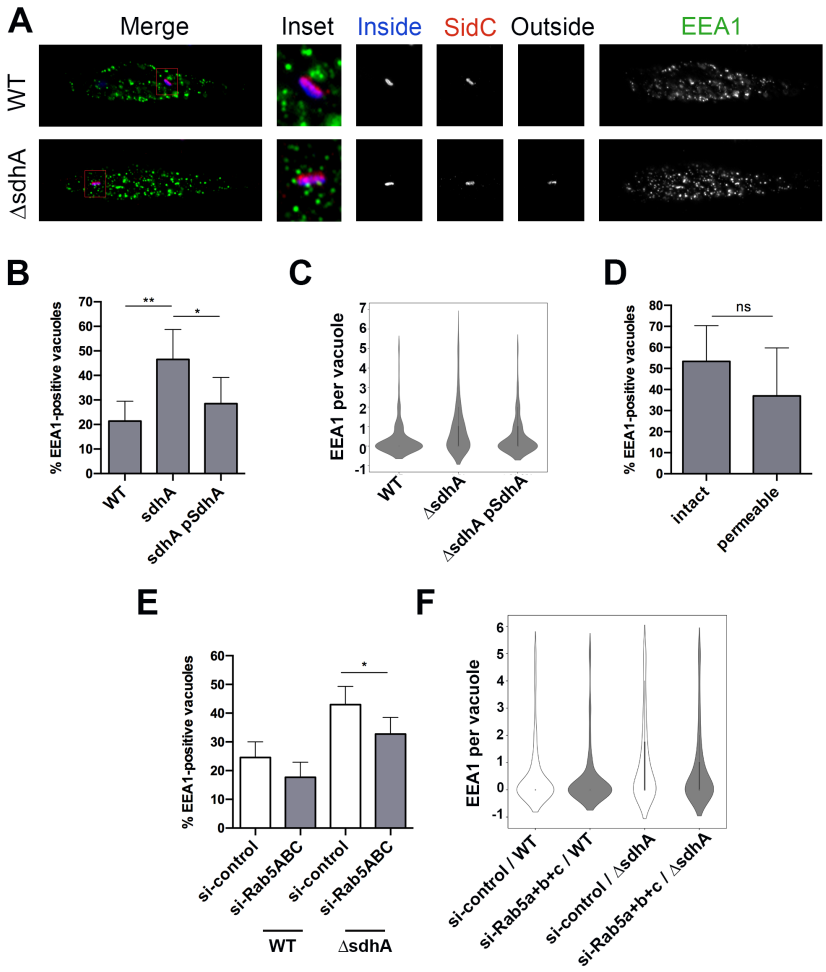

Figure 2. 6 The SdhA protein interferes with contact of EEA1-containing compartments with the LCV.

(A) Representative immunofluorescence microscopy images of the *Legionella*-containing vacuole in infected BMDMs at 4hpi, challenged with noted bacterial strains. Cells were probed with anti-*L. pneumophila* before and after permeabilization, to determine vacuole integrity (Materials and Methods) as well as anti-SidC and anti-EEA1 after permeabilization. EEA1 and SidC are pseudo-colored in green and red, respectively. Insets are magnified 3.25-fold from the original image by changing resolution. Other panels are identical resolution to original grabbed images. (B) Images from (A) were analyzed to quantify colocalization events between the vacuole and EEA1 (Materials and Methods). Total of 146 vacuoles from 2 experiments were analyzed. (C) Frequency distribution of colocalization events from (B). Interquartile range was calculated from integer values. (D) Lack of correlation between intact or cytosol-detected (permeable) Δ*sdhA* vacuoles and colocalization of EEA1 at the vacuole. (E) BMDMs nucleofected with siRNA were challenged with noted *L. pneumophila* strains and stained as in (A). Images were captured and analyzed after capture to quantify colocalization events of EEA1 at the vacuole) (Materials and Methods). Total of 182 vacuoles from 2 experiments were analyzed. (F) Frequency distribution of colocalization events from (E). Interquartile range was calculated from integer values

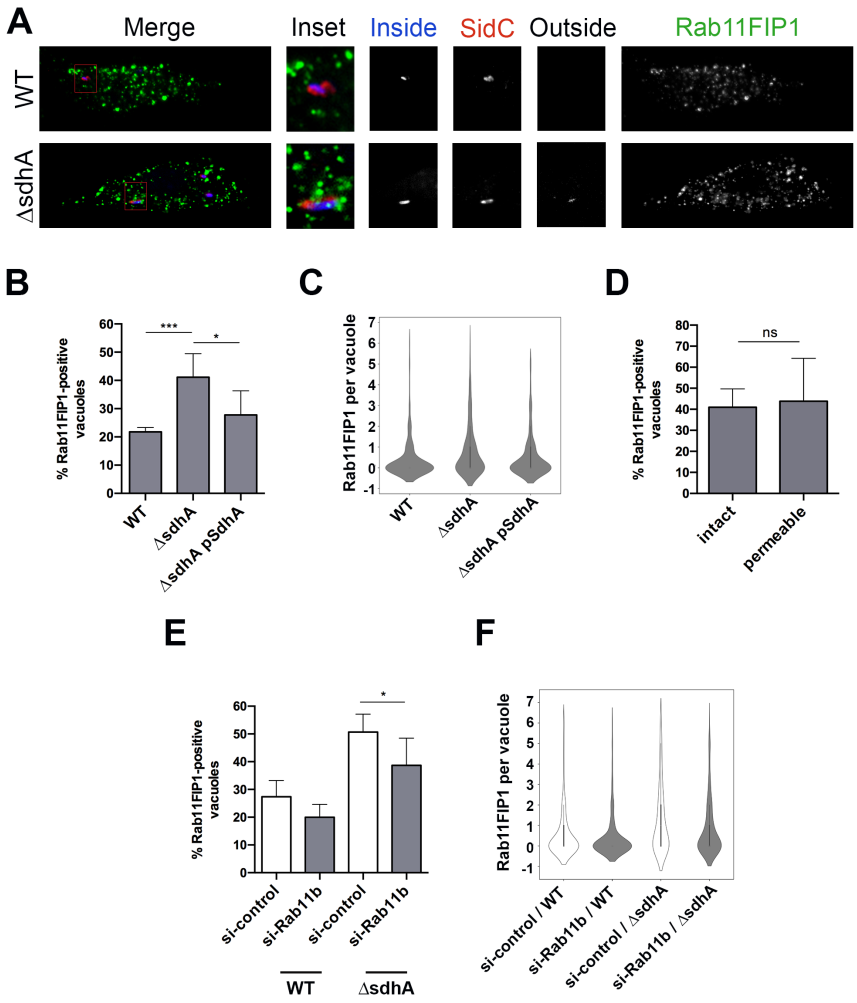

Figure 2. 7 Rab11FIP1 localizes to the ΔsdhA vacuole at a higher frequency compared to WT

(A) Representative immunofluorescence microscopy images of the *Legionella*-containing vacuole in infected BMDMs at 4hpi, challenged with noted bacterial strains. Cells were probed with anti-*L. pneumophila* before and after permeabilization, to determine vacuole integrity (Materials and Methods) as well as anti-Rab11FIP1 and SidC after permeabilization. Rab11FIP1 and SidC are pseudo-colored in green and red, respectively. Insets are magnified 3.25-fold from the original image by changing resolution. Other panels are identical resolution to original grabbed images. (B) Images from (A) were analyzed in Volocity to quantify colocalization events between the vacuole and Rab11FIP1. Total of 181 vacuoles from 2 experiments were analyzed. (C) Frequency distribution of colocalization events from (B). Interquartile range was calculated from integer values. (D) Lack of correlation between intact or cytosol-detected (permeable) Δ*sdhA* vacuoles and colocalization of Rab11FIP1 at the vacuole. (E) BMDMs were nucleofected with siRNA, were challenged with noted *L. pneumophila* strains and stained as in (A). Images were captured and analyzed after capture to to quantify colocalization events of Rab11FIP1 at the vacuole (Materials and Methods). Total of 158 vacuoles from 2 experiments were analyzed. (F) Frequency distribution of colocalization events from (E). Interquartile range was calculated from integer values.

2.3.5 The SdhA protein depresses localization of EEA1 and Rab11FIP1 about the L. pneumophila vacuole.

The localization of EEA1-positive compartments in the vicinity of LCVs during *L. pneumophila* challenge of BMDMs was next determined by immunofluorescence microscopy. After 4 hours of challenge, BMDMs were fixed and simultaneously stained for EEA1, cytosol-accessible bacteria, total bacteria, and SidC, (a marker of the LCV membrane; [95, 327]. EEA1-positive puncta were dispersed throughout the cell, and localization of the puncta about the LCV was determined by image analysis, quantifying the number of colocalization events between EEA1 and the vacuole (Figure 2.6A; Materials and Methods). The number of EEA1 colocalization events increased significantly at the Δ*sdhA* vacuole compared to the WT vacuole (Fig. 2.6A), consistent with the increase in vacuole integrity associated with knockdown of EEA1 (Fig. 2.5A). Furthermore, this phenotype was rescued by introduction of a plasmid encoding SdhA in the *L. pneumophila* Δ*sdhA* mutant (Figure 2.6B,C). There was no significant correlation between intact or disrupted Δ*sdhA* vacuoles and the EEA1 colocalization, which may be reflective of transient interactions (Figure 2.6D).

We found similar results after staining endogenous Rab11FIP1, a marker of recycling endosomes. Antibody against Rab11FIP1 labeled distinct puncta dispersed throughout the cell (Figure 2.7A). Similar to EEA1, Rab11FIP1 colocalized at a higher frequency with the Δ*sdhA* vacuole compared to the WT vacuole, with the phenotype rescued by complementation of SdhA on plasmid *in trans* (Figure 2.7B,C). Again, we observed no significant correlation between intact or disrupted Δ*sdhA* vacuoles and Rab11FIP1 colocalization (Figure 2.7D).

If aberrant increased localization of EEA1 and Rab11FIP1 with the Δ*sdhA* LCV is due to the action of the upstream Rab effectors, then knockdown of these Rabs should reverse this effect. As expected, simultaneous knockdown of all three Rab5 isoforms in BMDMS reduced the number of EEA1-positive compartments associated with Δ*sdhA* LCV during infection (Figure 2.6E,F). Similarly, as expected for a protein that functions in trafficking a component downstream of this GTPase, knockdown of Rab11b isoform reduced the number of Rab11FIP1 compartments associated with the Δ*sdhA* vacuole, (Figure 2.7E,F). Therefore, Rab proteins responsible for loss of LCV integrity are required for increased association of their downstream effectors to the dysfunctional *Legionella* Δ*sdhA*-containing compartment. This result is consistent with proposition that the compartments decorated by these effectors are responsible for the loss of integrity of the *L. pneumophila* Δ*sdhA*-containing vacuole.

2.4 Discussion

In this study, screens were performed that identified host membrane trafficking factors responsible for causing vacuole disruption and interfering with intracellular growth of an *L. pneumophila* Δ*sdhA* strain. We initially used a luciferase reporter assay to positively select for siRNA-depleted cells that showed increased intracellular growth of the mutant strain. Overall, 20 candidate genes were identified after screening 112 genes. To demonstrate specificity for knockdowns that result in increased LCV integrity relative to that observed in bone marrow-derived macrophages (BMDMs), we turned to high-throughput microscopy analysis to identify factors specifically involved in antagonizing vacuole integrity of the *L. pneumophila* Δ*sdhA* mutant. From a primary shRNA screen

introduced into BMDMs by lentivirus, we identified 8 candidate genes, with the majority being Rab GTPases involved in endocytic and membrane-recycling. Genes of particular interest were Rab5, Rab8, and Rab11. Strikingly, Rab11a had been previously implicated in regulated vacuole rupture as supporting intracellular growth after *Shigella* uptake into cultured cells [138, 139]. This raises the possibility that trafficking events that support intracellular growth of a cytosolic pathogen (*S. flexneri*) interfere with the biogenesis of the membrane surrounding an intravacuolar organism (*L. pneumophila*).

Validation of screen hits revealed that rescue of Δ*sdhA* vacuole integrity and growth was specific to depletion of individual isoforms. After silencing Rab5a, Rab5b, or Rab5c, we found that individual depletion of each isoform is sufficient to reduce vacuole disruption and the observed growth defect of the Δ*sdhA* strain (Figure 2.3A, 2.4A). This phenotype is consistent with previous studies demonstrating that the three isoforms localize to the same endocytic compartment and cooperatively regulate endocytic events [242]. Depletion of all three isoforms rescued the Δ*sdhA* phenotype to a similar degree as the depletion of individual isoforms, indicating that the isoforms function collectively rather than separately during trafficking.

In contrast to the situation with the Rab5 isoforms, specific silencing of Rab11b, but not Rab11a, enhanced the integrity of the Δ*sdhA* vacuole (Figure 2.3B, 2.4B). Furthermore, knockdown of both Rab11 isoforms produced a similar phenotype as individual knockdown of Rab11b, confirming that only Rab11b is required for Δ*sdhA* vacuole disruption It has been shown in other cell types that these two isoforms can localize to distinct compartments within the cell, which suggests a division of function between the two isoforms [262, 273]. Of particular note in this regard is Rab11 isoform

specificity that supports growth of *S. flextneri,* in which the Rab11A isoform appears critical but the Rab11B isoform does not. The isoform differences between the two pathogens may reflect spatial and temporal differences in the biogenesis and degradation of the bacterium-containing compartments. After uptake into host cells, depletion of Rab11A interferes with degradation of the *Shigella*-containing vacuole, while Rab11B has no documented effect. As degradation of the *Shigella*-containing vacuole occurs shortly after bacterial uptake at the periphery of cells, Rab11A may drive compartment destabilization in this region. In contrast, *Legionella* vacuole degradation occurs hours after infection, allowing access to perinuclear regions which could allow an interface with Rab11B-containing compartments.

A similar phenomenon was discovered when individual Rab8 isoforms were depleted. Silencing of Rab8b, but not Rab8a, increased the stability of vacuoles harboring the Δ*sdhA* strain and resulted in enhanced growth for the mutant (Figure 2.3C, 2.4C). Very little is known about the difference between the two Rab8 isoforms, although it is postulated that they function in both distinct and as well as overlapping compartments in various cell types [279, 328]. Unlike the situation with Rab11a/b knockdown of Rab8a in combination with Rab8b showed stronger rescue than individual depletion of the Rab8b isoform. This additive effect is consistent with a small pool of Rab8a that has either overlapping function or overlapping localization with Rab8b, resulting in a fraction of the Δ*sdhA*-containing vacuoles being destabilized by the Rab8a isoform.

We investigated if downstream effectors of the Rab GTPases were involved in facilitating Δ*sdhA* vacuole disruption. We demonstrated that depletion of the Rab5 effector EEA1 and the Rab11b effector Rab11FIP1 partially restored integrity of the

Δ*sdhA*-containing vacuole and intracellular growth of the mutant, generating phenotypes indistinguishable from depletion of the GTPases (Figure 2.5A, 2.5B). We also found that depletion of VAMP3, an interacting protein of both Rab8b and Rab11b, could result in an increased number of intact vacuoles harboring the Δ*sdhA* strain (Figure 2.5C) [283, 324, 325]. VAMP3 is SNARE protein that drives membrane fusion pointing to a model in which disruption of membrane integrity is a consequence of fusion with a compartment that destabilizes the LCV [329]. In turn, EEA1 is involved in tethering Rab5-positive endosomes to membranes enriched in PI(3)P, and Rab11FIP1 is known to be involved in docking recycling vesicles to membranes enriched in PI(3,4,5,)P_3 [268, 326]. We also found that depletion of Rab5 isoforms or Rab11b decreased the percentage of EEA1 and Rab11FIP1 localization at the Δ*sdhA* vacuole, respectively. Therefore, these proteins may define tethering (EEA1) docking (Rab11Fip1) and fusion (Vamp3) events downstream from the action of Rab5 and Rab11b isoforms, that drive destabilization of the vacuole harboring the mutant. Supporting this model, we found that EEA1 and Rab11FIP1 localized to the Δ*sdhA*-containing vacuole at a higher frequency compared to the WT-containing vacuole, indicating that they may play a direct role in destabilizing the vacuole harboring the mutant (Figure 2.6, 2.7).

The question of how Δ*sdhA* vacuole disruption occurs remains unclear. Surprisingly, neither EEA1 nor Rab11FIP1 recruitment showed any preference for intact or disrupted vacuoles harboring the Δ*sdhA* strain. It is possible that vacuole interactions with destabilizing compartments is transient, making it difficult to distinguish differences based on single time point assays. Alternatively, it is possible that there is a diversity of destabilizing compartments of different compositions, and probing for these two proteins

does not capture the total spectrum of compartments that can disrupt the vacuole. Of note is the possibility that the increased frequency of EEA1 and Rab11FIP1 at the Δ*sdhA* vacuole compared to WT is indicative of a phosphoinositide motif that recruits host proteins to mutant vacuole, and could increase the diversity of recruited material that is toxic for the compartment. The possibility of a unique lipid environment in the vacuole harboring the mutant is one explanation for why it is particularly sensitive to the action of the *L. pneumophila* lysophospholipase PlaA. [97]. Perhaps lipids are found on this vacuole, but are missing from the WT, that serve as substrates for PlaA.

Not considered here is the possibility that cargo being delivered to the Δ*sdhA* vacuole from the endocytic-recycling pathway directly promotes membrane disruption. Delivery of toxic cargo to the bacteria-containing vacuole has been observed in other pathogens, such as *Salmonella* [113]. It has been demonstrated in macrophages that Rab11 traffics the NADPH oxidase flavocytochrome B, and it is possible that this cargo could be delivered to the Δ*sdhA* vacuole resulting in oxidative destabilization [330]. It is interesting to note that vacuole degradation is an essential step necessary to release *S. flexneri* into the cytosol and initiate intracellular replication. These events appear to require recruitment of Rab11A-containing vesicles that could carry destabilizing cargo [138, 139]. Therefore, an event that for one pathogen is toxic, for another is an essential step in the biogenesis process leading to intracellular growth.

Altogether, this study describes a genetic screen that was able to identify a specific set of host factors that are required for Δ*sdhA* vacuole disruption. Future studies should elucidate the exact mechanism by which these proteins facilitate vacuole

disruption and the nature of the cargo being delivered to the vacuole that destabilizes the vacuole.

2.5 Supplemental Tables

ZMAD Value Key

		12 hpi		24 hpi	
Gene	**Accession**	**ZMAD value**	**Code**	**ZMAD value**	**Code**
DNM3	NM_172646	0.32		0.61	
ACTR2	NM_146243	0.19		-0.15	
ACTR3	NM_023735	1.38		1.05	
ADAM10	NM_007399	-1.4		-2.46	
AI642036	NM_001045520	0.01		0.28	
AMPH	NM_175007	0.28		-0.7	
AP1B1	NM_007454	-0.43		-1.03	
AP1M1	NM_007456	-1.49		-2.23	
AP1M2	NM_009678	-0.62		-0.54	
AP2A1	NM_001077264	-1.2		-2.29	
AP2A2	NM_007459	-0.78		-0.73	
AP2B1	NM_027915	0.67		-0.26	
AP2M1	NM_009679	-0.17		0.09	
ARF1	NM_007476	-0.81		-0.89	
ARF6	NM_007481	-0.78		-1.18	
ARFIP2	NM_029802	0.68		2.4	
ARPC1B	NM_023142	-0.99		-0.84	
ARPC2	NM_029711	-0.12		0.3	
Arpc3	NM_019824	0.62		0.1	
ARPC4	NM_026552	1.34		-0.4	
Arrb1	NM_178220	2.72		2.17	
ARRB2	NM_145429	1.66		0.91	

ATM	NM_007499	-0.73		-1.22
ATP6V0A1	NM_016920	-0.18		-0.29
BIN1	NM_001083334	0.69		0.53
C730014M21RIK	XM_356089	1.09		-0.03
CAMK1	NM_133926	1.23		0.54
CAV	NM_007616	-0.68		-0.14
CAV2	NM_016900	0.46		0.42
CAV3	NM_007617	-0.07		-0.73
CBL	NM_007619	0.41		0.61
CBLB	NM_001033238	-0.47		-0.24
CBLC	NM_023224	0		-0.07
CDC42	NM_009861	0.56		2.42
CIB1	NM_011870	1.27		0.69
CIB2	NM_019686	0.26		0.28
CLTA	NM_001080386	-1.08		-0.76
CLTB	NM_028870	0.56		-0.45
CLTC	NM_001003908	2.11		0.77
D6ERTD32E	NM_177466	1.84		-0.09
D9BWG0185E	NM_173781	-0.58		0
DAB2	NM_001008702	-0.96		-1.67
DIAP1	NM_007858	-0.96		-2.16
DNM	NM_010065	-0.16		-0.62
DNM2	NM_001039520	0.76		2.38
EEA1	NM_001001932	-2.26		-0.72
EFS	NM_010112	1.27		0.67
EPN1	NM_010147	0.28		1.14
EPN2	NM_010148	-0.66		-1.33
EPN3	NM_027984	-0.3		-0.68
EPS15	NM_007943	-1.03		-2.09
EPS15-RS	NM_007944	-1.24		-1.8
FYN	NM_001122892	-0.73		-2.12

GORASP1	NM_028976	0.15		-0.36
GRB2	NM_008163	0.47		-1.19
HIP1	NM_146001	-0.95		-0.52
HIP1R	NM_145070	0.88		0.83
Ihpk3	NM_173027	-0.43		-0.57
ITSN	NM_001110275	0		0.24
LIMK1	NM_010717	-1.06		-1.7
LOC385666	XM_001481287	0.61		0.7
MAP4K2	NM_009006	1.06		0.94
MAPK8IP	NM_011162	-0.29		-0.71
MAPK8IP2	NM_021921	0.79		0.35
MAPK8IP3	NM_013931	0.6		0.45
NEDD4L	NM_001114386	1.87		0.87
NSF	NM_008740	0.83		0.91
PACSIN1	NM_178365	0.99		0.24
PACSIN3	NM_030880	-0.19		0.09
PAK1	NM_011035	1.2		0.47
PICALM	NM_146194	-0.46		-0.14
PIK3C2G	NM_011084	1.2		0.84
PIK3CG	NM_020272	0.66		1.72
PIP5K1B	NM_008847	0.64		0.45
PSCD3	NM_011182	0.26		0.31
RAB11A	NM_017382	0.26		-0.49
RAB11B	NM_008997	1.62		-0.67
RAB3A	NM_009001	1		0.54
RAB3B	NM_023537	0.81		0.34
RAB3C	NM_023852	0.69		0.23
RAB3D	NM_031874	3.33		3.13
RAB4A	NM_009003	-0.04		0.95
RAB4B	NM_029391	2.42		1.56
RAB5A	NM_025887	0.84		0.46
RAB5B	NM_011229	2.66		1.21
RAB5C	NM_024456	2.38		3.16
RAB6	NM_024287	0.3		0.58
RAB7L1	NM_144875	0.72		0.83
RAB8A	NM_023126	1.63		0.54

RAB8B	NM_173413	0.61		0.43
RAC1	NM_009007	-0.67		-0.45
RHOA	NM_016802	-1.34		-2.6
ROCK1	NM_009071	2.23		0.93
ROCK2	NM_009072	0.1		0.15
SH3D1B	NM_011365	0.74		0.67
SH3GLB1	NM_019464	1		-0.31
SH3GLB2	NM_139302	-0.33		0.47
SNAP91	NM_013669	0.61		0.26
STAU1	NM_011490	0.03		0.33
SYNJ2	NM_001113351	-0.17		-0.03
SYT1	NM_009306	1.9		2.23
SYT2	NM_009307	-0.23		-0.35
VAMP1	NM_009496	0.08		3.3
VAMP2	NM_009497	-0.34		-0.75
VAPA	NM_013933	0.88		0.34
VAPB	NM_019806	0.21		0.57
VAV2	NM_009500	1.16		1.88
VIL2	NM_009510	0.04		0.32
WAS	NM_009515	1.12		0.32
WASF1	NM_031877	1.91		0.93
WASF2	NM_153423	-0.02		-0.77
WASF3	NM_145155	-0.01		0.73

Table 2. 3 Results of high-throughput siRNA screen for enhanced intracellular growth of *L. pneumophila* Δ*sdhA* Lux^{+}.

Gene	shRNA #	P value	Gene	shRNA #	P value
Actr10	1	0.1177	Rab27b	1	0.1458
Actr10	2	0.5923	Rab27b	2	0.7872
Actr10	3	0.8073	Rab27b	3	0.9675
Actr10	4	0.9793	RAB27B	4	0.0744
Arfip2	1	0.4932	Rab3d	1	0.0819
Arfip2	2	0.4412	Rab3d	2	0.3344
Arfip2	3	0.7436	Rab3d	3	0.7929
Arfip2	4	0.5418	Rab3d	4	0.8173
Arrb1	1	0.6047	Rab4b	1	0.4803
Arrb1	2	0.4322	Rab4b	2	0.3532

Arrb1	3	0.8456	Rab4b	3	0.6605
Arrb1	4	0.6144	RAB4B	4	0.0172
CDC42	1	0.4182	Rab5b	1	0.7291
CDC42	2	0.1961	Rab5b	2	0.0172
Cdc42	3	0.2991	Rab5b	3	0.7451
Cdc42	4	0.3578	Rab5b	4	0.5741
Cltc	1	0.3965	Rab5c	1	0.1399
Cltc	2	0.4765	Rab5c	2	0.5613
Cltc	3	0.532	Rab5c	3	0.4044
Cltc	4	0.1725	Rab5c	4	0.3601
Dnm2	1	0.5825	Rab8a	1	0.4154
Dnm2	2	0.3522	Rab8a	2	0.1749
Dnm2	3	0.0558	Rab8a	3	0.5073
Dnm2	4	0.2033	Rab8a	4	0.7256
Exph5	1	0.9414	Rab8b	1	0.5815
Exph5	2	0.6855	Rab8b	2	0.0181
Exph5	3	0.8026	Rab8b	3	0.858
Exph5	4	0.7788	RAB8B	4	0.4001
Rab11a	1	0.4995	Rock1	1	0.4832
Rab11a	2	0.6372	Rock1	2	0.006
Rab11a	3	0.8636	Rock1	3	0.8686
RAB11A	4	0.7568	Rock1	4	0.8534
Rab11b	1	0.9513	Syt1	1	0.3277
Rab11b	2	0.0293	Syt1	2	0.0346
Rab11b	3	0.2814	Syt1	3	0.6141
Rab11b	4	0.0091	SYT1	4	0.6419
Rab11fip5	4	0.6865	Sytl4	1	0.0549
Rab11fip5	1	0.4099	Sytl4	2	0.8449
Rab11fip5	2	0.519	Sytl4	3	0.6043
RAB11FIP5	4	0.2616	Sytl4	4	0.6921
Rab27a	1	0.469	Vamp1	1	0.5823
Rab27a	2	0.0048	Vamp1	2	0.5284
Rab27a	3	0.6966	Vamp1	3	0.3935
Rab27a	4	0.49	Vamp1	4	0.6897

Table 2. 4 shRNA screen against membrane trafficking genes

Gene	shRNA #	P value	Gene	shRNA #	P value
Exoc1	1	0.9318	Myo5b	1	0.3832
Exoc1	2	0.2858	Myo5b	2	0.4357

Exoc1	3	0.7806	Myo5b	3	0.6864
Exoc1	4	0.0756	Myo5b	4	0.3675
Exoc2	1	0.2719	Rab11a	1	0.7994
Exoc2	2	0.9959	Rab11a	2	0.0745
Exoc2	3	0.7262	Rab11a	3	0.4838
Exoc2	4	0.8977	RAB11A	4	0.9983
Exoc3	1	0.5506	Rab11b	1	0.5452
Exoc3	2	0.9824	Rab11b	2	0.4713
Exoc3	3	0.6841	Rab11b	3	0.0715
Exoc3	4	0.4311	Rab11b	4	0.2229
Exoc4	1	0.8072	Rab11fip1	1	0.327
Exoc4	2	0.4192	Rab11fip1	2	0.6949
Exoc4	3	0.0971	Rab11fip1	3	0.0616
Exoc4	4	0.8716	Rab11fip1	4	0.0041
EXOC5	1	0.5385	RAB11FIP2	1	0.6161
EXOC5	2	0.5588	Rab11fip2	2	0.9433
Exoc5	3	0.0179	Rab11fip2	3	0.2654
Exoc5	4	0.4602	Rab11fip2	4	0.6218
Exoc6	1	0.8661	Rab11fip3	1	0.338
Exoc6	2	0.9808	Rab11fip3	2	0.3315
Exoc6	3	0.6457	Rab11fip3	3	0.4513
Exoc6	4	0.796	Rab11fip3	4	0.0233
Exoc7	1	0.3209	Rab11fip4	1	0.4408
Exoc7	2	0.8242	Rab11fip4	2	0.8527
Exoc7	3	0.6668	Rab11fip4	3	0.4792
Exoc7	4	0.5208	Rab11fip4	4	0.4426
Exoc8	1	0.4807	Rab11fip5	1	0.3468
Exoc8	2	0.5697	Rab11fip5	2	0.4045
Exoc8	3	0.5392	Rab11fip5	3	0.7385
Exoc8	4	0.7132	Rab11fip5	4	0.305
Kif13a	1	0.2845	Sh3bp5	1	0.044
Kif13a	2	0.4443	Sh3bp5	2	0.1828
Kif13a	3	0.7925	Sh3bp5	3	0.7538
Kif13a	4	0.8098	Sh3bp5	4	0.4745
Kif5a	1	0.5565	Trappc2l	1	0.3474
Kif5a	2	0.1294	Trappc2l	2	0.2794
Kif5a	3	0.9502	Trappc2l	3	0.1306

KIF5A	4	0.4521	Trappc2l	4	0.6209
Kif5b	1	0.3848	Zfyve27	1	0.233
Kif5b	2	0.6111	Zfyve27	2	0.5971
Kif5b	3	0.4694	Zfyve27	3	0.7208
Kif5b	4	0.1674	Zfyve27	4	0.0281

Table 2. 5 shRNA screen against Rab11-associated genes

Chapter 3: Discussion & Future Directions

3.1 Summary

The results presented in this thesis demonstrate that components of the endocytic and recycling compartment are involved in the disruption of the Δ*sdhA* vacuole during *Legionella* infection within macrophages. We showed that depletion of Rab5 isoforms partially rescued the Δ*sdhA* defect in vacuole integrity and intracellular growth. Strikingly, we found that specific depletion of Rab11b or Rab8b, but not Rab11a or Rab8a isoforms, partially rescued the Δ*sdhA* defects. Furthermore, we showed that knockdown of downstream effectors EEA1, Rab11FIP1, or VAMP3 partially rescued the Δ*sdhA* defects. We went on to investigate the localization of EEA1 and Rab11FIP1 in the cell during *Legionella* infection and found that EEA1 and Rab11FIP1 colocalize with the Δ*sdhA* vacuole at a higher frequency compared to the WT vacuole.

3.2 Comparison to *Shigella* vacuole rupture model

Our findings are particularly interesting due to the roles that endocytic and recycling compartments play during *Shigella flexneri* pathogenesis. It was previously reported that Rab5 and Rab11 localize to the *Shigella*-containing vacuole immediately after uptake [138] [139]. Upon *Shigella*-induced internalization by epithelial cells, newly formed macropinosomes derived from the *Shigella* invasion site are recruited to the *Shigella*-containing vacuole. These macropinosomes are initially positive for Rab5 but are then converted to Rab11-positive macropinosomes [139] [331]. The recruitment of Rab11-positive macropinosomes is tightly connected to the conversion of $PI(4,5)P_2$ to PI(5)P on the vacuole by *Shigella* T3SS substrate IpgD. Infection with an *ipgD* mutant exhibits a delay in Rab11 recruitment to the vacuole. By live microscopy, it was

demonstrated that the recruitment of Rab11 occurs immediately before the vacuole ruptures, since galectin-3, a marker for disrupted membranes, accumulates at the vacuole immediately after Rab11 signal begins to diminish. These steps occur in a matter of minutes, as the *Shigella* vacuole ruptures within 10 minutes of pathogen invasion. It is postulated that a fusion event occurs between the Rab11-positive macropinosomes and the *Shigella*-containing vacuole, causing the observed vacuole rupture [139] [331].

These findings of Jost Enninga and colleagues provide the intriguing model that the endocytic-recycling events that support intracellular growth of a cytosolic pathogen (*Shigella flexneri*) could interfere with the vacuole integrity of an intravacuolar pathogen (*Legionella pneumophila*). One difference between Enninga and colleagues' findings and our findings is that they observed vacuole rupture of WT *Shigella* to be dependent on the Rab11a isoform, while Rab11b had no documented effect. In contrast, we found that Δ*sdhA* vacuole disruption is dependent on Rab11b, not on Rab11a. One difference in approach is that Enninga and colleagues performed their assays in HeLa cells and we performed our assays in RAW and bone marrow-derived macrophages. Cell type differences between assays may contribute to the isoform differences observed. However, we found that knockdown of Rab11 isoforms in HeLa cells and subsequent *Legionella* infection still resulted in the stimulation of Δ*sdhA* intracellular growth in si-Rab11b treated cells (Appendix, Figure 4.1). Therefore, we postulate isoform differences between the two pathogens may reflect spatial and temporal differences between the biogenesis and degradation of each pathogen-containing vacuole. The step of *Shigella* vacuolar rupture takes place rapidly (<10 min) after bacterial internalization within epithelial cells [139]. In contrast, after uptake, the Δ*sdhA* vacuole traffics to a perinuclear region of the

host cell before vacuole disruption is observed at 4 hours post-infection [97]. Rab11a and Rab11b have been shown to localize to distinct compartments within the cell, consistent with a division of function between the two isoforms. Rab11b primarily localizes to perinuclear regions of the cell, perfectly situated to affect vacuole dynamics in the absence of SdhA protein. We speculate that Rab11b drives degradation in the absence of SdhA due to the nearby locales of Rab11b and the LCV. Additionally, we hypothesize that *Shigella* vacuolar rupture by Rab11a occurs adjacent to the plasma membrane, nearby to Rab11a compartments and distant from the site of residence of Rab11b.

3.3 Future Directions

3.3.1 Rab11 and the exocyst complex

Both the *Shigella*-containing vacuole and the Δ*sdhA Legionella*-containing vacuole do not recruit Lamp1 (lysosome marker) or show acidification upon vacuole disruption [331] [97]. These observations suggest that vacuole rupture of both pathogens is mediated by direct physical contacts between Rab11-positive vesicles and the pathogen-containing vacuole. Furthermore, these Rab11 positive vesicles seem to be derived from a Rab5→Rab11 endocytic-recycling pathway, since double knockdown experiments demonstrated no difference to single knockdown experiments (Figure 4.2). Such contacts may be an outcome of "misdirected" trafficking events toward the pathogen-containing vacuole instead of their intended recycling to the plasma membrane. In uninfected cells, Rab11-positive recycling endosomes are recycled back to the plasma membrane by the exocyst complex and myosin V (MyoV), which traffics along radial actin filaments [332]. These recycling endosomes are then tethering to the plasma membrane through the direct interaction of Rab11-MyoV with the exocyst component

Exoc6 (Sec15), which forms a tripartite docking complex at the cell surface together with other exocyst components. After docking, Exoc6 interacts with SNARE complexes to mediate vesicle fusion with the plasma membrane [333] [334]. Of note is that from a yeast two-hybrid screen, the N-terminal domain of SdhA was found to bind to Exoc6 (unpublished data).

In this study, we tested for genes related to Rab11 by a secondary shRNA screen in BMDMs. The shRNA screen assessed for any knockdown conditions that could rescue the vacuole integrity defect of the Δ*sdhA* mutant at 6 hours post-infection. A subset of genes that was tested included components of the exocyst complex (Exoc1-8) (Figure 2.2C). Interestingly, knockdown of Exoc6 did not rescue Δ*sdhA* vacuole disruption phenotype. Furthermore, knockdown of other exocyst components also did not rescue Δ*sdhA* vacuole disruption. These results can be explained by two possibilities. The first possibility is that sufficient depletion of the exocyst components by shRNAs did not occur. For this reason, it is important to test knockdown efficiency of exocyst components by immunoblot for future experiments. In particular, immunoblotting after nucleofection of Exoc6 siRNA in BMDMs would be an important experiment to perform. If Exoc6 is efficiently depleted, then we can proceed to validate if knockdown of Exoc6 rescues Δ*sdhA* vacuole disruption. The second possibility for why depletion of exocyst components did not rescue Δ*sdhA* vacuole integrity is that the exocyst complex may not be involved in Rab11-mediated disruption of the Δ*sdhA* vacuole. Rab11 not only participates is anterograde exocytic trafficking but also retrograde cargo movement. Next, I will describe how the retromer complex and autophagic trafficking might be implicated in Δ*sdhA* vacuole rupture.

3.3.2 Rab11, the retromer complex, and autophagy

A few studies have reported that Rab11 may function in concert with the retromer to facilitate recycling events [335] [336] [337]. The retromer is a heteropentameric complex composed of vacuolar protein sorting (Vps) proteins (Vps35, Vps26, and Vps29) and membrane-associated sorting nexins (SNX1, SNX2, SNX5, SNX6) [338]. Rab11 has been implicated together with Vps26/29/35 to traffic cargo from the sorting endosome to the recycling endosome [336] [337]. Rab11 has also shown to colocalize on endosomes with SNX4, a retromer-related sorting nexin involved in endosomal sorting [335]. Interestingly, we have found that knockdown of retromer component SNX1 rescues Δ*sdhA* vacuole integrity (Figure 4.2). Past reports together with our findings suggest that there is a link between Rab11-positive endosomes and the retromer complex, and that the vacuole harboring the Δ*sdhA* strain is dysfunctional as a consequence of physical contact with these components. Future investigations will require analysis of individual retromer components during Δ*sdhA* infection by microscopy.

The retromer serves a wide variety of cellular functions including recycling numerous cargoes from endosomes to the plasma membrane, facilitating autophagy, and retrograde trafficking of the lysosome receptor CI-M6PR [339] [340] [341]. In addition to recycling, Rab11 has also been reported to be mediate autophagy. In *Drosophila melanogaster*, Rab11 is known to remove the protein Hook, a negative regulator of endosome maturation, from mature late endosomes. This event was shown to facilitate the fusion of endosomes and autophagosomes [342]. It has also been reported that Rab11a recruits autophagy-related proteins WIP2 and subsequently ATG16L1/ATG5/ATG12 to vesicle membranes enriched in PI(3)P. This interaction, in

turn, links autophagy marker LC3 to the vesicle membrane [343]. Lastly, Rab11 was found to colocalize on vesicles positive for autophagic proteins ATG9 and ULK1 [344]. These previous findings raise the possibility that Rab11 is interacting with the Δ*sdhA* vacuole and coordinating the shuttle of the vacuole to the autophagic pathway. More evidence supporting this hypothesis is that the autophagic marker LC3 was found to colocalize with the Δ*sdhA* vacuoles 4-fold more than with WT vacuoles at 4hpi [97]. It would be interesting to evaluate if this LC3 colocalization at the Δ*sdhA* vacuole is reduced after cells are treated with siRNA against Rab11b. If so, it would point to a model that Rab11b mediates trafficking of the LCV to the autophagic pathway, which causes Δ*sdhA* vacuole disruption.

3.3.3 Investigate mechanism of how Δ*sdhA* vacuole disrupts

The question of how disruption of the vacuole surrounding the Δ*sdhA* strain occurs remains unclear. We believe that factors involved in the disruption of the Δ*sdhA* vacuole are different than the factors involved in disruption of WT vacuole, possibly because WT vacuole disruption factors prevent vacuole establishment while Δ*sdhA* vacuole disruption factors prevent vacuole maintenance. From this body of work, I found that components of the endocytic-recycling pathway prevent vacuole maintenance and disrupt the Δ*sdhA* vacuole at 4-6hpi. Specifically, Rab effectors EEA1 and Rab11FIP1 were found to be involved in the mutant vacuole disruption. Surprisingly, disrupted and intact vacuoles harboring the Δ*sdhA* strain showed equivalent levels of EEA1/Rab11FIP1 colocalization by microscopy. Because our analysis was performed from a single time point, and interaction with these potentially disruptive compartment maybe transient, we

believe that we may have missed important events in our assay strategy, making it difficult to distinguish differences based on single time point assays. Future studies to image EEA1 and Rab11FIP1 during *Legionella* infection with live microscopy to understand the transient kinetics of disruption will be helpful in handling this shortcoming. Live image microscopy would also assist in elucidating where EEA1 and Rab11FIP1 compartments are derived from. In the findings of Enninga and colleagues, the Rab5-positive and subsequently Rab11-positive macropinosomes were derived from compartments proximal to the *Shigella* invasion site. It has been reported that the ruffling that occurs during *Shigella* internalization also induce macropinosome formation [139]. It would be interesting to examine where EEA1 or Rab11FIP1 compartments are derived during Δ*sdhA* infection. Based on our evidence that Rab11b is found in a perinuclear region and has an effect on Δ*sdhA* vacuole integrity, we hypothesize that EEA1 and Rab11FIP1 are also derived from a perinuclear compartment and that is why we observe colocalization with the Δ*sdhA* vacuole at 4hpi.

An alternative explanation for differences in EEA1 and Rab11FIP1 localization at intact or disrupted Δ*sdhA* vacuoles is that that there is a diversity of destabilizing compartments of different compositions, and probing for these two proteins does not capture the total spectrum of compartments that can disrupt the vacuole. Although we demonstrated that depletion of v-SNARE VAMP3 rescues Δ*sdhA* vacuole integrity and intracellular growth, we did not closely inspect the localization of VAMP3 during *Legionella* infection. Perhaps a difference in VAMP3 recruitment can be discerned for intact or disrupted vacuoles harboring the Δ*sdhA* strain. VAMP3 is an interacting protein of not only Rab11 but also Rab8 [283, 324, 325]. We did not closely examine by

microscopy if Rab8 and its other interacting proteins, such as Trip8b, Mss4, and AS160, are localizing to the Δ*sdhA* vacuole. Furthermore, other proteins that arose as hits in the primary shRNA screen were also not closely examined by microscopy. These candidate hits were two proteins that modulate exocytotic membrane docking and fusion events, RAB27B and SYT1, and two proteins that are associated with endocytosis, RAB4B and ROCK1. This finding raises the possibility that Δ*sdhA* vacuole disruption may involve multiple pathways, some of which may be dependent on the location of the vacuole and whether in interfaces with exocytic or endocytic trafficking pathways.

There is possibility that the increased frequency of EEA1 and Rab11FIP1 at the Δ*sdhA* vacuole compared to the WT vacuole is indicative of a phosphoinositide motif that recruits host proteins to the mutant vacuole. This is also a question Enninga and investigators raised in relation to *Shigella* infection, since Rab11 recruitment to the *Shigella*-containing vacuole is dependent on the *Shigella* inositol phosphate phosphatase IpgD substrate [139]. It would be interesting to investigate if there are also differences in phosphoinositide composition between the Δ*sdhA* and WT vacuole. In particular, it would be intriguing to investigate if the EEA1 binding motif PI(3)P or the Rab11FIP1 binding motifs PI(3,4,5)P_3 or phosphatidic acid (PA) are present on the Δ*sdhA* vacuole but not the WT vacuole. It would also be worthwhile to investigate the series of enzymes involved in the conversion of the above-mentioned phosphoinositides; one potential enzyme is 5-phosphatase OCRL, which has been shown to directly bind SdhA. The possibility of a unique lipid environment in the Δ*sdhA* vacuole could also explain why it is particularly sensitive to the action of the *L. pneumophila* lysophospholipase PlaA [97].

Perhaps lipids are found on this vacuole, but are missing from the WT, that serve as substrates for PlaA.

We also contemplate that the cargo being delivered to the Δ*sdhA* vacuole from the endocytic-recycling pathway may disrupt the membrane vacuole about the Δ*sdhA* strain. Delivery of toxic cargo to the bacteria-containing vacuole has been observed in other pathogens, such as *Salmonella* [113]. It has been demonstrated in macrophages that Rab11 traffics the NADPH oxidase flavocytochrome B, and it is possible that this cargo could be delivered to the Δ*sdhA* vacuole resulting in oxidative destabilization [330]. Identification of the type of cargo delivered to the vacuole is another aim of future experiments.

The connected pathway relationship between Rab5, Rab8b and Rab11b has been reported in the literature and combination knockdown experiments can be informative, as indicated by Figure 4.2. It is possible that EEA1 localization at the LCV may change in Rab11b or Rab8b knockdown experiments. Additionally, Rab11FIP1 localization at the LCV may change in Rab5 knockdown experiments. These knockdown experiments need to be tested in the future.

Of note, it is possible that Rab knockdown may slow the rate of phagocytosis/vacuolar maturation during infection and this may alternatively explain the phenotypes observed in this body of work. The phenotypes may be due to a delay in vacuole establishment rather than a specific defect in vacuole maintenance. To test this hypothesis, markers involved in vacuolar establishment that are distinguishable from markers involved in vacuolar maintenance will have to be observed over time in

knockdown conditions. Time-course microscopy experiments will be best suited for testing this hypothesis.

Lastly, we are curious to investigate if a similar set of host proteins that cause Δ*sdhA* vacuole disruption in macrophages is also causing vacuole disruption in amoeba. Although Rab proteins are conserved between species, differences have been identified between mammalian and amoeba Rab proteins [345] [346] [347]. These differences could also potentially provide an explanation for the role of SdhA homologs SdhB and SidH, as a Δ*sdhA*Δ*sdhB*Δ*sidH* strain produces an aggravated defect in intracellular growth compared to the Δ*sdhA* strain alone. Since Δ*sdhA* vacuole disruption occurs both in amoeba and macrophages, it will be interesting to investigate if the host proteins causing vacuole disruption are species-dependent.

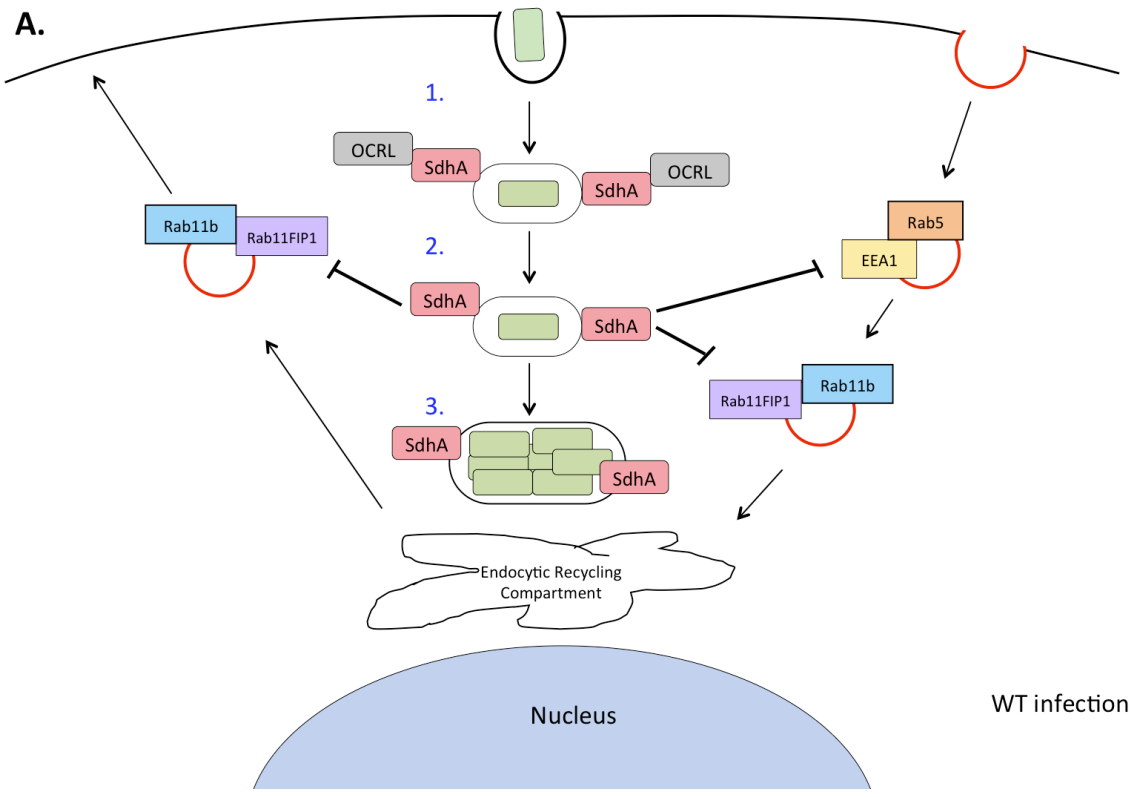

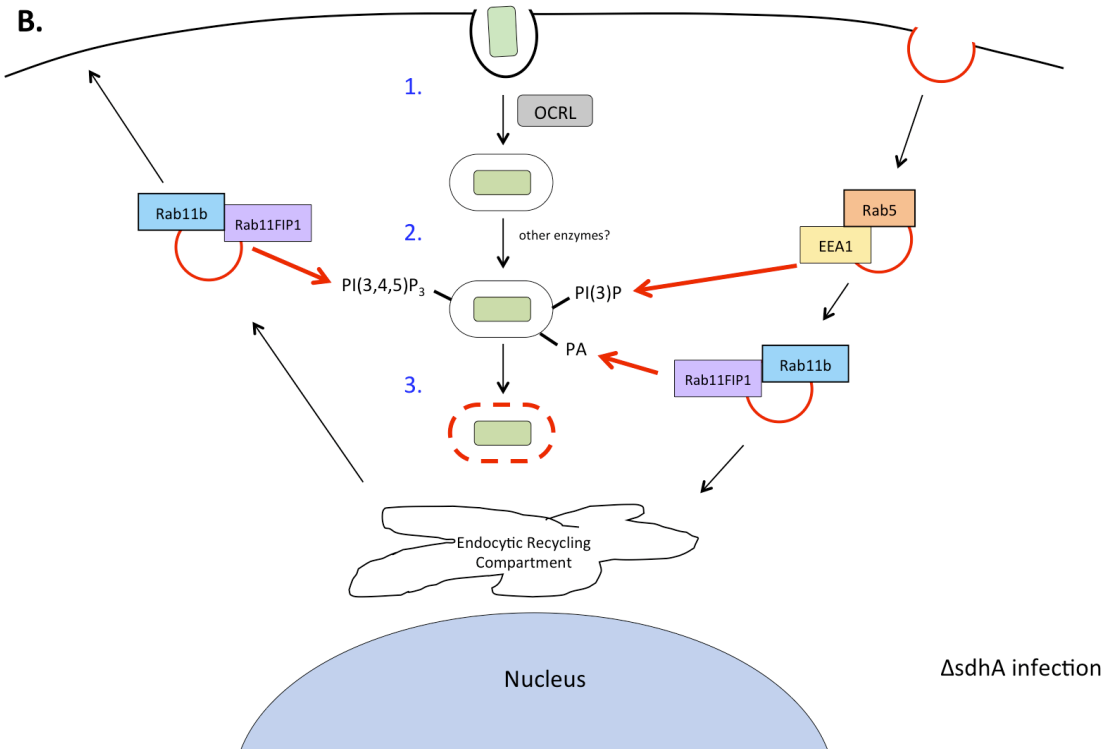

Figure 3. 1 Model for SdhA-mediated prevention of *Legionella* vacuole disruption
A). WT infection model. 1) After uptake of *Legionella*, SdhA sequesters OCRL from performing its 5-phosphatase activity. This inhibition of OCRL activity prevents the lipid content of the WT vacuole from being modified. 2) The WT vacuole does not contain lipids that signal the recruitment of endocytic and recycling components to the vacuole. 3) As a result, fusion of endocytic-recycling vesicles does not occur and the vacuole remains intact, allowing for it to expand and accommodate *Legionella* replication.
B) Δ*sdhA* infection model. 1) After uptake of *Legionella*, OCRL performs its 5-phosphatase activity either directly on the vacuole or on nearby vesicles that are incorporated into the vacuole. 2) In addition to OCRL, other enzymes may modify the lipid content of ΔsdhA vacuole such that the vacuole contains lipids PI(3)P, PI(3,4,5)P_3, and phosphatidic acid (PA). These lipids recruit EEA1-Rab5-positive vesicles and Rab11FIP1-Rab11-positive vesicles to the Δ*sdhA* vacuole, where they make contact and fuse with the vacuole. 3) The action of vacuole fusion with endocytic-recycling compartments may directly disrupt the vacuole. Alternatively, the incorporation of these compartments into the vacuole may provide a substrate for PlaA phospholipase activity, which in turn will disrupt the vacuole.

3.4 Model & Conclusion

In this body of work, the Rab GTPases Rab5, Rab11, and Rab8 have been implicated in driving disruption of membrane integrity of the vacuole surrounding the

Δ*sdhA* mutant during infection of mouse macrophages. The downstream effectors EEA1, Rab11FIP1, and VAMP3 appear to be associated with this disruption, and are involved in facilitating membrane fusion events during vesicle trafficking in the cell. EEA1, an effector of Rab5, is involved in the tethering of Rab5-positive endosomes to membranes enriched in PI(3)P [251]. Rab11FIP1, an effector of Rab11, is known to be involved in docking of recycling vesicles to membranes enriched in $PI(3,4,5)P_3$ and phosphatidic acid [268]. VAMP3, an effector of Rab11 and Rab8, is a v-SNARE protein that drives membrane fusion [283] [284]. Altogether, the results presented in this thesis point to a model in which disruption of the Δ*sdhA* vacuole membrane is a consequence of fusion with the above described compartments (Figure 3.1).

In this model, the Δ*sdhA* vacuole acquires a phosphoinositide substrate that is absent on the WT vacuole (Figure 3.1B). This phosphoinositide substrate is converted, by interacting enzymes, to three potential substrates: PI(3)P, $PI(3,4,5)P_3$, or phosphatidic acid. The substrates are generated prior to 4 hours of infection, at which point either Rab5-activated EEA1 binds PI(3)P or Rab11-Rab11FIP1 bind $PI(3,4,5)P_3$ or phosphatidic acid. This results in tethering and docking of vesicles to the ΔsdhA vacuole and allows for recruitment of SNARE proteins (in particular VAMP3). The v-SNARE VAMP3 together with t-SNAREs facilitates the fusion of host vesicles on the Δ*sdhA* vacuoles. Vesicle fusion may directly cause membrane disruption. Additionally, membrane disruption could be caused by PlaA, which directly interacts with the fused lipid substrates derived from the host vesicles. These events expose the Δ*sdhA* bacteria to the cytosol. The WT vacuole, however, evades accumulation of toxic phospholipids at the LCV. We hypothesize SdhA sequesters the 5-phosphatase OCRL, thus preventing

downstream phosphoinositide metabolism events from occurring at the vacuole (Figure 3.1A).

Through this research, we elucidated which specific host proteins are involved in disrupting the Δ*sdhA* vacuole. We learned that components of the endocytic and recycling pathway (Rab5, Rab11, and Rab8) are involved in exacerbating the integrity of the Δ*sdhA* vacuole. Furthermore, the downstream effectors EEA1, Rab11FIP1, and VAMP3 are involved in facilitating this disruption event. We learned that both *Shigella* and Δ*sdhA* interface a Rab11 trafficking pathway, albeit a Rab11a pathway for *Shigella* and a Rab11b pathway for Δ*sdhA*. The similarity between *Legionella* and *Shigella* interactions with a common endocytic-recycling pathway provides an example of how a host process can either promote or interfere with pathogen replication, depending on the strategy used for intracellular growth. Future studies should elucidate the exact mechanism by which endocytic-recycling proteins facilitate vacuole disruption.

Chapter 4: Appendix

A)

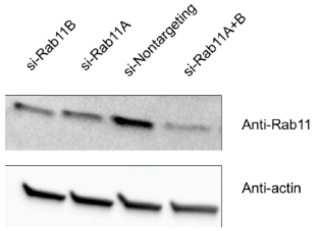

B)

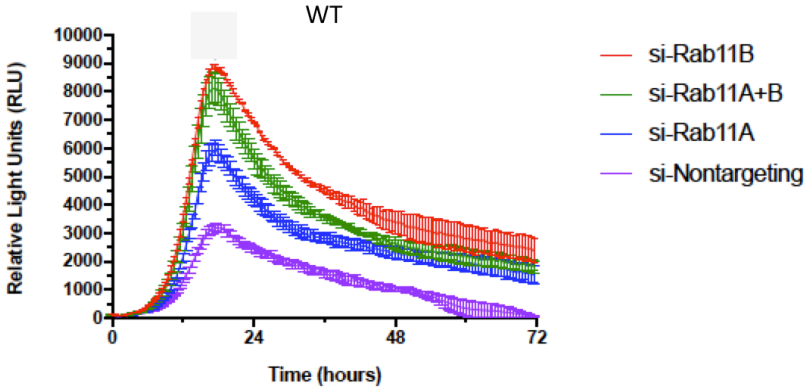

C)

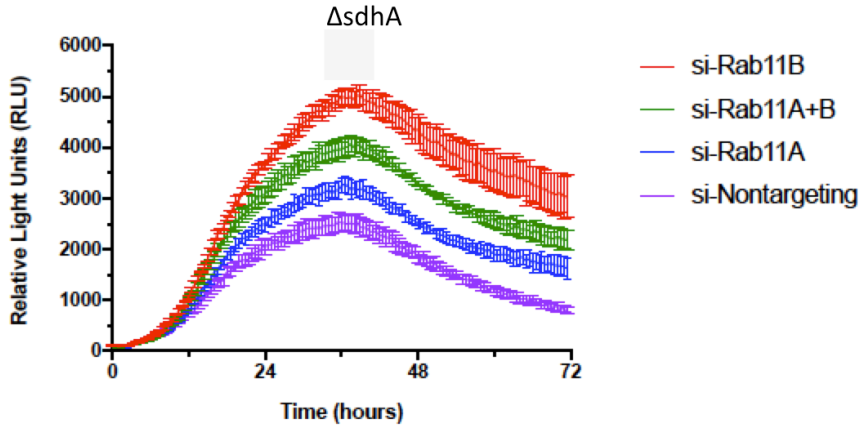

Figure 4. 1 Δ*sdhA* intracellular growth in Rab11 isoform-depleted HeLa cells
A) Transfection efficiency of 50nM siRNA against Rab11 isoforms in HeLa cells**.** B) Intracellular growth of WT-lux strain in siRNA treated HeLa cells. C) Intracellular growth of ΔsdhA-lux strain in siRNA treated HeLa cells.

A)

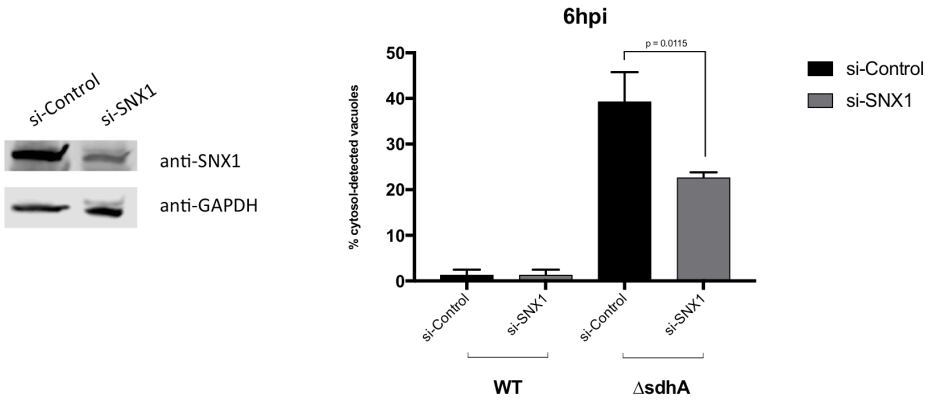

B)

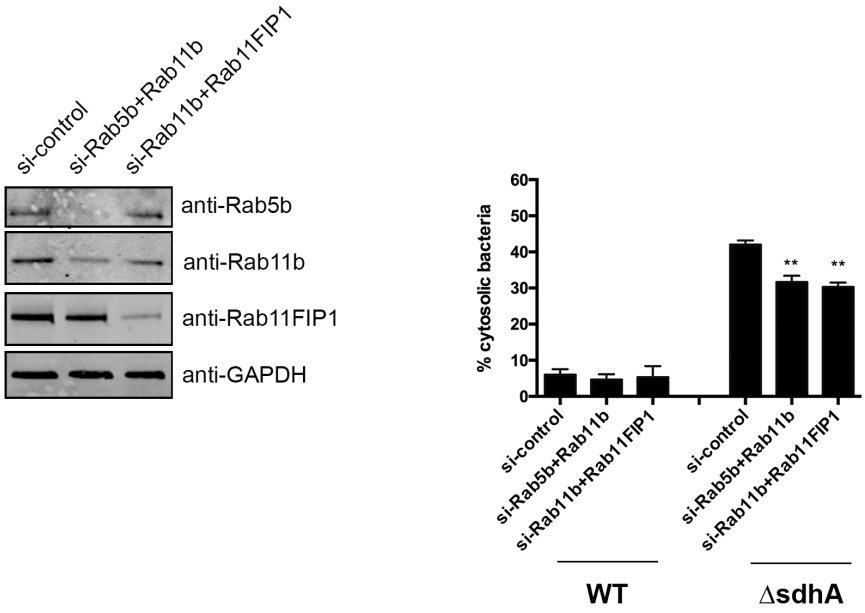

Figure 4. 2 Depletion of SNX1 and double knockdowns partially rescue ΔsdhA vacuole permeability

A) BMDMs were nucleofected with control siRNA or si-SNX1. Knockdown efficiency was measured by immunoblot (left). Nucleofected BMDMs were infected with WT or Δ*sdhA* for 6 hours and then fixed and stained for cytosol-detected bacteria as previously described in Methods. Percent cytosol-detected bacteria were quantified for each condition (right). B) BMDMs were nucleofected with control siRNA, si-Rab5b+Rab11b, or si-Rab11b+Rab11FIP1. Knockdown efficiency was measured by immunoblot (left). Nucleofected BMDMs were infected with WT or Δ*sdhA* for 6 hours and then fixed and stained for cytosol-detected bacteria as previously described in Methods. Percent cytosol-detected bacteria were quantified for each condition (right).

Chapter 5: Bibliography

1. Rowbotham, T.J., *Preliminary report on the pathogenicity of Legionella pneumophila for freshwater and soil amoebae.* J Clin Pathol, 1980. **33**(12): p. 1179-83.
2. Solomon, J.M., et al., *Intracellular growth of Legionella pneumophila in Dictyostelium discoideum, a system for genetic analysis of host-pathogen interactions.* Infect Immun, 2000. **68**(5): p. 2939-47.
3. Taylor, M., K. Ross, and R. Bentham, *Legionella, protozoa, and biofilms: interactions within complex microbial systems.* Microb Ecol, 2009. **58**(3): p. 538-47.
4. Newton, H.J., et al., *Molecular pathogenesis of infections caused by Legionella pneumophila.* Clin Microbiol Rev, 2010. **23**(2): p. 274-98.
5. O'Connor, T.J., et al., *Minimization of the Legionella pneumophila genome reveals chromosomal regions involved in host range expansion.* Proc Natl Acad Sci U S A, 2011. **108**(36): p. 14733-40.
6. Bruggemann, H., C. Cazalet, and C. Buchrieser, *Adaptation of Legionella pneumophila to the host environment: role of protein secretion, effectors and eukaryotic-like proteins.* Curr Opin Microbiol, 2006. **9**(1): p. 86-94.
7. Ge, J. and F. Shao, *Manipulation of host vesicular trafficking and innate immune defence by Legionella Dot/Icm effectors.* Cell Microbiol, 2011. **13**(12): p. 1870-80.
8. Hubber, A. and C.R. Roy, *Modulation of host cell function by Legionella pneumophila type IV effectors.* Annu Rev Cell Dev Biol, 2010. **26**: p. 261-83.
9. Shin, S. and C.R. Roy, *Host cell processes that influence the intracellular survival of Legionella pneumophila.* Cell Microbiol, 2008. **10**(6): p. 1209-20.
10. Xu, L. and Z.Q. Luo, *Cell biology of infection by Legionella pneumophila.* Microbes Infect, 2013. **15**(2): p. 157-67.
11. Isberg, R.R., T.J. O'Connor, and M. Heidtman, *The Legionella pneumophila replication vacuole: making a cosy niche inside host cells.* Nat Rev Microbiol, 2009. **7**(1): p. 13-24.
12. Horwitz, M.A., *Formation of a novel phagosome by the Legionnaires' disease bacterium (Legionella pneumophila) in human monocytes.* J Exp Med, 1983. **158**(4): p. 1319-31.
13. Ensminger, A.W. and R.R. Isberg, *Legionella pneumophila Dot/Icm translocated substrates: a sum of parts.* Curr Opin Microbiol, 2009. **12**(1): p. 67-73.
14. McDade, J.E., et al., *Legionnaires' disease: isolation of a bacterium and demonstration of its role in other respiratory disease.* N Engl J Med, 1977. **297**(22): p. 1197-203.
15. Cianciotto, N.P., H. Hilbi, and C. Buchrieser, *Legionnaires' Disease*, in *The Prokaryotes: Human Microbiology*, E. Rosenberg, et al., Editors. 2013, Springer Berlin Heidelberg: Berlin, Heidelberg. p. 147-217.
16. Fraser, D.W., *The challenges were legion.* The Lancet Infectious Diseases, 2005. **5**(4): p. 237-241.

17. Terranova, W., M.L. Cohen, and D.W. Fraser, *1974 outbreak of Legionnaires' Disease diagnosed in 1977. Clinical and epidemiological features.* Lancet, 1978. **2**(8081): p. 122-4.
18. Cunha, B.A., *Legionnaires' disease: clinical differentiation from typical and other atypical pneumonias.* Infect Dis Clin North Am, 2010. **24**(1): p. 73-105.
19. Hilbi, H., et al., *Update on Legionnaires' disease: pathogenesis, epidemiology, detection and control.* Mol Microbiol, 2010. **76**(1): p. 1-11.
20. Edelstein, P.H., *Antimicrobial chemotherapy for legionnaires' disease: a review.* Clin Infect Dis, 1995. **21 Suppl 3**: p. S265-76.
21. Kinchen, J.M. and K.S. Ravichandran, *Phagosome maturation: going through the acid test.* Nat Rev Mol Cell Biol, 2008. **9**(10): p. 781-95.
22. Deng, M., et al., *Increased expression of reticulon 3 in neurons leads to reduced axonal transport of beta site amyloid precursor protein-cleaving enzyme 1.* J Biol Chem, 2013. **288**(42): p. 30236-45.
23. Horwitz, M.A., *The Legionnaires' disease bacterium (Legionella pneumophila) inhibits phagosome-lysosome fusion in human monocytes.* J Exp Med, 1983. **158**(6): p. 2108-26.
24. Krska, D., et al., *C3larvin toxin, an ADP-ribosyltransferase from Paenibacillus larvae.* J Biol Chem, 2015. **290**(3): p. 1639-53.
25. Horwitz, M.A., *Phagocytosis of the Legionnaires' disease bacterium (Legionella pneumophila) occurs by a novel mechanism: engulfment within a pseudopod coil.* Cell, 1984. **36**(1): p. 27-33.
26. Swanson, M.S. and R.R. Isberg, *Association of Legionella pneumophila with the macrophage endoplasmic reticulum.* Infect Immun, 1995. **63**(9): p. 3609-20.
27. Robinson, C.G. and C.R. Roy, *Attachment and fusion of endoplasmic reticulum with vacuoles containing Legionella pneumophila.* Cell Microbiol, 2006. **8**(5): p. 793-805.
28. Tilney, L.G., et al., *How the parasitic bacterium Legionella pneumophila modifies its phagosome and transforms it into rough ER: implications for conversion of plasma membrane to the ER membrane.* J Cell Sci, 2001. **114**(Pt 24): p. 4637-50.
29. Kagan, J.C. and C.R. Roy, *Legionella phagosomes intercept vesicular traffic from endoplasmic reticulum exit sites.* Nat Cell Biol, 2002. **4**(12): p. 945-54.
30. Kotewicz, K.M., et al., *A Single Legionella Effector Catalyzes a Multistep Ubiquitination Pathway to Rearrange Tubular Endoplasmic Reticulum for Replication.* Cell Host Microbe, 2017. **21**(2): p. 169-181.
31. Alli, O.A., et al., *Temporal pore formation-mediated egress from macrophages and alveolar epithelial cells by Legionella pneumophila.* Infect Immun, 2000. **68**(11): p. 6431-40.
32. Berger, K.H. and R.R. Isberg, *Two distinct defects in intracellular growth complemented by a single genetic locus in Legionella pneumophila.* Mol Microbiol, 1993. **7**(1): p. 7-19.
33. Marra, A., et al., *Identification of a Legionella pneumophila locus required for intracellular multiplication in human macrophages.* Proc Natl Acad Sci U S A, 1992. **89**(20): p. 9607-11.

34. Segal, G. and H.A. Shuman, *Characterization of a new region required for macrophage killing by Legionella pneumophila.* Infect Immun, 1997. **65**(12): p. 5057-66.
35. Kubori, T., et al., *Native structure of a type IV secretion system core complex essential for Legionella pathogenesis.* Proc Natl Acad Sci U S A, 2014. **111**(32): p. 11804-9.
36. Vincent, C.D., et al., *Identification of the core transmembrane complex of the Legionella Dot/Icm type IV secretion system.* Mol Microbiol, 2006. **62**(5): p. 1278-91.
37. Ghosal, D., et al., *Molecular architecture, polar targeting and biogenesis of the Legionella Dot/Icm T4SS.* Nat Microbiol, 2019. **4**(7): p. 1173-1182.
38. Chetrit, D., et al., *A unique cytoplasmic ATPase complex defines the Legionella pneumophila type IV secretion channel.* Nat Microbiol, 2018. **3**(6): p. 678-686.
39. Vincent, C.D., et al., *Identification of the DotL coupling protein subcomplex of the Legionella Dot/Icm type IV secretion system.* Mol Microbiol, 2012. **85**(2): p. 378-91.
40. Bardill, J.P., J.L. Miller, and J.P. Vogel, *IcmS-dependent translocation of SdeA into macrophages by the Legionella pneumophila type IV secretion system.* Mol Microbiol, 2005. **56**(1): p. 90-103.
41. Sutherland, M.C., et al., *The Legionella IcmSW complex directly interacts with DotL to mediate translocation of adaptor-dependent substrates.* PLoS Pathog, 2012. **8**(9): p. e1002910.
42. Cambronne, E.D. and C.R. Roy, *The Legionella pneumophila IcmSW complex interacts with multiple Dot/Icm effectors to facilitate type IV translocation.* PLoS Pathog, 2007. **3**(12): p. e188.
43. Burstein, D., et al., *Genomic analysis of 38 Legionella species identifies large and diverse effector repertoires.* Nat Genet, 2016. **48**(2): p. 167-75.
44. Gomez-Valero, L., et al., *More than 18,000 effectors in the Legionella genus genome provide multiple, independent combinations for replication in human cells.* Proc Natl Acad Sci U S A, 2019. **116**(6): p. 2265-2273.
45. Fontana, M.F., et al., *Secreted bacterial effectors that inhibit host protein synthesis are critical for induction of the innate immune response to virulent Legionella pneumophila.* PLoS Pathog, 2011. **7**(2): p. e1001289.
46. Liu, Y. and Z.Q. Luo, *The Legionella pneumophila effector SidJ is required for efficient recruitment of endoplasmic reticulum proteins to the bacterial phagosome.* Infect Immun, 2007. **75**(2): p. 592-603.
47. Banga, S., et al., *Legionella pneumophila inhibits macrophage apoptosis by targeting pro-death members of the Bcl2 protein family.* Proc Natl Acad Sci U S A, 2007. **104**(12): p. 5121-6.
48. Heidtman, M., et al., *Large-scale identification of Legionella pneumophila Dot/Icm substrates that modulate host cell vesicle trafficking pathways.* Cell Microbiol, 2009. **11**(2): p. 230-48.
49. Kagan, J.C., et al., *Legionella subvert the functions of Rab1 and Sec22b to create a replicative organelle.* J Exp Med, 2004. **199**(9): p. 1201-11.

50. Losick, V.P. and R.R. Isberg, *NF-kappaB translocation prevents host cell death after low-dose challenge by Legionella pneumophila.* J Exp Med, 2006. **203**(9): p. 2177-89.
51. Gaspar, A.H. and M.P. Machner, *VipD is a Rab5-activated phospholipase A1 that protects Legionella pneumophila from endosomal fusion.* Proc Natl Acad Sci U S A, 2014. **111**(12): p. 4560-5.
52. Shohdy, N., et al., *Pathogen effector protein screening in yeast identifies Legionella factors that interfere with membrane trafficking.* Proc Natl Acad Sci U S A, 2005. **102**(13): p. 4866-71.
53. Ku, B., et al., *VipD of Legionella pneumophila targets activated Rab5 and Rab22 to interfere with endosomal trafficking in macrophages.* PLoS Pathog, 2012. **8**(12): p. e1003082.
54. Xu, L., et al., *Inhibition of host vacuolar H+-ATPase activity by a Legionella pneumophila effector.* PLoS Pathog, 2010. **6**(3): p. e1000822.
55. Laguna, R.K., et al., *A Legionella pneumophila-translocated substrate that is required for growth within macrophages and protection from host cell death.* Proc Natl Acad Sci U S A, 2006. **103**(49): p. 18745-50.
56. Sherwood, R.K. and C.R. Roy, *A Rab-centric perspective of bacterial pathogen-occupied vacuoles.* Cell Host Microbe, 2013. **14**(3): p. 256-68.
57. Haneburger, I. and H. Hilbi, *Phosphoinositide lipids and the Legionella pathogen vacuole.* Curr Top Microbiol Immunol, 2013. **376**: p. 155-73.
58. Machner, M.P. and R.R. Isberg, *A bifunctional bacterial protein links GDI displacement to Rab1 activation.* Science, 2007. **318**(5852): p. 974-7.
59. Arasaki, K. and C.R. Roy, *Legionella pneumophila promotes functional interactions between plasma membrane syntaxins and Sec22b.* Traffic, 2010. **11**(5): p. 587-600.
60. Arasaki, K., D.K. Toomre, and C.R. Roy, *The Legionella pneumophila effector DrrA is sufficient to stimulate SNARE-dependent membrane fusion.* Cell Host Microbe, 2012. **11**(1): p. 46-57.
61. Machner, M.P. and R.R. Isberg, *Targeting of host Rab GTPase function by the intravacuolar pathogen Legionella pneumophila.* Dev Cell, 2006. **11**(1): p. 47-56.
62. Cheng, W., et al., *Structural insights into a unique Legionella pneumophila effector LidA recognizing both GDP and GTP bound Rab1 in their active state.* PLoS Pathog, 2012. **8**(3): p. e1002528.
63. Cherfils, J., *Arf GTPases and their effectors: assembling multivalent membrane-binding platforms.* Curr Opin Struct Biol, 2014. **29**: p. 67-76.
64. Jackson, C.L., *GEF-effector interactions.* Cell Logist, 2014. **4**(2): p. e943616.
65. Nagai, H., et al., *A bacterial guanine nucleotide exchange factor activates ARF on Legionella phagosomes.* Science, 2002. **295**(5555): p. 679-82.
66. Wasilko, D.J. and Y. Mao, *Exploiting the ubiquitin and phosphoinositide pathways by the Legionella pneumophila effector, SidC.* Curr Genet, 2016. **62**(1): p. 105-8.
67. Dolinsky, S., et al., *The Legionella longbeachae Icm/Dot substrate SidC selectively binds phosphatidylinositol 4-phosphate with nanomolar affinity and promotes pathogen vacuole-endoplasmic reticulum interactions.* Infect Immun, 2014. **82**(10): p. 4021-33.

68. Gazdag, E.M., et al., *The structure of the N-terminal domain of the Legionella protein SidC.* J Struct Biol, 2014. **186**(1): p. 188-94.
69. Hsu, F., et al., *The Legionella effector SidC defines a unique family of ubiquitin ligases important for bacterial phagosomal remodeling.* Proc Natl Acad Sci U S A, 2014. **111**(29): p. 10538-43.
70. Ingmundson, A., et al., *Legionella pneumophila proteins that regulate Rab1 membrane cycling.* Nature, 2007. **450**(7168): p. 365-9.
71. Mihai Gazdag, E., et al., *Mechanism of Rab1b deactivation by the Legionella pneumophila GAP LepB.* EMBO Rep, 2013. **14**(2): p. 199-205.
72. Dong, N., et al., *Modulation of membrane phosphoinositide dynamics by the phosphatidylinositide 4-kinase activity of the Legionella LepB effector.* Nat Microbiol, 2016. **2**: p. 16236.
73. Neunuebel, M.R., et al., *De-AMPylation of the small GTPase Rab1 by the pathogen Legionella pneumophila.* Science, 2011. **333**(6041): p. 453-6.
74. Tan, Y. and Z.Q. Luo, *Legionella pneumophila SidD is a deAMPylase that modifies Rab1.* Nature, 2011. **475**(7357): p. 506-9.
75. Mukherjee, S., et al., *Modulation of Rab GTPase function by a protein phosphocholine transferase.* Nature, 2011. **477**(7362): p. 103-6.
76. Pan, X., et al., *Ankyrin repeat proteins comprise a diverse family of bacterial type IV effectors.* Science, 2008. **320**(5883): p. 1651-4.
77. Finsel, I., et al., *The Legionella effector RidL inhibits retrograde trafficking to promote intracellular replication.* Cell Host Microbe, 2013. **14**(1): p. 38-50.
78. Kubori, T., A. Hyakutake, and H. Nagai, *Legionella translocates an E3 ubiquitin ligase that has multiple U-boxes with distinct functions.* Mol Microbiol, 2008. **67**(6): p. 1307-19.
79. Kubori, T., et al., *Legionella metaeffector exploits host proteasome to temporally regulate cognate effector.* PLoS Pathog, 2010. **6**(12): p. e1001216.
80. Ensminger, A.W. and R.R. Isberg, *E3 ubiquitin ligase activity and targeting of BAT3 by multiple Legionella pneumophila translocated substrates.* Infect Immun, 2010. **78**(9): p. 3905-19.
81. Wong, K., et al., *Structural Mimicry by a Bacterial F Box Effector Hijacks the Host Ubiquitin-Proteasome System.* Structure, 2017. **25**(2): p. 376-383.
82. Qiu, J., et al., *Ubiquitination independent of E1 and E2 enzymes by bacterial effectors.* Nature, 2016. **533**(7601): p. 120-4.
83. Belyi, Y., et al., *Lgt: a family of cytotoxic glucosyltransferases produced by Legionella pneumophila.* J Bacteriol, 2008. **190**(8): p. 3026-35.
84. Shen, X., et al., *Targeting eEF1A by a Legionella pneumophila effector leads to inhibition of protein synthesis and induction of host stress response.* Cell Microbiol, 2009. **11**(6): p. 911-26.
85. Belyi, Y., et al., *Legionella pneumophila glucosyltransferase inhibits host elongation factor 1A.* Proc Natl Acad Sci U S A, 2006. **103**(45): p. 16953-8.
86. Mateyak, M.K. and T.G. Kinzy, *eEF1A: thinking outside the ribosome.* J Biol Chem, 2010. **285**(28): p. 21209-13.
87. Guo, Z., et al., *A Legionella effector modulates host cytoskeletal structure by inhibiting actin polymerization.* Microbes Infect, 2014. **16**(3): p. 225-36.

88. Kim, S. and P.A. Coulombe, *Emerging role for the cytoskeleton as an organizer and regulator of translation.* Nat Rev Mol Cell Biol, 2010. **11**(1): p. 75-81.
89. Ge, J., et al., *A Legionella type IV effector activates the NF-kappaB pathway by phosphorylating the IkappaB family of inhibitors.* Proc Natl Acad Sci U S A, 2009. **106**(33): p. 13725-30.
90. Losick, V.P., et al., *LnaB: a Legionella pneumophila activator of NF-kappaB.* Cell Microbiol, 2010. **12**(8): p. 1083-97.
91. Abu-Zant, A., et al., *Anti-apoptotic signalling by the Dot/Icm secretion system of L. pneumophila.* Cell Microbiol, 2007. **9**(1): p. 246-64.
92. Chen, G.Y., et al., *A Genetic Screen Reveals that Synthesis of 1,4-Dihydroxy-2-Naphthoate (DHNA), but Not Full-Length Menaquinone, Is Required for Listeria monocytogenes Cytosolic Survival.* MBio, 2017. **8**(2).
93. Liu, B.C., et al., *Constitutive Interferon Maintains GBP Expression Required for Release of Bacterial Components Upstream of Pyroptosis and Anti-DNA Responses.* Cell Rep, 2018. **24**(1): p. 155-168 e5.
94. Vande Walle, L. and M. Lamkanfi, *Pyroptosis.* Curr Biol, 2016. **26**(13): p. R568-R572.
95. Luo, Z.Q. and R.R. Isberg, *Multiple substrates of the Legionella pneumophila Dot/Icm system identified by interbacterial protein transfer.* Proc Natl Acad Sci U S A, 2004. **101**(3): p. 841-6.
96. Ninio, S., et al., *The Legionella IcmS-IcmW protein complex is important for Dot/Icm-mediated protein translocation.* Mol Microbiol, 2005. **55**(3): p. 912-26.
97. Creasey, E.A. and R.R. Isberg, *The protein SdhA maintains the integrity of the Legionella-containing vacuole.* Proc Natl Acad Sci U S A, 2012. **109**(9): p. 3481-6.
98. Pilla, D.M., et al., *Guanylate binding proteins promote caspase-11-dependent pyroptosis in response to cytoplasmic LPS.* Proc Natl Acad Sci U S A, 2014. **111**(16): p. 6046-51.
99. Piro, A.S., et al., *Detection of Cytosolic Shigella flexneri via a C-Terminal Triple-Arginine Motif of GBP1 Inhibits Actin-Based Motility.* MBio, 2017. **8**(6).
100. Akoh, C.C., et al., *GDSL family of serine esterases/lipases.* Prog Lipid Res, 2004. **43**(6): p. 534-52.
101. Flieger, A., B. Neumeister, and N.P. Cianciotto, *Characterization of the gene encoding the major secreted lysophospholipase A of Legionella pneumophila and its role in detoxification of lysophosphatidylcholine.* Infect Immun, 2002. **70**(11): p. 6094-106.
102. Attree, O., et al., *The Lowe's oculocerebrorenal syndrome gene encodes a protein highly homologous to inositol polyphosphate-5-phosphatase.* Nature, 1992. **358**(6383): p. 239-42.
103. Zhang, X., et al., *Cell lines from kidney proximal tubules of a patient with Lowe syndrome lack OCRL inositol polyphosphate 5-phosphatase and accumulate phosphatidylinositol 4,5-bisphosphate.* J Biol Chem, 1998. **273**(3): p. 1574-82.
104. Kuhle, V., G.L. Abrahams, and M. Hensel, *Intracellular Salmonella enterica redirect exocytic transport processes in a Salmonella pathogenicity island 2-dependent manner.* Traffic, 2006. **7**(6): p. 716-30.

105. Rajashekar, R., et al., *Live cell imaging reveals novel functions of Salmonella enterica SPI2-T3SS effector proteins in remodeling of the host cell endosomal system.* PLoS One, 2014. **9**(12): p. e115423.
106. Stein, M.A., et al., *Identification of a Salmonella virulence gene required for formation of filamentous structures containing lysosomal membrane glycoproteins within epithelial cells.* Mol Microbiol, 1996. **20**(1): p. 151-64.
107. Paz, I., et al., *Galectin-3, a marker for vacuole lysis by invasive pathogens.* Cell Microbiol, 2010. **12**(4): p. 530-44.
108. Boucrot, E., et al., *The intracellular fate of Salmonella depends on the recruitment of kinesin.* Science, 2005. **308**(5725): p. 1174-8.
109. Patel, S., et al., *Caspase-3 cleavage of Salmonella type III secreted effector protein SifA is required for localization of functional domains and bacterial dissemination.* Gut Microbes, 2019. **10**(2): p. 172-187.
110. Brumell, J.H., et al., *SifA permits survival and replication of Salmonella typhimurium in murine macrophages.* Cell Microbiol, 2001. **3**(2): p. 75-84.
111. Dumont, A., et al., *SKIP, the host target of the Salmonella virulence factor SifA, promotes kinesin-1-dependent vacuolar membrane exchanges.* Traffic, 2010. **11**(7): p. 899-911.
112. Sindhwani, A., et al., *Salmonella exploits the host endolysosomal tethering factor HOPS complex to promote its intravacuolar replication.* PLoS Pathog, 2017. **13**(10): p. e1006700.
113. McGourty, K., et al., *Salmonella inhibits retrograde trafficking of mannose-6-phosphate receptors and lysosome function.* Science, 2012. **338**(6109): p. 963-7.
114. Gao, Y., et al., *The Pearling Transition Provides Evidence of Force-Driven Endosomal Tubulation during Salmonella Infection.* MBio, 2018. **9**(3).
115. Ruiz-Albert, J., et al., *Complementary activities of SseJ and SifA regulate dynamics of the Salmonella typhimurium vacuolar membrane.* Mol Microbiol, 2002. **44**(3): p. 645-61.
116. Camacho, E.M., et al., *Engineering Salmonella as intracellular factory for effective killing of tumour cells.* Sci Rep, 2016. **6**: p. 30591.
117. Ray, K., et al., *Tracking the dynamic interplay between bacterial and host factors during pathogen-induced vacuole rupture in real time.* Cell Microbiol, 2010. **12**(4): p. 545-56.
118. Schroeder, N., et al., *The virulence protein SopD2 regulates membrane dynamics of Salmonella-containing vacuoles.* PLoS Pathog, 2010. **6**(7): p. e1001002.
119. Krieger, V., et al., *Reorganization of the endosomal system in Salmonella-infected cells: the ultrastructure of Salmonella-induced tubular compartments.* PLoS Pathog, 2014. **10**(9): p. e1004374.
120. Ramsden, A.E., et al., *The SPI-2 type III secretion system restricts motility of Salmonella-containing vacuoles.* Cell Microbiol, 2007. **9**(10): p. 2517-29.
121. Moest, T., et al., *Contribution of bacterial effectors and host proteins to the composition and function of Salmonella-induced tubules.* Cell Microbiol, 2018. **20**(12): p. e12951.
122. Wesolowski, J. and F. Paumet, *Taking control: reorganization of the host cytoskeleton by Chlamydia.* F1000Res, 2017. **6**: p. 2058.

123. Al-Zeer, M.A., et al., *Chlamydia trachomatis remodels stable microtubules to coordinate Golgi stack recruitment to the chlamydial inclusion surface.* Mol Microbiol, 2014. **94**(6): p. 1285-97.
124. Wesolowski, J., et al., *Chlamydia Hijacks ARF GTPases To Coordinate Microtubule Posttranslational Modifications and Golgi Complex Positioning.* MBio, 2017. **8**(3).
125. Kumar, Y. and R.H. Valdivia, *Actin and intermediate filaments stabilize the Chlamydia trachomatis vacuole by forming dynamic structural scaffolds.* Cell Host Microbe, 2008. **4**(2): p. 159-69.
126. Jorgensen, I., et al., *The Chlamydia protease CPAF regulates host and bacterial proteins to maintain pathogen vacuole integrity and promote virulence.* Cell Host Microbe, 2011. **10**(1): p. 21-32.
127. Robertson, D.K., et al., *Inclusion biogenesis and reactivation of persistent Chlamydia trachomatis requires host cell sphingolipid biosynthesis.* PLoS Pathog, 2009. **5**(11): p. e1000664.
128. Hanada, K., et al., *CERT-mediated trafficking of ceramide.* Biochim Biophys Acta, 2009. **1791**(7): p. 684-91.
129. Hanada, K., et al., *Molecular machinery for non-vesicular trafficking of ceramide.* Nature, 2003. **426**(6968): p. 803-9.
130. Huitema, K., et al., *Identification of a family of animal sphingomyelin synthases.* EMBO J, 2004. **23**(1): p. 33-44.
131. Derre, I., R. Swiss, and H. Agaisse, *The lipid transfer protein CERT interacts with the Chlamydia inclusion protein IncD and participates to ER-Chlamydia inclusion membrane contact sites.* PLoS Pathog, 2011. **7**(6): p. e1002092.
132. Kumagai, K., et al., *Both the N- and C- terminal regions of the Chlamydial inclusion protein D (IncD) are required for interaction with the pleckstrin homology domain of the ceramide transport protein CERT.* Biochem Biophys Res Commun, 2018. **505**(4): p. 1070-1076.
133. Elwell, C.A., et al., *Chlamydia trachomatis co-opts GBF1 and CERT to acquire host sphingomyelin for distinct roles during intracellular development.* PLoS Pathog, 2011. **7**(9): p. e1002198.
134. Stanhope, R., et al., *IncV, a FFAT motif-containing Chlamydia protein, tethers the endoplasmic reticulum to the pathogen-containing vacuole.* Proc Natl Acad Sci U S A, 2017. **114**(45): p. 12039-12044.
135. Wong, K.W., *The Role of ESX-1 in Mycobacterium tuberculosis Pathogenesis.* Microbiol Spectr, 2017. **5**(3).
136. Simeone, R., et al., *Phagosomal rupture by Mycobacterium tuberculosis results in toxicity and host cell death.* PLoS Pathog, 2012. **8**(2): p. e1002507.
137. Simeone, R., et al., *Cytosolic access of Mycobacterium tuberculosis: critical impact of phagosomal acidification control and demonstration of occurrence in vivo.* PLoS Pathog, 2015. **11**(2): p. e1004650.
138. Mellouk, N., et al., *Shigella subverts the host recycling compartment to rupture its vacuole.* Cell Host Microbe, 2014. **16**(4): p. 517-30.
139. Weiner, A., et al., *Macropinosomes are Key Players in Early Shigella Invasion and Vacuolar Escape in Epithelial Cells.* PLoS Pathog, 2016. **12**(5): p. e1005602.

140. Mellouk, N. and J. Enninga, *Cytosolic Access of Intracellular Bacterial Pathogens: The Shigella Paradigm.* Front Cell Infect Microbiol, 2016. **6**: p. 35.
141. Choy, A., et al., *The Legionella effector RavZ inhibits host autophagy through irreversible Atg8 deconjugation.* Science, 2012. **338**(6110): p. 1072-6.
142. Rolando, M., et al., *Legionella pneumophila S1P-lyase targets host sphingolipid metabolism and restrains autophagy.* Proc Natl Acad Sci U S A, 2016. **113**(7): p. 1901-6.
143. Baxt, L.A. and M.B. Goldberg, *Host and bacterial proteins that repress recruitment of LC3 to Shigella early during infection.* PLoS One, 2014. **9**(4): p. e94653.
144. Campbell-Valois, F.X., et al., *Escape of Actively Secreting Shigella flexneri from ATG8/LC3-Positive Vacuoles Formed during Cell-To-Cell Spread Is Facilitated by IcsB and VirA.* MBio, 2015. **6**(3): p. e02567-14.
145. Ogawa, M., et al., *Escape of intracellular Shigella from autophagy.* Science, 2005. **307**(5710): p. 727-31.
146. Kreibich, S., et al., *Autophagy Proteins Promote Repair of Endosomal Membranes Damaged by the Salmonella Type Three Secretion System 1.* Cell Host Microbe, 2015. **18**(5): p. 527-37.
147. Lopez-Jimenez, A.T., et al., *The ESCRT and autophagy machineries cooperate to repair ESX-1-dependent damage at the Mycobacterium-containing vacuole but have opposite impact on containing the infection.* PLoS Pathog, 2018. **14**(12): p. e1007501.
148. Personnic, N., et al., *Subversion of Retrograde Trafficking by Translocated Pathogen Effectors.* Trends Microbiol, 2016. **24**(6): p. 450-462.
149. Chi, R.J., M.S. Harrison, and C.G. Burd, *Biogenesis of endosome-derived transport carriers.* Cell Mol Life Sci, 2015. **72**(18): p. 3441-3455.
150. Mirrashidi, K.M., et al., *Global Mapping of the Inc-Human Interactome Reveals that Retromer Restricts Chlamydia Infection.* Cell Host Microbe, 2015. **18**(1): p. 109-21.
151. Elwell, C.A., et al., *Chlamydia interfere with an interaction between the mannose-6-phosphate receptor and sorting nexins to counteract host restriction.* Elife, 2017. **6**.
152. Yao, J., et al., *Mechanism of inhibition of retromer transport by the bacterial effector RidL.* Proc Natl Acad Sci U S A, 2018. **115**(7): p. E1446-E1454.
153. Romano-Moreno, M., et al., *Molecular mechanism for the subversion of the retromer coat by the Legionella effector RidL.* Proc Natl Acad Sci U S A, 2017. **114**(52): p. E11151-E11160.
154. Barlocher, K., A. Welin, and H. Hilbi, *Formation of the Legionella Replicative Compartment at the Crossroads of Retrograde Trafficking.* Front Cell Infect Microbiol, 2017. **7**: p. 482.
155. Welin, A., S. Weber, and H. Hilbi, *Quantitative Imaging Flow Cytometry of Legionella-Infected Dictyostelium Amoebae Reveals the Impact of Retrograde Trafficking on Pathogen Vacuole Composition.* Appl Environ Microbiol, 2018. **84**(11).

156. Patrick, K.L., et al., *Quantitative Yeast Genetic Interaction Profiling of Bacterial Effector Proteins Uncovers a Role for the Human Retromer in Salmonella Infection.* Cell Syst, 2018. **7**(3): p. 323-338 e6.
157. Braun, V., et al., *Sorting nexin 3 (SNX3) is a component of a tubular endosomal network induced by Salmonella and involved in maturation of the Salmonella-containing vacuole.* Cell Microbiol, 2010. **12**(9): p. 1352-67.
158. McDonough, J.A., et al., *Host pathways important for Coxiella burnetii infection revealed by genome-wide RNA interference screening.* MBio, 2013. **4**(1): p. e00606-12.
159. Miller, H.E., C.L. Larson, and R.A. Heinzen, *Actin polymerization in the endosomal pathway, but not on the Coxiella-containing vacuole, is essential for pathogen growth.* PLoS Pathog, 2018. **14**(4): p. e1007005.
160. Alberts A, J.A., Lewis J, Raff M, Roberts K, Walter P., *Molecular Biology of the Cell.* Garland Science, 2008.
161. Goode, B.L., D.G. Drubin, and G. Barnes, *Functional cooperation between the microtubule and actin cytoskeletons.* Curr Opin Cell Biol, 2000. **12**(1): p. 63-71.
162. Mitchison, T.J., *Actin based motility on retraction fibers in mitotic PtK2 cells.* Cell Motil Cytoskeleton, 1992. **22**(2): p. 135-51.
163. Kasza, K.E. and J.A. Zallen, *Dynamics and regulation of contractile actin-myosin networks in morphogenesis.* Curr Opin Cell Biol, 2011. **23**(1): p. 30-8.
164. Skau, C.T. and C.M. Waterman, *Specification of Architecture and Function of Actin Structures by Actin Nucleation Factors.* Annu Rev Biophys, 2015. **44**: p. 285-310.
165. Wang, Y.L., *Exchange of actin subunits at the leading edge of living fibroblasts: possible role of treadmilling.* J Cell Biol, 1985. **101**(2): p. 597-602.
166. Cooper, J.A. and D.A. Schafer, *Control of actin assembly and disassembly at filament ends.* Curr Opin Cell Biol, 2000. **12**(1): p. 97-103.
167. Houdusse, A. and H.L. Sweeney, *How Myosin Generates Force on Actin Filaments.* Trends Biochem Sci, 2016. **41**(12): p. 989-997.
168. Breitsprecher, D. and B.L. Goode, *Formins at a glance.* J Cell Sci, 2013. **126**(Pt 1): p. 1-7.
169. Brouhard, G.J., *Dynamic instability 30 years later: complexities in microtubule growth and catastrophe.* Mol Biol Cell, 2015. **26**(7): p. 1207-10.
170. Mitchison, T. and M. Kirschner, *Dynamic instability of microtubule growth.* Nature, 1984. **312**(5991): p. 237-42.
171. Alushin, G.M., et al., *High-resolution microtubule structures reveal the structural transitions in alphabeta-tubulin upon GTP hydrolysis.* Cell, 2014. **157**(5): p. 1117-29.
172. McIntosh, J.R. and T. Hays, *A Brief History of Research on Mitotic Mechanisms.* Biology (Basel), 2016. **5**(4).
173. Wittmann, T., A. Hyman, and A. Desai, *The spindle: a dynamic assembly of microtubules and motors.* Nat Cell Biol, 2001. **3**(1): p. E28-34.
174. Andersen, S.S., *Spindle assembly and the art of regulating microtubule dynamics by MAPs and Stathmin/Op18.* Trends Cell Biol, 2000. **10**(7): p. 261-7.
175. Hirokawa, N., et al., *Kinesin superfamily motor proteins and intracellular transport.* Nat Rev Mol Cell Biol, 2009. **10**(10): p. 682-96.

176. Miki, H., et al., *All kinesin superfamily protein, KIF, genes in mouse and human.* Proc Natl Acad Sci U S A, 2001. **98**(13): p. 7004-11.
177. Hirokawa, N., Y. Noda, and Y. Okada, *Kinesin and dynein superfamily proteins in organelle transport and cell division.* Curr Opin Cell Biol, 1998. **10**(1): p. 60-73.
178. Woehlke, G. and M. Schliwa, *Walking on two heads: the many talents of kinesin.* Nat Rev Mol Cell Biol, 2000. **1**(1): p. 50-8.
179. Hancock, W.O. and J. Howard, *Processivity of the motor protein kinesin requires two heads.* J Cell Biol, 1998. **140**(6): p. 1395-405.
180. Spudich, J.A., *Molecular motors take tension in stride.* Cell, 2006. **126**(2): p. 242-4.
181. Yildiz, A., et al., *Intramolecular strain coordinates kinesin stepping behavior along microtubules.* Cell, 2008. **134**(6): p. 1030-41.
182. Yagi, T., *Bioinformatic approaches to dynein heavy chain classification.* Methods Cell Biol, 2009. **92**: p. 1-9.
183. Reck-Peterson, S.L., et al., *Single-molecule analysis of dynein processivity and stepping behavior.* Cell, 2006. **126**(2): p. 335-48.
184. Kardon, J.R. and R.D. Vale, *Regulators of the cytoplasmic dynein motor.* Nat Rev Mol Cell Biol, 2009. **10**(12): p. 854-65.
185. Holzbaur, E.L. and R.B. Vallee, *DYNEINS: molecular structure and cellular function.* Annu Rev Cell Biol, 1994. **10**: p. 339-72.
186. Vaughan, K.T. and R.B. Vallee, *Cytoplasmic dynein binds dynactin through a direct interaction between the intermediate chains and p150Glued.* J Cell Biol, 1995. **131**(6 Pt 1): p. 1507-16.
187. Schroer, T.A., *Dynactin.* Annu Rev Cell Dev Biol, 2004. **20**: p. 759-79.
188. Holzbaur, E.L., et al., *Homology of a 150K cytoplasmic dynein-associated polypeptide with the Drosophila gene Glued.* Nature, 1991. **351**(6327): p. 579-83.
189. Waterman-Storer, C.M., S. Karki, and E.L. Holzbaur, *The p150Glued component of the dynactin complex binds to both microtubules and the actin-related protein centractin (Arp-1).* Proc Natl Acad Sci U S A, 1995. **92**(5): p. 1634-8.
190. Holleran, E.A., et al., *beta III spectrin binds to the Arp1 subunit of dynactin.* J Biol Chem, 2001. **276**(39): p. 36598-605.
191. King, S.J. and T.A. Schroer, *Dynactin increases the processivity of the cytoplasmic dynein motor.* Nat Cell Biol, 2000. **2**(1): p. 20-4.
192. Ross, J.L., et al., *Processive bidirectional motion of dynein-dynactin complexes in vitro.* Nat Cell Biol, 2006. **8**(6): p. 562-70.
193. Martin, T.F., *Phosphoinositide lipids as signaling molecules: common themes for signal transduction, cytoskeletal regulation, and membrane trafficking.* Annu Rev Cell Dev Biol, 1998. **14**: p. 231-64.
194. Di Paolo, G. and P. De Camilli, *Phosphoinositides in cell regulation and membrane dynamics.* Nature, 2006. **443**(7112): p. 651-7.
195. Janetopoulos, C. and P. Devreotes, *Phosphoinositide signaling plays a key role in cytokinesis.* J Cell Biol, 2006. **174**(4): p. 485-90.
196. Simonsen, A., et al., *The role of phosphoinositides in membrane transport.* Curr Opin Cell Biol, 2001. **13**(4): p. 485-92.

197. Takenawa, T. and T. Itoh, *Phosphoinositides, key molecules for regulation of actin cytoskeletal organization and membrane traffic from the plasma membrane.* Biochim Biophys Acta, 2001. **1533**(3): p. 190-206.
198. Toker, A., *Phosphoinositides and signal transduction.* Cell Mol Life Sci, 2002. **59**(5): p. 761-79.
199. Jones, D.R. and I. Varela-Nieto, *Diabetes and the role of inositol-containing lipids in insulin signaling.* Mol Med, 1999. **5**(8): p. 505-14.
200. Logothetis, D.E., et al., *Channelopathies linked to plasma membrane phosphoinositides.* Pflugers Arch, 2010. **460**(2): p. 321-41.
201. Pendaries, C., et al., *Phosphoinositide signaling disorders in human diseases.* FEBS Lett, 2003. **546**(1): p. 25-31.
202. McLaughlin, S., et al., *PIP(2) and proteins: interactions, organization, and information flow.* Annu Rev Biophys Biomol Struct, 2002. **31**: p. 151-75.
203. De Craene, J.O., et al., *Phosphoinositides, Major Actors in Membrane Trafficking and Lipid Signaling Pathways.* Int J Mol Sci, 2017. **18**(3).
204. Ungewickell, A., et al., *The inositol polyphosphate 5-phosphatase Ocrl associates with endosomes that are partially coated with clathrin.* Proc Natl Acad Sci U S A, 2004. **101**(37): p. 13501-6.
205. Zhang, X., et al., *The protein deficient in Lowe syndrome is a phosphatidylinositol-4,5-bisphosphate 5-phosphatase.* Proc Natl Acad Sci U S A, 1995. **92**(11): p. 4853-6.
206. McCrea, H.J., et al., *All known patient mutations in the ASH-RhoGAP domains of OCRL affect targeting and APPL1 binding.* Biochem Biophys Res Commun, 2008. **369**(2): p. 493-9.
207. Faucherre, A., et al., *Lowe syndrome protein OCRL1 interacts with Rac GTPase in the trans-Golgi network.* Hum Mol Genet, 2003. **12**(19): p. 2449-56.
208. Ponting, C.P., *A novel domain suggests a ciliary function for ASPM, a brain size determining gene.* Bioinformatics, 2006. **22**(9): p. 1031-5.
209. Hagemann, N., et al., *Crystal structure of the Rab binding domain of OCRL1 in complex with Rab8 and functional implications of the OCRL1/Rab8 module for Lowe syndrome.* Small GTPases, 2012. **3**(2): p. 107-10.
210. Rodriguez-Gabin, A.G., et al., *Interaction of Rab31 and OCRL-1 in oligodendrocytes: its role in transport of mannose 6-phosphate receptors.* J Neurosci Res, 2010. **88**(3): p. 589-604.
211. Dressman, M.A., et al., *Ocrl1, a PtdIns(4,5)P(2) 5-phosphatase, is localized to the trans-Golgi network of fibroblasts and epithelial cells.* J Histochem Cytochem, 2000. **48**(2): p. 179-90.
212. Grieve, A.G., et al., *Lowe Syndrome protein OCRL1 supports maturation of polarized epithelial cells.* PLoS One, 2011. **6**(8): p. e24044.
213. Nandez, R., et al., *A role of OCRL in clathrin-coated pit dynamics and uncoating revealed by studies of Lowe syndrome cells.* Elife, 2014. **3**: p. e02975.
214. Luo, N., et al., *OCRL localizes to the primary cilium: a new role for cilia in Lowe syndrome.* Hum Mol Genet, 2012. **21**(15): p. 3333-44.
215. Erdmann, K.S., et al., *A role of the Lowe syndrome protein OCRL in early steps of the endocytic pathway.* Dev Cell, 2007. **13**(3): p. 377-90.

216. Billcliff, P.G., et al., *OCRL1 engages with the F-BAR protein pacsin 2 to promote biogenesis of membrane-trafficking intermediates.* Mol Biol Cell, 2016. **27**(1): p. 90-107.
217. Itoh, T., et al., *Role of the ENTH domain in phosphatidylinositol-4,5-bisphosphate binding and endocytosis.* Science, 2001. **291**(5506): p. 1047-51.
218. Varnai, P. and T. Balla, *Visualization of phosphoinositides that bind pleckstrin homology domains: calcium- and agonist-induced dynamic changes and relationship to myo-[3H]inositol-labeled phosphoinositide pools.* J Cell Biol, 1998. **143**(2): p. 501-10.
219. Takei, K. and V. Haucke, *Clathrin-mediated endocytosis: membrane factors pull the trigger.* Trends Cell Biol, 2001. **11**(9): p. 385-91.
220. Wennerberg, K. and C.J. Der, *Rho-family GTPases: it's not only Rac and Rho (and I like it).* J Cell Sci, 2004. **117**(Pt 8): p. 1301-12.
221. Madrid, A.S. and K. Weis, *Nuclear transport is becoming crystal clear.* Chromosoma, 2006. **115**(2): p. 98-109.
222. Kahn, R.A., et al., *Arf family GTPases: roles in membrane traffic and microtubule dynamics.* Biochem Soc Trans, 2005. **33**(Pt 6): p. 1269-72.
223. Pfeffer, S.R., *Rab GTPases: specifying and deciphering organelle identity and function.* Trends Cell Biol, 2001. **11**(12): p. 487-91.
224. Stenmark, H. and V.M. Olkkonen, *The Rab GTPase family.* Genome Biol, 2001. **2**(5): p. REVIEWS3007.
225. Khosravi-Far, R., et al., *Isoprenoid modification of rab proteins terminating in CC or CXC motifs.* Proc Natl Acad Sci U S A, 1991. **88**(14): p. 6264-8.
226. Gomes, A.Q., et al., *Membrane targeting of Rab GTPases is influenced by the prenylation motif.* Mol Biol Cell, 2003. **14**(5): p. 1882-99.
227. Segev, N., *Ypt/rab gtpases: regulators of protein trafficking.* Sci STKE, 2001. **2001**(100): p. re11.
228. Chavrier, P., et al., *Hypervariable C-terminal domain of rab proteins acts as a targeting signal.* Nature, 1991. **353**(6346): p. 769-72.
229. Seabra, M.C. and C. Wasmeier, *Controlling the location and activation of Rab GTPases.* Curr Opin Cell Biol, 2004. **16**(4): p. 451-7.
230. Sonnichsen, B., et al., *Distinct membrane domains on endosomes in the recycling pathway visualized by multicolor imaging of Rab4, Rab5, and Rab11.* J Cell Biol, 2000. **149**(4): p. 901-14.
231. Echard, A., et al., *Interaction of a Golgi-associated kinesin-like protein with Rab6.* Science, 1998. **279**(5350): p. 580-5.
232. Hill, E., M. Clarke, and F.A. Barr, *The Rab6-binding kinesin, Rab6-KIFL, is required for cytokinesis.* EMBO J, 2000. **19**(21): p. 5711-9.
233. Stenmark, H., *Rab GTPases as coordinators of vesicle traffic.* Nat Rev Mol Cell Biol, 2009. **10**(8): p. 513-25.
234. Gorvel, J.P., et al., *rab5 controls early endosome fusion in vitro.* Cell, 1991. **64**(5): p. 915-25.
235. Bucci, C., et al., *The small GTPase rab5 functions as a regulatory factor in the early endocytic pathway.* Cell, 1992. **70**(5): p. 715-28.
236. Zerial, M. and H. McBride, *Rab proteins as membrane organizers.* Nat Rev Mol Cell Biol, 2001. **2**(2): p. 107-17.

237. Roberts, R.L., et al., *Endosome fusion in living cells overexpressing GFP-rab5.* J Cell Sci, 1999. **112 (Pt 21)**: p. 3667-75.
238. Zeigerer, A., et al., *Rab5 is necessary for the biogenesis of the endolysosomal system in vivo.* Nature, 2012. **485**(7399): p. 465-70.
239. Wilson, D.B. and M.P. Wilson, *Identification and subcellular localization of human rab5b, a new member of the ras-related superfamily of GTPases.* J Clin Invest, 1992. **89**(3): p. 996-1005.
240. Chiariello, M., C.B. Bruni, and C. Bucci, *The small GTPases Rab5a, Rab5b and Rab5c are differentially phosphorylated in vitro.* FEBS Lett, 1999. **453**(1-2): p. 20-4.
241. Chen, P.I., et al., *Rab5 isoforms differentially regulate the trafficking and degradation of epidermal growth factor receptors.* J Biol Chem, 2009. **284**(44): p. 30328-38.
242. Bucci, C., et al., *Co-operative regulation of endocytosis by three Rab5 isoforms.* FEBS Lett, 1995. **366**(1): p. 65-71.
243. Ali, B.R., et al., *Multiple regions contribute to membrane targeting of Rab GTPases.* J Cell Sci, 2004. **117**(Pt 26): p. 6401-12.
244. Christoforidis, S., et al., *Phosphatidylinositol-3-OH kinases are Rab5 effectors.* Nat Cell Biol, 1999. **1**(4): p. 249-52.
245. Simonsen, A., et al., *EEA1 links PI(3)K function to Rab5 regulation of endosome fusion.* Nature, 1998. **394**(6692): p. 494-8.
246. Shin, H.W., et al., *An enzymatic cascade of Rab5 effectors regulates phosphoinositide turnover in the endocytic pathway.* J Cell Biol, 2005. **170**(4): p. 607-18.
247. Kutateladze, T.G., et al., *Phosphatidylinositol 3-phosphate recognition by the FYVE domain.* Mol Cell, 1999. **3**(6): p. 805-11.
248. Das, S. and D.G. Lambright, *Membrane Trafficking: An Endosome Tether Meets a Rab and Collapses.* Curr Biol, 2016. **26**(20): p. R927-R929.
249. Stenmark, H., et al., *Endosomal localization of the autoantigen EEA1 is mediated by a zinc-binding FYVE finger.* J Biol Chem, 1996. **271**(39): p. 24048-54.
250. Gaullier, J.M., et al., *FYVE fingers bind PtdIns(3)P.* Nature, 1998. **394**(6692): p. 432-3.
251. Callaghan, J., et al., *Direct interaction of EEA1 with Rab5b.* Eur J Biochem, 1999. **265**(1): p. 361-6.
252. Lawe, D.C., et al., *Sequential roles for phosphatidylinositol 3-phosphate and Rab5 in tethering and fusion of early endosomes via their interaction with EEA1.* J Biol Chem, 2002. **277**(10): p. 8611-7.
253. McBride, H.M., et al., *Oligomeric complexes link Rab5 effectors with NSF and drive membrane fusion via interactions between EEA1 and syntaxin 13.* Cell, 1999. **98**(3): p. 377-86.
254. Ullrich, O., et al., *Rab11 regulates recycling through the pericentriolar recycling endosome.* J Cell Biol, 1996. **135**(4): p. 913-24.
255. Wang, X., et al., *Regulation of vesicle trafficking in madin-darby canine kidney cells by Rab11a and Rab25.* J Biol Chem, 2000. **275**(37): p. 29138-46.
256. Goldenring, J.R., et al., *Enrichment of rab11, a small GTP-binding protein, in gastric parietal cells.* Am J Physiol, 1994. **267**(2 Pt 1): p. G187-94.

257. Ren, M., et al., *Hydrolysis of GTP on rab11 is required for the direct delivery of transferrin from the pericentriolar recycling compartment to the cell surface but not from sorting endosomes.* Proc Natl Acad Sci U S A, 1998. **95**(11): p. 6187-92.
258. Urbe, S., et al., *Rab11, a small GTPase associated with both constitutive and regulated secretory pathways in PC12 cells.* FEBS Lett, 1993. **334**(2): p. 175-82.
259. Satoh, A.K., et al., *Rab11 mediates post-Golgi trafficking of rhodopsin to the photosensitive apical membrane of Drosophila photoreceptors.* Development, 2005. **132**(7): p. 1487-97.
260. Lock, J.G. and J.L. Stow, *Rab11 in recycling endosomes regulates the sorting and basolateral transport of E-cadherin.* Mol Biol Cell, 2005. **16**(4): p. 1744-55.
261. Welz, T., J. Wellbourne-Wood, and E. Kerkhoff, *Orchestration of cell surface proteins by Rab11.* Trends Cell Biol, 2014. **24**(7): p. 407-15.
262. Lapierre, L.A., et al., *Rab11b resides in a vesicular compartment distinct from Rab11a in parietal cells and other epithelial cells.* Exp Cell Res, 2003. **290**(2): p. 322-31.
263. Silvis, M.R., et al., *Rab11b regulates the apical recycling of the cystic fibrosis transmembrane conductance regulator in polarized intestinal epithelial cells.* Mol Biol Cell, 2009. **20**(8): p. 2337-50.
264. Sugawara, K., et al., *Rab11 and its effector Rip11 participate in regulation of insulin granule exocytosis.* Genes Cells, 2009. **14**(4): p. 445-56.
265. Butterworth, M.B., et al., *Rab11b regulates the trafficking and recycling of the epithelial sodium channel (ENaC).* Am J Physiol Renal Physiol, 2012. **302**(5): p. F581-90.
266. Best, J.M., et al., *Small GTPase Rab11b regulates degradation of surface membrane L-type Cav1.2 channels.* Am J Physiol Cell Physiol, 2011. **300**(5): p. C1023-33.
267. Zhang, X.M., et al., *Sec15 is an effector for the Rab11 GTPase in mammalian cells.* J Biol Chem, 2004. **279**(41): p. 43027-34.
268. Lindsay, A.J. and M.W. McCaffrey, *The C2 domains of the class I Rab11 family of interacting proteins target recycling vesicles to the plasma membrane.* J Cell Sci, 2004. **117**(Pt 19): p. 4365-75.
269. Horgan, C.P. and M.W. McCaffrey, *The dynamic Rab11-FIPs.* Biochem Soc Trans, 2009. **37**(Pt 5): p. 1032-6.
270. Horgan, C.P., et al., *Rab11-FIP3 localises to a Rab11-positive pericentrosomal compartment during interphase and to the cleavage furrow during cytokinesis.* Biochem Biophys Res Commun, 2004. **319**(1): p. 83-94.
271. Marie, N., A.J. Lindsay, and M.W. McCaffrey, *Rab coupling protein is selectively degraded by calpain in a Ca2+-dependent manner.* Biochem J, 2005. **389**(Pt 1): p. 223-31.
272. Peden, A.A., et al., *The RCP-Rab11 complex regulates endocytic protein sorting.* Mol Biol Cell, 2004. **15**(8): p. 3530-41.
273. Kelly, E.E., C.P. Horgan, and M.W. McCaffrey, *Rab11 proteins in health and disease.* Biochem Soc Trans, 2012. **40**(6): p. 1360-7.
274. Caswell, P.T., et al., *Rab-coupling protein coordinates recycling of alpha5beta1 integrin and EGFR1 to promote cell migration in 3D microenvironments.* J Cell Biol, 2008. **183**(1): p. 143-55.

275. Lindsay, A.J., et al., *Rab coupling protein (RCP), a novel Rab4 and Rab11 effector protein.* J Biol Chem, 2002. **277**(14): p. 12190-9.
276. Huber, L.A., et al., *Rab8, a small GTPase involved in vesicular traffic between the TGN and the basolateral plasma membrane.* J Cell Biol, 1993. **123**(1): p. 35-45.
277. Huber, L.A., P. Dupree, and C.G. Dotti, *A deficiency of the small GTPase rab8 inhibits membrane traffic in developing neurons.* Mol Cell Biol, 1995. **15**(2): p. 918-24.
278. Peranen, J., et al., *Rab8 promotes polarized membrane transport through reorganization of actin and microtubules in fibroblasts.* J Cell Biol, 1996. **135**(1): p. 153-67.
279. Chen, S., et al., *Rab8b and its interacting partner TRIP8b are involved in regulated secretion in AtT20 cells.* J Biol Chem, 2001. **276**(16): p. 13209-16.
280. Nuoffer, C., et al., *Mss4 does not function as an exchange factor for Rab in endoplasmic reticulum to Golgi transport.* Mol Biol Cell, 1997. **8**(7): p. 1305-16.
281. Miinea, C.P., et al., *AS160, the Akt substrate regulating GLUT4 translocation, has a functional Rab GTPase-activating protein domain.* Biochem J, 2005. **391**(Pt 1): p. 87-93.
282. Armstrong, J., et al., *Identification of a novel member of the Rab8 family from the rat basophilic leukaemia cell line, RBL.2H3.* J Cell Sci, 1996. **109 (Pt 6)**: p. 1265-74.
283. Finetti, F., et al., *The small GTPase Rab8 interacts with VAMP-3 to regulate the delivery of recycling T-cell receptors to the immune synapse.* J Cell Sci, 2015. **128**(14): p. 2541-52.
284. Zhu, S., et al., *Rab11a-Rab8a cascade regulates the formation of tunneling nanotubes through vesicle recycling.* J Cell Sci, 2018. **131**(19).
285. Bonifacino, J.S. and B.S. Glick, *The mechanisms of vesicle budding and fusion.* Cell, 2004. **116**(2): p. 153-66.
286. Jahn, R. and R.H. Scheller, *SNAREs--engines for membrane fusion.* Nat Rev Mol Cell Biol, 2006. **7**(9): p. 631-43.
287. Chen, Y.A. and R.H. Scheller, *SNARE-mediated membrane fusion.* Nat Rev Mol Cell Biol, 2001. **2**(2): p. 98-106.
288. Fasshauer, D., et al., *Conserved structural features of the synaptic fusion complex: SNARE proteins reclassified as Q- and R-SNAREs.* Proc Natl Acad Sci U S A, 1998. **95**(26): p. 15781-6.
289. Prekeris, R., *Rabs, Rips, FIPs, and Endocytic Membrane Traffic.* TheScientificWorldJOURNAL, 2003. **3**.
290. Hanson, P.I., et al., *Structure and conformational changes in NSF and its membrane receptor complexes visualized by quick-freeze/deep-etch electron microscopy.* Cell, 1997. **90**(3): p. 523-35.
291. Weber, H.S. and S.E. Cyran, *Transvenous "snare-assisted" coil occlusion of patent ductus arteriosus.* Am J Cardiol, 1998. **82**(2): p. 248-51.
292. Rice, L.M. and A.T. Brunger, *Crystal structure of the vesicular transport protein Sec17: implications for SNAP function in SNARE complex disassembly.* Mol Cell, 1999. **4**(1): p. 85-95.

293. Mayer, A., W. Wickner, and A. Haas, *Sec18p (NSF)-driven release of Sec17p (alpha-SNAP) can precede docking and fusion of yeast vacuoles.* Cell, 1996. **85**(1): p. 83-94.
294. Zeng, Q., et al., *The cytoplasmic domain of Vamp4 and Vamp5 is responsible for their correct subcellular targeting: the N-terminal extenSion of VAMP4 contains a dominant autonomous targeting signal for the trans-Golgi network.* J Biol Chem, 2003. **278**(25): p. 23046-54.
295. Steegmaier, M., et al., *Vesicle-associated membrane protein 4 is implicated in trans-Golgi network vesicle trafficking.* Mol Biol Cell, 1999. **10**(6): p. 1957-72.
296. Zeng, Q., et al., *A novel synaptobrevin/VAMP homologous protein (VAMP5) is increased during in vitro myogenesis and present in the plasma membrane.* Mol Biol Cell, 1998. **9**(9): p. 2423-37.
297. Wong, S.H., et al., *Endobrevin, a novel synaptobrevin/VAMP-like protein preferentially associated with the early endosome.* Mol Biol Cell, 1998. **9**(6): p. 1549-63.
298. Antonin, W., et al., *The R-SNARE endobrevin/VAMP-8 mediates homotypic fusion of early endosomes and late endosomes.* Mol Biol Cell, 2000. **11**(10): p. 3289-98.
299. McMahon, H.T., et al., *Cellubrevin is a ubiquitous tetanus-toxin substrate homologous to a putative synaptic vesicle fusion protein.* Nature, 1993. **364**(6435): p. 346-9.
300. Volchuk, A., et al., *Cellubrevin is a resident protein of insulin-sensitive GLUT4 glucose transporter vesicles in 3T3-L1 adipocytes.* J Biol Chem, 1995. **270**(14): p. 8233-40.
301. Feng, D., et al., *Subcellular distribution of 3 functional platelet SNARE proteins: human cellubrevin, SNAP-23, and syntaxin 2.* Blood, 2002. **99**(11): p. 4006-14.
302. Galli, T., et al., *Tetanus toxin-mediated cleavage of cellubrevin impairs exocytosis of transferrin receptor-containing vesicles in CHO cells.* J Cell Biol, 1994. **125**(5): p. 1015-24.
303. Tayeb, M.A., et al., *Inhibition of SNARE-mediated membrane traffic impairs cell migration.* Exp Cell Res, 2005. **305**(1): p. 63-73.
304. Murray, R.Z., et al., *Syntaxin 6 and Vti1b form a novel SNARE complex, which is up-regulated in activated macrophages to facilitate exocytosis of tumor necrosis Factor-alpha.* J Biol Chem, 2005. **280**(11): p. 10478-83.
305. Cunha, B.A., A. Burillo, and E. Bouza, *Legionnaires' disease.* Lancet, 2016. **387**(10016): p. 376-385.
306. Horwitz, M.A. and F.R. Maxfield, *Legionella pneumophila inhibits acidification of its phagosome in human monocytes.* J Cell Biol, 1984. **99**(6): p. 1936-43.
307. Horwitz, M.A. and S.C. Silverstein, *Legionnaires' disease bacterium (Legionella pneumophila) multiples intracellularly in human monocytes.* J Clin Invest, 1980. **66**(3): p. 441-50.
308. Segal, G., M. Feldman, and T. Zusman, *The Icm/Dot type-IV secretion systems of Legionella pneumophila and Coxiella burnetii.* FEMS Microbiol Rev, 2005. **29**(1): p. 65-81.
309. Asrat, S., et al., *Bacterial pathogen manipulation of host membrane trafficking.* Annu Rev Cell Dev Biol, 2014. **30**: p. 79-109.

310. Creasey, E.A. and R.R. Isberg, *Maintenance of vacuole integrity by bacterial pathogens.* Curr Opin Microbiol, 2014. **17**: p. 46-52.
311. Wiater, L.A., et al., *Early events in phagosome establishment are required for intracellular survival of Legionella pneumophila.* Infect Immun, 1998. **66**(9): p. 4450-60.
312. Aachoui, Y., et al., *Caspase-11 protects against bacteria that escape the vacuole.* Science, 2013. **339**(6122): p. 975-8.
313. Shi, J., et al., *Cleavage of GSDMD by inflammatory caspases determines pyroptotic cell death.* Nature, 2015. **526**(7575): p. 660-5.
314. Coers, J., et al., *Restriction of Legionella pneumophila growth in macrophages requires the concerted action of cytokine and Naip5/Ipaf signalling pathways.* Cell Microbiol, 2007. **9**(10): p. 2344-57.
315. Ensminger, A.W., et al., *Experimental evolution of Legionella pneumophila in mouse macrophages leads to strains with altered determinants of environmental survival.* PLoS Pathog, 2012. **8**(5): p. e1002731.
316. de Jesus-Diaz, D.A., et al., *Host Cell S Phase Restricts Legionella pneumophila Intracellular Replication by Destabilizing the Membrane-Bound Replication Compartment.* MBio, 2017. **8**(4).
317. Byrne, B. and M.S. Swanson, *Expression of Legionella pneumophila virulence traits in response to growth conditions.* Infect Immun, 1998. **66**(7): p. 3029-34.
318. Auerbuch, V., D.T. Golenbock, and R.R. Isberg, *Innate immune recognition of Yersinia pseudotuberculosis type III secretion.* PLoS Pathog, 2009. **5**(12): p. e1000686.
319. Chung, N., et al., *Median absolute deviation to improve hit selection for genome-scale RNAi screens.* J Biomol Screen, 2008. **13**(2): p. 149-58.
320. Huang, L., et al., *The E Block motif is associated with Legionella pneumophila translocated substrates.* Cell Microbiol, 2011. **13**(2): p. 227-45.
321. Pelegrin, P., C. Barroso-Gutierrez, and A. Surprenant, *P2X7 receptor differentially couples to distinct release pathways for IL-1beta in mouse macrophage.* J Immunol, 2008. **180**(11): p. 7147-57.
322. Franceschini, A., et al., *STRING v9.1: protein-protein interaction networks, with increased coverage and integration.* Nucleic Acids Res, 2013. **41**(Database issue): p. D808-15.
323. Pfeffer, S. and D. Aivazian, *Targeting Rab GTPases to distinct membrane compartments.* Nat Rev Mol Cell Biol, 2004. **5**(11): p. 886-96.
324. Wilcke, M., et al., *Rab11 regulates the compartmentalization of early endosomes required for efficient transport from early endosomes to the trans-golgi network.* J Cell Biol, 2000. **151**(6): p. 1207-20.
325. Banerjee, M., et al., *Cellubrevin/vesicle-associated membrane protein-3-mediated endocytosis and trafficking regulate platelet functions.* Blood, 2017. **130**(26): p. 2872-2883.
326. Christoforidis, S., et al., *The Rab5 effector EEA1 is a core component of endosome docking.* Nature, 1999. **397**(6720): p. 621-5.
327. Weber, S.S., et al., *Legionella pneumophila exploits PI(4)P to anchor secreted effector proteins to the replicative vacuole.* PLoS Pathog, 2006. **2**(5): p. e46.

328. Sato, T., et al., *Rab8a and Rab8b are essential for several apical transport pathways but insufficient for ciliogenesis.* J Cell Sci, 2014. **127**(Pt 2): p. 422-31.
329. Hu, C., D. Hardee, and F. Minnear, *Membrane fusion by VAMP3 and plasma membrane t-SNAREs.* Exp Cell Res, 2007. **313**(15): p. 3198-209.
330. Casbon, A.J., et al., *Macrophage NADPH oxidase flavocytochrome B localizes to the plasma membrane and Rab11-positive recycling endosomes.* J Immunol, 2009. **182**(4): p. 2325-39.
331. Lopez-Montero, N. and J. Enninga, *Diverted recycling-Shigella subversion of Rabs.* Small GTPases, 2018. **9**(5): p. 365-374.
332. Pylypenko, O., et al., *Structural basis of myosin V Rab GTPase-dependent cargo recognition.* Proc Natl Acad Sci U S A, 2013. **110**(51): p. 20443-8.
333. Kasai, H., N. Takahashi, and H. Tokumaru, *Distinct initial SNARE configurations underlying the diversity of exocytosis.* Physiol Rev, 2012. **92**(4): p. 1915-64.
334. Guichard, A., V. Nizet, and E. Bier, *RAB11-mediated trafficking in host-pathogen interactions.* Nat Rev Microbiol, 2014. **12**(9): p. 624-34.
335. van Weering, J.R., P. Verkade, and P.J. Cullen, *SNX-BAR proteins in phosphoinositide-mediated, tubular-based endosomal sorting.* Semin Cell Dev Biol, 2010. **21**(4): p. 371-80.
336. Hsiao, J.C., et al., *Intracellular Transport of Vaccinia Virus in HeLa Cells Requires WASH-VPEF/FAM21-Retromer Complexes and Recycling Molecules Rab11 and Rab22.* J Virol, 2015. **89**(16): p. 8365-82.
337. Walsh, R.B., et al., *Opposing functions for retromer and Rab11 in extracellular vesicle cargo traffic at synapses.* bioRxiv, 2019: p. 645713.
338. Seaman, M.N., *The retromer complex - endosomal protein recycling and beyond.* J Cell Sci, 2012. **125**(Pt 20): p. 4693-702.
339. Wang, S., et al., *The retromer complex is required for rhodopsin recycling and its loss leads to photoreceptor degeneration.* PLoS Biol, 2014. **12**(4): p. e1001847.
340. Jimenez-Orgaz, A., et al., *Control of RAB7 activity and localization through the retromer-TBC1D5 complex enables RAB7-dependent mitophagy.* EMBO J, 2018. **37**(2): p. 235-254.
341. Cui, Y., et al., *Retromer has a selective function in cargo sorting via endosome transport carriers.* J Cell Biol, 2019. **218**(2): p. 615-631.
342. Szatmari, Z., et al., *Rab11 facilitates cross-talk between autophagy and endosomal pathway through regulation of Hook localization.* Mol Biol Cell, 2014. **25**(4): p. 522-31.
343. Puri, C., et al., *The RAB11A-Positive Compartment Is a Primary Platform for Autophagosome Assembly Mediated by WIPI2 Recognition of PI3P-RAB11A.* Dev Cell, 2018. **45**(1): p. 114-131 e8.
344. Longatti, A., et al., *TBC1D14 regulates autophagosome formation via Rab11- and ULK1-positive recycling endosomes.* J Cell Biol, 2012. **197**(5): p. 659-75.
345. Padh, H., et al., *A post-lysosomal compartment in Dictyostelium discoideum.* J Biol Chem, 1993. **268**(9): p. 6742-7.
346. Cardelli, J., *Phagocytosis and macropinocytosis in Dictyostelium: phosphoinositide-based processes, biochemically distinct.* Traffic, 2001. **2**(5): p. 311-20.

347. Maniak, M., *Conserved features of endocytosis in Dictyostelium.* Int Rev Cytol, 2002. **221**: p. 257-87.